Aus dem

Institut für Pharmakologie und Toxikologie der Bundeswehr

Precision-Cut Lung Slices (PCLS): Optimization of Long-Term Cold Storage and use as model for reactivation of organophosphorus-compound inhibited AChE

Dissertation

zum Erwerb des Doctor of Philosophy (Ph.D.) an der Medizinischen Fakultät der Ludwig-Maximilians-Universität München

vorgelegt von

Fee Marie Victoria Gölitz

aus

Mannheim / Deutschland

Jahr

2025

Mit Genehmigung der Medizinischen Fakultät der
Ludwig-Maximilians-Universität München

Erstes Gutachten:	Prof. Dr. Timo Wille
Zweites Gutachten:	Prof. Dr. Thomas Gudermann
Drittes Gutachten:	Prof. Dr. Joachim Heinrich
Viertes Gutachten:	Prof. Dr. Anja Horn-Bochtler

Dekan: Prof. Dr. med. Thomas Gudermann

Tag der mündlichen Prüfung: 16.09.2025

Affidavit

Affidavit

Gölitz, Fee

Surname, first name

Street

Zip code, town, country

I hereby declare, that the submitted thesis entitled:

Precision-Cut Lung Slices (PCLS): Optimization of Long-Term Cold Storage and use as model for reactivation of organophosphorus-compound inhibited AChE

is my own work. I have only used the sources indicated and have not made unauthorised use of services of a third party. Where the work of others has been quoted or reproduced, the source is always given.

I further declare that the dissertation presented here has not been submitted in the same or similar form to any other institution for the purpose of obtaining an academic degree.

Munich, 24.09.2025 Fee Gölitz

place, date Signature doctoral candidate

Confirmation of congruency

LMU LUDWIG-MAXIMILIANS-UNIVERSITÄT MÜNCHEN

Promotionsbüro Medizinische Fakultät

MMRS

Confirmation of congruency between printed and electronic version of the doctoral thesis

Gölitz, Fee

Surname, first name

Street

Zip code, town, country

I hereby declare, that the submitted thesis entitled:

Precision-Cut Lung Slices (PCLS): Optimization of Long-Term Cold Storage and use as model for reactivation of organophosphorus-compound inhibited AChE

is congruent with the printed version both in content and format.

Munich, 24.09.2025

place, date

Fee Gölitz

Signature doctoral candidate

Table of contents

List of abbreviations

AChE	Acetylcholinesterase
ACh	Acetylcholine
ADOC	4-Amino-2-((diethylamino)methyl)phenol
ATCh	Acetylthiocholine
BuChE	Butyrylcholinesterase
COPD	Chronic Obstructive Pulmonary Disease
CVX	Chinese VX
CWC	Chemical Weapon Convention
DMEM/F12	Dulbecco’s Modified Eagle's Medium / Nutrient Mixture F-12
DMSO	Dimethyl Sulfoxide
DTNB	5,5'-Dithiobis(2-nitrobenzoic acid)
EFSA	European Food Safety Authority
ELISA	Enzyme-linked immunosorbent assay
Eto	Ethopropazine
GA	Tabun
GB	Sarin
GD	Soman
GF	Cyclosarin
H&E	Hematoxylin and Eosin
hPCLS	human Precision-Cut Lung Slices
IF	Immunofluorescence
NOX-6	Non-Oxime-6
OBI	Obidoxime
OP	Organophosphorus
OPCW	Organisation for the Prohibition of Chemical Weapons
OPNA	Organophosphorus nerve agent
PAM	Pralidoxime
PCLS	Precision-Cut Lung Slices
POX	Phosphylated Oximes
PTE C23AL	Phosphotriesterase C23AL
qPCR	quantitative Polymerase Chain Reaction
RNA	Ribonucleic Acid

RVX	Russian VX
3R	Reduction, Refinement, Replacement
TNB^-	5-Thio-2-nitrobenzoate

List of publications and presentations

Publications of the cumulative dissertation:

Publication I: Gölitz F, Herbert J, Worek F, Wille T (2023). AChE reactivation in precision-cut lung slices following organophosphorus compound poisoning. *Toxicology Letters*, Volume 392, Pages 75-83, DOI:10.1016/j.toxlet.2023.12.014

Publication II: M. Camila Melo-Narvaez †, Fee Gölitz †, Eshita Jain, Janine Gote-Schniering, Mircea Gabriel Stoleriu, Wilhelm Bertrams, Bernd Schmeck, Ali Önder Yildirim, Ursula Rauen, Timo Wille*, Mareike Lehmann (2025). Cold storage of human precision-cut lung slices in TiProtec preserves cellular composition and transcriptional responses and enables on-demand mechanistic studies. *Respiratory Research*, Volume 26, Article Number 57, Pages 1-19, DOI:10.1186/s12931-025-03132-w †M. Camila Melo-Narvaez and Fee Gölitz contributed equally to this work. *Correspondence author.

Conference contributions:

Oral and Poster presentations:

1. **Investigation of novel therapeutic approaches in organophosphate induced lung injury using Precision-Cut Lung slices (PCLS),** Fee Gölitz, Franz Worek, Timo Wille, GRK 2338 Annual Retreat, Herrsching, 2022
2. **Reactivation of organophosphorus compound-inhibited acetylcholinesterase in rat Precision-Cut Lung slices,** Fee Gölitz, Franz Worek, Timo Wille, German Pharmtox Summit (GPTS), Ulm, 2023
3. **Precision-Cut Lung Slices in acetylcholinesterase reactivator research: comparison of colorimetrically determined AChE activity and airway responsiveness,** Fee Gölitz, Franz Worek, Timo Wille, Annual meeting of the Society of Toxicology (SOT), Nashville, 2023
4. **Determination of organophosphorus compound inhibited AChE activity: Precision-Cut Lung slices (PCLS) as a useful model for AChE reactivator research,** Fee Gölitz, Franz Worek, Timo Wille, Medical chemical defense conference (MCDC), Munich, 2023
5. **Determination of organophosphorus compound inhibited AChE activity: Precision cut lung slices as a useful model for AChE reactivator research,** Fee Gölitz, Franz Worek, Timo Wille, Forum Junger Wissenschaftler, Frankfurt, 2023
6. **Precision cut lung slices as a versatile research tool: AChE reactivator research and cold-storage preservation**, GRK 2338 Annual Retreat, Tutzing, 2023
7. **Precision Cut Lung Slices in Acetylcholinesterase Reactivator Research: Assessing AChE Activity and Airway Responsiveness**, Fee Gölitz, Franz Worek, Timo Wille, European Association of Poisons Centers and Clinical Toxicologist (EAPCCT), Munich, 2024
8. **„Lungengewebeschnitte“ in der Wehrmedizinischen Toxikologie: Vom „Lungengummibärchen“ zum hochfunktionellen Präzisionslungenschnitt**, Fee Gölitz, 55. Kongress der DGWMP e. V., Augsburg, 2024

List of figures and tables

1. Authors Contributions to the Publications

1.1 Contributions to Publication I

Gölitz F, Herbert J, Worek F, Wille T (2023). AChE reactivation in precision-cut lung slices following organophosphorus compound poisoning. *Toxicology Letters*, Volume 392, Pages 75-83, DOI:10.1016/j.toxlet.2023.12.014

Journal listing in “Web of science” - “Clarivate” - “Journal Citation Reports” (2023): *Toxicology Letters*: Rank by Journal Impact Factor/ Category Toxicology 49 of 106; Rank by Journal Citation Indicator/ Category Toxicology 27 of 106.

The activity of acetylcholinesterase (AChE) was assessed for the first time in intact precision-cut lung slices (PCLS). To measure the effects of organophosphorus nerve agents (OPNAs) and reactivators on AChE activity at the molecular level, PCLS were used as a more complex *ex vivo* model compared to previously employed systems, such as isolated AChE. Additionally, functional measurements were performed, with a primary focus on examining airway responses following exposure to OPNAs and subsequent treatment with various reactivators. A correlation between molecular and functional levels was established. With this method the use of animals in science can be reduced in the future. Furthermore, reactivator candidates can be evaluated more quickly in a reliable, complex model closer to the physiological reality.

Below, I have outlined my specific contributions to this research.

Gölitz F:

1. **Project Initiation and Planning:**
- Literature research
- Preliminary measurements regarding:
  - Amount of PCLS/measurement needed
  - PTE concentration needed
  - Timing requirements
- Project and experiment design

2. **Experiment Implementation:**
- Generation and culture of PCLS
- Establishment of the AChE activity measurement method (based on the Ellman Assay) in intact PCLS
- Airway activity measurements by video microscopy
- Data collection

3. **Analysis and Visualization:**
- Data analysis
- Statistical data analysis
- Visualization of data and figure generation

4. **Manuscript Development and Submission Process:**
- Writing of the original manuscript draft
- Addressing the reviewers' comments
- Writing a detailed response to the reviewers
- Preparation of the revised manuscript

The contributions of the co-authors to the publication Gölitz F. et al. in *Toxicology Letters* (2023) are listed below.

Herbert J:

1. **Project Initiation:**
- Literature research
- Preliminary tests with lung homogenate and single PCLS
- Pre-evaluations for bronchoconstriction experiment
2. **Manuscript Development:**
- Manuscript reviewing and editing of the original manuscript draft

Worek F:

1. **Project Initiation and Planning:**
- Scientific advice
2. **Analysis:**
- Data discussion
3. **Manuscript Development and Submission Process:**
- Manuscript reviewing and editing of the original manuscript draft

Wille T:

1. **Project Initiation and Planning:**
- Literature research
- Project and experiment design
- Project supervision and scientific advice
2. **Analysis:**
- Data discussion
3. **Manuscript Development and Submission Process:**
- Manuscript reviewing and editing of the original manuscript draft
- Addressing the reviewers' comments
- Corresponding author for submission

1.2 Contributions to Publication II

M. Camila Melo-Narvaez †, Fee Gölitz †, Eshita Jain, Janine Gote-Schniering, Mircea Gabriel Stoleriu, Wilhelm Bertrams, Bernd Schmeck, Ali Önder Yildirim, Ursula Rauen, Timo Wille*, Mareike Lehmann* (2025). Cold storage of human precision-cut lung slices in TiProtec preserves cellular composition and transcriptional responses and enables on-demand mechanistic studies. *Respiratory Research*, Volume 26, Article Number 57, Pages 1-19, DOI:10.1186/s12931-025-03132-w †M. Camila Melo-Narvaez and Fee Gölitz contributed equally to this work. *Corresponding authors.

Journal listing in “Web of science” - “Clarivate” - “Journal Citation Reports” (2023*): Respiratory Research*: Rank by Journal Impact Factor/ Category Respiratory System 17 of 101; Rank by Journal Citation Indicator/ Category 17 of 101.

The study evaluated the efficacy of TiProtec®, a specifically designed tissue preservation solution, for the long-term cold storage of human precision-cut lung slices (hPCLS). For this purpose, hPCLS were stored in DMEM/F-12 (Dulbecco’s Modified Eagle's Medium), TiProtec, or TiProtec without iron chelators for up to 28 days. Assessments included various methods covering a wide range of endpoints (e.g. viability, metabolic activity, tissue structure, transcriptomics). Results indicated that TiProtec effectively preserved the viability, metabolic activity, transcriptional profile, and cellular composition of hPCLS for up to 14 days. Furthermore, cold storage did not significantly induce cellular senescence in hPCLS. Additionally, hPCLS maintained their functional responsiveness to fibrotic stimuli.

These findings highlight the potential of TiProtec to optimize long-term cold storage of hPCLS, ensuring their viability and functionality for on-demand mechanistic studies and drug discovery in Respiratory Research.

Below, I have outlined my specific contributions to this research, as well as the ones from Melo-Narvaez M C, with whom the first authorship is shared equally.

Gölitz F:

1. **Project Initiation and Planning:**
- Literature research
- Project and experiment design
2. **Experiment Implementation:**
- Preparation of fresh cold storage solutions following the transfer from the Rauen lab
- hPCLS culture
- hPCLS RNA (Ribonucleic Acid) isolation
- hPCLS staining and imaging
- Viability and metabolic activity measurements
3. **Analysis and Visualization:**
- Statistical data analysis
- Visualization of data and figure generation
4. **Manuscript Development and Submission Process:**
- Writing of the original manuscript draft
- Addressing the reviewers’ comments

Melo-Narvaez M C:

1. **Project Planning:**
- Literature research
- Project and experiment design
2. **Experiment implementation:**
- Generation and culture of hPCLS
- hPCLS RNA isolation and qPCR (quantitative Polymerase Chain Reaction)
- hPCLS staining and imaging
3. **Analysis and Visualization:**
- Image analysis
- Bulk RNA sequencing analysis
- Statistical data analysis
- Visualization of data and figure generation
4. **Manuscript Development and Submission Process:**
- Writing of the original manuscript draft
- Addressing the reviewers' comments

The contributions of the co-authors to the publication Melo-Narvaez M C and Gölitz F et al. in *Respiratory Research* (2025) are listed below:

Jain E:

1. **Experiment Implementation:**
- Generation and culture of hPCLS
- hPCLS RNA isolation and qPCR
- hPCLS staining and imaging

Gote-Schniering J:

1. **Analysis and Visualization:**
- Bulk RNA sequencing analysis
- Statistical data analysis
2. **Manuscript Development and Submission Process:**
- Manuscript writing
- Addressing the reviewers' comments

Stoleriu M G:

1. **Clinical Sample Contribution:**
- Generation of clinical samples

Bertrams W:

1. **Analysis:**
- Bulk RNA sequencing analysis
2. **Manuscript Development:**
- Manuscript review

Schmeck B:

1. Manuscript review and scientific advice

Yildirim A Ö:

1. Scientific advice

Rauen U:

1. **Experiment Implementation:**
- Preparation of cold storage solutions
- Provision of iron chelators
2. **Manuscript Development and Submission Process:**
- Manuscript writing and reviewing
- Addressing the reviewers' comments
- Scientific advice

Wille T:

1. **Project Initiation and Planning:**
- Literature Research
- Project and experiment design
- Project supervision and scientific advice
2. **Analysis and Visualization:**
- Data discussion
3. **Manuscript Development and Submission Process:**
- Manuscript writing and reviewing
- Addressing the reviewers' comments
- Corresponding author

Lehmann M:

1. **Project Planning:**
- Literature research
- Project and experiment design
- Project supervision and scientific advice
2. **Analysis and Visualization:**
- Data analysis
- Figure generation
3. **Manuscript Development and Submission Process:**
- Manuscript writing and reviewing
- Addressing the reviewers' comments
- Corresponding author for submission

2. Introductory summary

2.1 Background and Importance of Organophosphorus (OP) Compounds

Tabun (GA) and sarin (GB) were the first organophosphorus nerve agents (OPNAs) developed in the 1930s by Gerhard Schrader, who worked at I.G. Farben in Leverkusen, Germany. The two compounds were the result of a pesticide development program. Yet, the extreme toxicity of these organophosphorus (OP) compounds led to their further development as chemical weapons. In the early 1940s, cyclosarin (GF) and soman (GD) were synthesized by Gerhard Schrader in Leverkusen and by Richard Kuhn in Heidelberg. (Karalliedde et al. 2001; Marrs 2007) As these agents were developed in Germany, they are referred to as the G-agent series (Worek et al. 2016a).

Subsequently, the V-series agents, named for their "venomous" or "vicious" properties, were developed, with VX emerging in the 1950s. Slightly modified analogs such as RVX (Russian VX) and CVX (Chinese VX) followed (Chauhan et al. 2008). These compounds share a basic structure derived from Schrader's patented "alkyl formula" (Schrader 1950; Schrader et al. 1958) *(Fig.1)*.

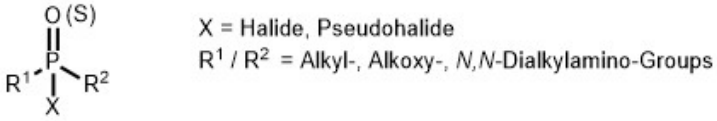

Fig 1. Schrader's "alkyl formula" created with ChemDraw Version 21.0.0.

Today, OP compounds continue to pose a significant threat due to their ongoing use as pesticides and as chemical weapons. While the use of OP pesticides has declined, particularly in Europe, industrial accidents and cases of self-poisoning remain a problem in other regions of the world, especially in Southeast Asia (Gunnell und Eddleston 2003; Eddleston et al. 2005). The decrease in use of OP pesticides in agriculture is caused by the strict regulations of national authorities and the European Food Safety Authority (EFSA 2024; European Comission 2024). The use of OPNAs as chemical weapons was banned through the “Chemical Weapon Convention in 1997: Convention on the Prohibition of the Development, Production, Stockpiling and Use of Chemical Weapons and on their Destruction” (Organisation for the Prohibition of Chemical Weapons 07.06.2020). Despite these efforts, there is an ongoing threat of dangerous OPNA use such as in Syria, Malaysia, Great Britain, and Russia (Dolgin 2013; John et al. 2018; Nakagawa und Tu 2018; Steindl et al. 2021; Vale et al. 2018).

Although the use of OPNAs for assassinations is relatively rare, the potential for high-impact releases with significant danger to a wider population (hybrid warfare) underscores the need for improved therapeutic options, since current treatments are often insufficient. Moreover, the unpredictability of exposure scenarios, whether from accidental OP pesticide poisoning or deliberate OPNA attacks, makes timely and effective medical response challenging. (Bey und Walter 2002)

2.2 Acetylcholinesterase (AChE)-Inhibition Related Complications Following OP Compound Exposure and Current Therapeutic Options

OP compounds bind covalently to acetylcholinesterase (AChE), resulting in an inhibition of the enzyme, which, in its physiological state, cleaves the neurotransmitter acetylcholine (ACh) (Alkondon et al. 2009). The AChE inhibition is caused through the phosphorylation or phosphonylation (termed as phosphylation) of the hydroxyl group of the amino acid serine located in the active center of this pivotal enzyme (Holmstedt 1959). As a result of the AChE inhibition, ACh can no longer be cleaved in the synaptic cleft. The ACh overflow leads to an overstimulation of the muscarinic and nicotinic receptors, this may result in a cholinergic crisis (Marrs 1993). A cholinergic crisis is defined by various symptoms, including bronchorrhea, bronchoconstriction, bradycardia, muscle paralysis, tachycardia and convulsions. In the extreme, the cholinergic crisis may be lethal due to respiratory failure (Grob 1956; Aktories et al. 2022).

Since many years a triple therapy consisting of a muscarinic receptor antagonist (atropine or scopolamine), an AChE reactivator (oxime) and a benzodiazepine (diazepam or midazolam) is used to treat patients after OP compound exposure (Eddleston et al. 2008). It is crucial to treat patients as early as possible since the mortality rate is higher without prompt treatment. To counteract the overstimulation of muscarinic receptors atropine is given in a rapid escalating dose scheme (atropinisation). The continuation of the atropine administration is often necessary and needs to be carefully titrated to avoid atropine overdosing with symptoms like tachycardia, intestinal atony and pyrexia (Moffatt et al. 2010; Aktories et al. 2022). Rapid and early administration of oximes is also important (Eyer 2003), as it enables the reactivation of inhibited AChE by first forming a Michaelis-type phosphyl-AChE-oxime complex and then subsequently removing the phosphyl moiety from AChE through oxime-induced phosphylation (Eyer 2003; Worek et al. 2004). With some OP compounds, such as dimethyl-OP pesticides, a beneficial spontaneous reactivation might occur due to a dephosphylation of the phosphylated AChE via hydrolysis (Worek et al. 1999; Worek et al. 2004). However, if oximes are not applied in time, the phosphylated AChE “ages” through a hydrolytic dealkylation, making enzyme inhibition irreversible due to increased binding stability between AChE and the OP compound (Worek et al. 2004) (*Fig. 2*). For neuroprotection and to combat symptoms like agitation or seizures benzodiazepines are administered.

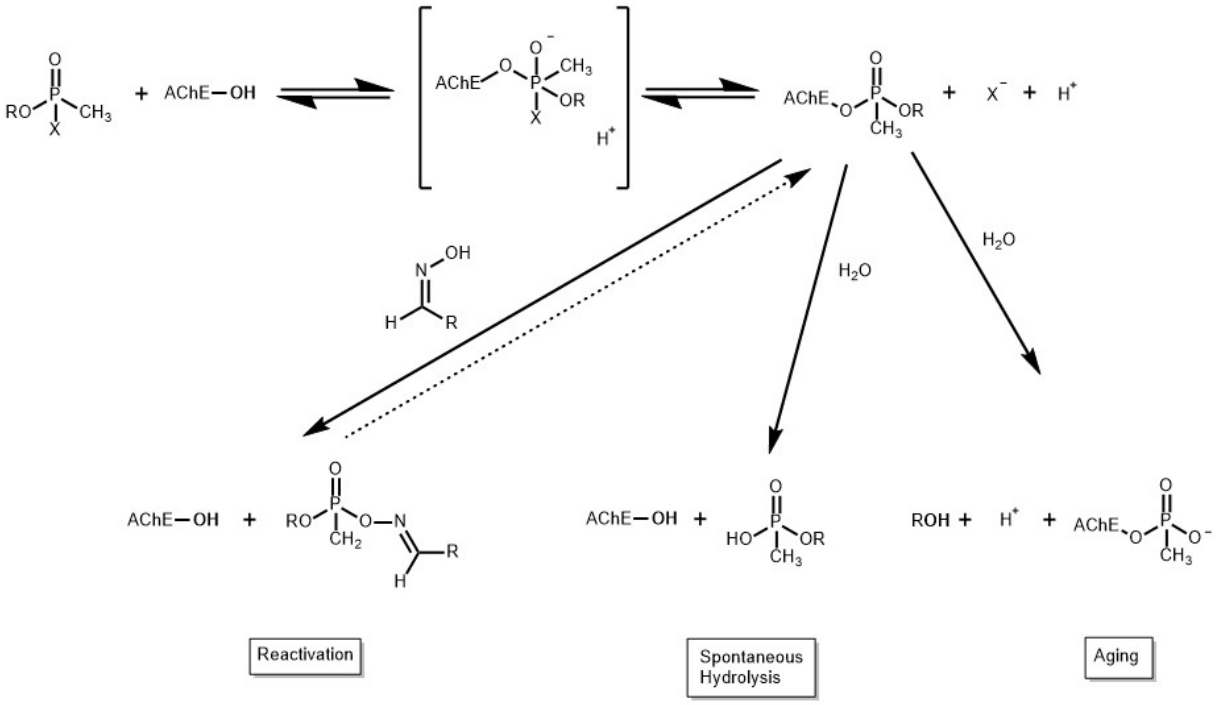

Fig 2. Reaction pathways at the hydroxyl residue in the active site of acetylcholinesterase (AChE) upon interaction with organophosphorus (OP) compounds, leading to AChE inhibition. Afterwards the following key processes are possible: Reactivation by oximes, spontaneous hydrolysis, and irreversible aging. Adapted from (Worek et al. 2004) and created with ChemDraw Version 21.0.0.

Currently, the standard triple therapy after OP poisoning often lacks effectiveness, particularly in cases involving certain OP compounds such as cyclosarin or tabun, where the reactivation of AChE by obidoxime (OBI) has proven to be notably low (Worek et al. 2004). Furthermore, the synthesis of OP analogs is possible, resulting in OPNAs with different properties as their parent compounds. For example, derivatives of tabun and sarin have shown significantly altered characteristics (Aurbek et al. 2010). Additionally, the possibility of inventing new OPNA structures - potentially accelerated by the misuse of artificial intelligence (Urbina et al. 2022) - underlines the urgent need for more effective broad-spectrum AChE reactivators. As a result, extensive development programs from various organizations aim to improve the therapeutic efficacy through intensive research (Worek und Thiermann 2013; Worek et al. 2020).

2.3 Challenges in Developing and Testing AChE Reactivators

For several decades research has been carried out to find new AChE reactivators (Worek und Thiermann 2013; Worek et al. 2020), but various challenges still occur regarding this research:

Reactivation kinetics, for example, depend on the specific combination of the OP compound and the oxime used. Certain combinations exhibit only weak reactivation, as most oximes have only a small spectrum and reactivate the AChE inhibited by a particular OP too slow (Worek et al. 2016b). This highlights the need for broad-spectrum oximes. As an interim solution, various oximes were combined, not only to broaden their effectiveness spectrum, but also with the aim to increase reactivation performance (Worek et al. 2007). Another hurdle is the lacking ability of oximes to penetrate the blood brain barrier due to their chemical structure and their associated positive charge resulting in hydrophilicity (Worek und Thiermann 2013; Kalász et al. 2015). To overcome these obstacles, experimental reactivators with “non-oxime” structures have been developed. Notably, some of these compounds are based on 4-amino-2-((diethylamino)methyl)phenol (ADOC) (Koning et al. 2018). However, a persistent obstacle, regardless of whether oximes or non-oxime reactivators (NOX) are used, is the potential formation of a new AChE inhibiting compound - the so called phosphylated reactivators (Ashani et al. 2003; Becker et al. 2010). Again, these challenges highlight the necessity to continue research regarding safe and effective AChE reactivators.

As respiratory failure due to bronchorrhea, bronchoconstriction and flaccid paralysis of diaphragm and intercostal muscles may result in death of patients, lung tissue is of high importance for research on AChE reactivator candidates’ effectiveness. Currently, the Ellman assay is a key tool in research to assess the ability of OP compounds to inhibit AChE and to evaluate therapeutic reactivators *in vitro* or *ex vivo*. It allows precise measurement of the AChE activity, offering insights into the dynamics of enzyme inhibition and reactivation. For this purpose the enzyme can be obtained from various sources including the electric organs of the electric ray and electric eel, from erythrocyte membranes, so called ghosts, or even from tissue homogenates such as lung or brain (Dodge et al. 1963; Worek et al. 2002; Worek et al. 2012; Wigenstam et al. 2022). However, these *in vitro* models cannot map systemic and physiological functions highlighting the need for more complex alternatives. In the past, *in vivo* experiments with rodents were performed earlier in drug development than it is ethically justifiable today, while human *in vivo* studies remain entirely unfeasible. Additionally, *in vivo* animal experiments are time-intensive, expensive and complex to analyze due to the various interfering factors.

Given these limitations, and as the British statistician George Box once said, “Essentially, all models are wrong, but some are useful” (Box 1976), a more refined and useful lung model is required to evaluate new therapeutic approaches after OP exposure. To address this, Precision-Cut Lung Slices (PCLS) from rats were used here as an *ex vivo* model, offering both ethical advantages and a closer approximation of physiological conditions.

2.4 New Approaches: Focus on Precision-Cut Lung Slices (PCLS)

PCLS are a versatile and robust *ex vivo* lung model which has been used in respiratory research for several years, the model became popular when tissue cutting with microtomes and vibratomes became an option (Liu et al. 2019; Koziol-White et al. 2024). Still, the PCLS preparation process is laborious and time-consuming. Due to the lung's lack of solid consistency, stabilization is

achieved through the instillation of agarose, which solidifies upon cooling. The “gummy bear-like” lung tissue is then sliced into PCLS. These are then stored overnight to recover and are afterwards ready for experimental use.

PCLS offer unique research opportunities, due to their preserved natural tissue architecture, including airways, blood vessels, parenchyma, and resident cell types. By using PCLS one must consider high individual variations based on their different tissue area origins, which can be an advantage and a disadvantage at the same time. On the one hand, multiple anatomical regions of the lung and different disease stages, depending on the patient, can be represented. On the other hand, the reproducibility and comparability are complicated, as not all regions are suitable for the same type of experiments, such as those involving airways or arteries for example. Today PCLS are widely used to study lung biology, toxicology, and the progression of diseases, such as fibrosis and Chronic Obstructive Pulmonary Disease (COPD), as well as to investigate the effects of pollutants, pathogens, and novel therapeutic approaches (Alsafadi et al. 2017; Alsafadi et al. 2020; Tigges et al. 2022; Herbert et al. 2023; Lehmann et al. 2024).

Improvements in imaging techniques, assay development, lung tissue preparation and storage have further enhanced the quality of PCLS experiments and enabled the exploration of new model options. In recent years cytotoxic and pro-inflammatory effects were studied using various assays, including metabolic tests and imaging techniques like the Alamar Blue assay, ELISAs (Enzyme-linked immunosorbent assays) and confocal microscopy for example (Neuhaus et al. 2018). Functional parameters such as ciliary beating and the airway or artery responsiveness have also been addressed (Paddenberg et al. 2014; Herbert et al. 2019; Herbert et al. 2023).

PCLS can be derived from various species, with human tissue (from healthy or diseased patients) considered to be the gold standard (Lehmann et al. 2024). However, human tissue access is limited and provides a substantial logistical burden in comparison to access to animal tissue, such as from rats and mice. The use of PCLS aligns with the 3R principle proposed by Russell and Burch (Russell und Burch 1992), which emphasizes not only reduction but also refinement and replacement of animal experiments. Through the large amount of PCLS gained from one rat lung (~ approx. 200 PCLS) the number of animals used is significantly reduced. Nevertheless, strategies to optimize the use of human PCLS (hPCLS), and to overcome the limited hPCLS availability, are needed, alongside with studies examining species-specific differences (Lehmann et al. 2024). Strategies such as long-term cold storage and cryopreservation would help to uncouple the timing of experiments from hPCLS preparation and further maximize the amount of hPCLS used for experiments, while simultaneously ensuring accurate evaluations of disease mechanisms and new therapeutic approaches.

In conclusion, PCLS offer a wide range of applications in respiratory research, but their full potential has yet to be realized. Further optimization could unlock additional possibilities for this promising model.

2.5 Application of the Ellman Assay in OP Toxicity Research

The Ellman assay is a widely used spectrophotometric method for quantifying the AChE activity. Developed in 1961, this assay is based on the hydrolysis of acetylthiocholine (ATCh) by AChE. (Ellman et al. 1961) The resulting thiocholine reacts with the chromogenic agent DTNB (5,5'-dithiobis(2-nitrobenzoic acid)), forming the yellow product TNB^- (5-thio-2-nitrobenzoate), the absorption of which was originally measured at 412 nm with a photometer. The TNB^- formation rate

is directly proportional to the AChE activity, making this assay a simple, fast, and cost-effective tool for kinetic studies, occupational health monitoring, and diagnosing OP compound exposure and its effect on AChE activity. (Worek et al. 2012)

To understand the efficacy of new therapeutics and to optimize treatment strategies the assay is essential for quick evaluations of new therapeutic candidates. Various improvements of the Ellman assay allow high-throughput screening using microplate-based systems or automated liquid-handling platforms, facilitating large-scale evaluation of inhibitors and reactivators (Wille et al. 2010).

Despite its utility, the Ellman assay has limitations that must be considered when planning experiments. If the AChE is sourced from erythrocytes or tissue with strong blood circulation the associated hemoglobin must be considered since its Soret band overlaps with TNB^- absorption at 412 nm, complicating measurements in erythrocyte lysates. This can be mitigated by using light of different wavelengths, such as maximum 436 nm, though this reduces sensitivity. Additionally, side reactions, such as the interaction of DTNB with thiol groups and the “oximolysis” of the oximes with ATCh, may blur the results. Substrate hydrolysis is sensitive to pH and temperature, requiring careful control of assay conditions to ensure reproducibility. (Worek et al. 2012)

Specific challenges arise when studying the reactivation of OP-inhibited AChE. Free OP in samples can re-inhibit reactivated AChE, and spontaneous enzyme reactivation and inhibitor aging substantially influence the results. Moreover, oxime-based reactivation generates phosphyl oxime (POX) intermediates, which may act as potent secondary inhibitors (Ashani et al. 2003). Oximes in high concentrations can also inhibit AChE directly or react with the substrate (oximolysis), hampering measurements (Sinko et al. 2007). These issues necessitate precise control of enzyme and oxime concentrations, along with appropriate corrections for background activity.

Understanding these limitations and optimizing experimental conditions, the Ellman assay remains a powerful and versatile method for studying AChE activity, OP toxicity, and therapeutic reactivation strategies.

2.6 PCLS and their Application in AChE Reactivation Research (Publication I)

Despite the lethality of OPNAs the medical countermeasures remain insufficient (e.g. AChE reactivators), necessitating testing novel reactivator compounds with meaningful models.

Historically, research using lung tissue in form of PCLS has focused on functional effects, such as airway constriction; for the development of treatment strategies airway recovery was primarily investigated (Martin et al. 1996; Seehase et al. 2011; Herbert et al. 2019). Therapeutic evaluations centered on airway relaxation (Wigenstam et al. 2021), leaving the primary toxic mechanism - AChE inhibition - underexplored in intact PCLS. Until now, attempts to measure AChE activity in lung tissue relies mainly on lung tissue lysates (Wigenstam et al. 2022), which preclude any functional or dynamic assessments in intact lung tissue.

Recognizing this gap, the AChE activity was measured in PCLS, which served as an *ex vivo* model, in which the tissue architecture is preserved (*Fig*. 3). Therefore, PCLS provide the unique opportunity to analyze both molecular-level responses (AChE activity) and functional-level responses (airway changes) - offering a dual assessment that lysate-based systems cannot provide.

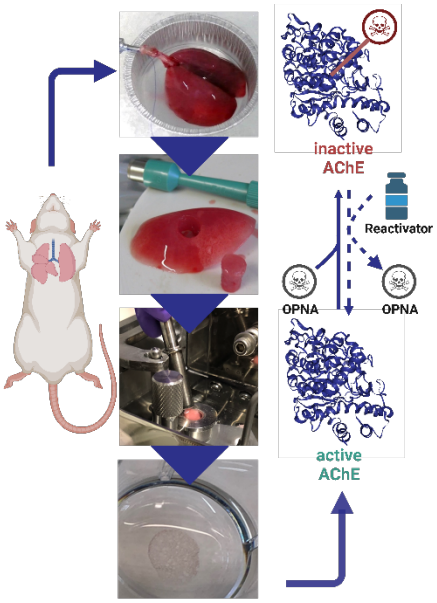

Fig. 3 Illustration of the Precision-Cut Lung Slice (PCLS) preparation workflow and key processes at the acetylcholinesterase (AChE) level, including organophosphorus nerve agent (OPNA)-induced inhibition and subsequent application of reactivators (Created in BioRender. Gölitz, F. (2025) https://BioRender.com/lqonumk).

In this study a platform to screen and evaluate AChE reactivator candidates in a physiologically more relevant context than with lysates or isolated AChE was established. PCLS were exposed to a broad spectrum of nerve agents, including GF, VX, or GB, to evaluate their inhibitory effects on lung tissue AChE and the responsiveness of PCLS to reactivation after OPNA exposure and subsequent reactivator therapy. Our study employed two established oximes, OBI and HI-6, alongside the novel non-oxime reactivator NOX-6.

Various steps of the experimental design were optimized: To address the low AChE activity in lung tissue and in order to prevent interference from butyrylcholinesterase (BuChE), ethopropazine (Eto) was utilized as a selective BuChE inhibitor. The measurement wavelength was optimized to 436 nm, minimizing hemoglobin interference while preserving the sensitivity of the Ellman assay. Additionally, pre-incubation with DTNB was conducted to avoid potential side reactions between DTNB and free sulfur-containing groups within the tissue during the measurement itself, ensuring accurate and reliable measurements of AChE activity. To eliminate residues of excess OPNAs and to prevent re-inhibition of reactivated AChE, a phosphotriesterase (PTE C23AL) was introduced to the assay medium, ensuring an OPNA-free environment (Cherny et al. 2013; Goldsmith et al. 2016). This innovative setup enabled AChE activity monitoring after treatment with both POX-forming and non-POX-forming reactivators. Introducing wash steps, as demonstrated with NOX-6 (a POX-forming reactivator (Koning et al. 2018), is essential for the method as POX formation depends on the concentrations of both the reactivator and the inhibited AChE.

The findings underscore the potential of PCLS as a cutting-edge model for OPNA research, particularly for early and high-throughput analysis of reactivators. By integrating molecular and functional level endpoints the utility of PCLS in understanding the interplay between AChE activity and airway constriction was demonstrated. The inclusion of various nerve agents and reactivators further underlines the model's robustness. Sarin-inhibited AChE showed the highest reactivation (OBI > HI-6), followed by VX-inhibited AChE (OBI > NOX-6 > HI-6). In contrast, no significant reactivation was observed for cyclosarin-inhibited AChE. Airway recovery data showed a similar

trend, emphasizing that OBI treatment was more effective for sarin-exposed airways compared to cyclosarin-exposed airways.

This work represents an advance in identifying promising reactivator candidates, moving beyond traditional approaches combining assessment of enzymatic and functional data. Thus, PCLS can drive the development of more effective countermeasures against OPNA poisoning.

2.7 Cold-Storage of Human PCLS (Publication II)

Assessing toxicological aspects and evaluating the potential of future drugs (Liu et al. 2019; Al-safadi et al. 2020; Koziol-White et al. 2024), hPCLS should be the benchmark to avoid species-specific differences. However, the limited availability of human lung tissue and due to the logistical burden by its generation, transport and storage, the widespread application of hPCLS is restricted (Lehmann et al. 2024). The viability and functionality of the PCLS under cell culture conditions (37 °C, 5% CO_2, and 100% air humidity) lasts for approximately two weeks, with a substantial decrease of quality over time, depending on the particular storage conditions (Neuhaus et al. 2017). To address the challenge of optimal tissue usage and to improve the availability of hPCLS, the efficacy of a tissue preservation solution, TiProtec®, both with and without iron chelators (*Table 1*), was evaluated for long-term cold storage of hPCLS.

Table 1. Composition of TiProtec.

Ingredients	Concentration [mmol/L]
Cl^-	103.1
Na^+	16
K^+	93
$H_2PO_4^-$	1
Mg^{2+}	8
Ca^{2+}	0.05
Glycine	10
Alanine	5
α-Ketoglutarate	2
Aspartate	5
N-Acetylhistidine	30
Tryptophan	2
Sucrose	20
Glucose	10
Deferoxamine*	0.1
LK 614*	0.02
pH	7.0

* Not present in TiProtec (-).

In this study, hPCLS generated from peritumor control tissues from non-chronic lung disease patients were stored in DMEM/F-12, TiProtec, or TiProtec (-) at 4°C for up to 28 days. All solutions were enriched with 1% penicillin/streptomycin. Tissue viability, metabolic activity, and structural integrity were evaluated using Live/Dead™ staining, the Alamar Blue assay and Hematoxylin and Eosin (H&E) staining. Furthermore, transcriptional changes and signaling pathways were analyzed using bulk RNA sequencing. Cold storage-induced senescence was evaluated using transcriptomics and immunofluorescence (IF) staining. Finally, to test the functionality of cold-stored hPCLS, samples were exposed to a fibrotic cocktail, and fibrotic responses were assessed with RT-qPCR and IF.

The results demonstrate that TiProtec preserves the viability, metabolic activity, and structural integrity of hPCLS for up to 14 days. Furthermore, it downregulated pathways associated with cell death, inflammation, and hypoxia, while upregulating protective pathways against oxidative stress. After 14 days no significant changes of the cellular senescence were observed, as determined by transcriptional profiling and IF staining. The ability to study functional aspects of lung tissue was retained: cold-stored hPCLS responded well to fibrotic stimuli, showing upregulation of genes for key extracellular matrix proteins such as fibronectin and collagen 1 as well as myofibroblast markers, including alpha smooth-muscle actin.

The findings underscore the benefits of TiProtec for preserving hPCLS for extended periods, making it possible to conduct on-demand experiments in the future. Unlike cryopreservation, which carries risks such as ice crystal formation, cold storage at 4°C is a more gentle long-term storage method (Pegg 2015). It allows easy handling during transport and storage, as no liquid nitrogen and no cryoprotectants like dimethyl sulfoxide (DMSO), which shows membrane toxicity and causes oxidative damage, are needed, thereby simplifying logistical challenges (Elliott et al. 2017; Tigges et al. 2021).

Building on previous studies that demonstrated TiProtec's efficacy in rat PCLS (Tigges et al. 2021), this study highlights the solution's suitability for long-term cold storage of human lung tissue. By preserving transcriptional integrity, cellular composition, and responsiveness to experimental stimuli, cold storage in TiProtec enables tissue banking, collaboration between research groups, and the repurposing of excess hPCLS for future experiments. This approach represents a step forward in translational lung research.

2.8 Concluding Remarks

This research aimed to have a dual impact by addressing two distinct but complementary projects: first, to advance the discovery and optimization of novel AChE reactivators by providing a physiologically relevant model that allows to study key aspects of OPNA toxicity and AChE reactivation (Publication I); and second, to enhance the utility and accessibility of the PCLS model, with a particular focus on hPCLS (Publication II).

The first objective centered on utilizing PCLS as an advanced, physiologically relevant *ex vivo* model to evaluate therapeutic interventions after OP poisoning. Special attention was given to the reactivation of AChE and its correlation with other physiological factors, such as airway response. This study introduced a novel method for analyzing AChE activity in intact PCLS, enabling the early identification of promising reactivators in a more complex model, than currently used ones. Using intact PCLS, allows for a more in-depth evaluation of candidate reactivators, linking enzymatic and functional responses. Notably, the correlation between AChE activity and airway response underscores the potential role of reactivators, alongside antimuscarinic drugs, in treating

life-threatening airway constriction following OPNA exposure. These findings represent a significant step forward in developing more effective therapeutic strategies against OP toxicity.

The second objective focused on addressing key challenges related to the availability, preservation, and long-term viability and functionality of human lung tissue in the PCLS model. Building upon the work of Tigges et al., who demonstrated the possibility of long-term cold storage for rat PCLS (Tigges et al. 2021), this project extended those findings to the more complex and clinically relevant context of hPCLS. This study demonstrated the efficacy of TiProtec, in preserving hPCLS for up to 14 days. TiProtec maintained tissue viability, metabolic activity, structural integrity, and cellular composition, while also preserving the capacity of hPCLS to elicit a fibrotic response. Transcriptomical changes associated with cold storage in TiProtec were characterized, providing a reference for future research. This optimizes the use of precious human lung tissue, enabling tissue banking, sample shipping and sharing, as well as on-demand processing. These improvements significantly expand the potential applications of hPCLS in translational lung research.

In conclusion, this work establishes PCLS as a versatile and physiologically relevant platform for bridging the gap between *in vitro* and *in vivo* studies, enabling the reliable evaluation of AChE reactivators and advancing the field of OPNA toxicity research. Additionally, the improved preservation protocol for hPCLS represents a major step forward in the efficient and collaborative use of human lung tissue. Together, these advancements contribute to a more robust and accessible framework for both therapeutic discovery and lung research.

3. Publication I

Toxicology Letters 392 (2024) 75–83

Contents lists available at ScienceDirect

Toxicology Letters

journal homepage: www.journals.elsevier.com/toxicology-letters

AChE reactivation in precision-cut lung slices following organophosphorus compound poisoning

Fee Gölitz [a,b], Julia Herbert [c], Franz Worek [a], Timo Wille [a,1,*]

[a] Bundeswehr Institute of Pharmacology and Toxicology, Munich, Germany
[b] Walther-Straub-Institute of Pharmacology and Toxicology, Ludwig-Maximilians-University, Munich, Germany
[c] Department of Pharmacology and Toxicology, Ernest Mario School of Pharmacy, Rutgers University, Piscataway, NJ, USA

ARTICLE INFO

Editor: Dr. Angela Mally

Keywords:
Lung toxicity
Nerve agents
Oximes
PCLS
3 R

ABSTRACT

Precision-cut lung slices (PCLS) are a suitable model for analyzing the acetylcholinesterase (AChE) activity and subsequent effects after exposure to organophosphorus (OP) compounds. In this study, the AChE activity was determined in intact PCLS for the first time. Since the current standard therapy for OP poisoning (atropine + oxime + benzodiazepine) lacks efficiency, reliable models to study novel therapeutic substances are needed. Models should depict pathophysiological mechanisms and help to evaluate the beneficial effects of new therapeutics. Here PCLS were exposed to three organophosphorus nerve agents (OPNAs): sarin (GB), cyclosarin (GF), and VX. They were then treated with three reactivators: HI-6, obidoxime (OBI), and a non-oxime (NOX-6). The endpoints investigated in this study were the AChE activity and the airway area (AA) change. OPNA exposure led to very low residual AChE activities. Depending on the reactivator properties different AChE reactivation results were measured. GB-inhibited PCLS-AChE was reactivated best, followed by VX and GF. To substantiate these findings and to understand the connection between the molecular and the functional levels in a more profound way the results were correlated to the AA changes. These investigations underline the importance of reactivator use and point to the possibilities for future improvements in the treatment of OPNA-exposed victims.

1. Introduction

Recent organophosphorus nerve agent (OPNA) attacks in Syria (Dolgin, 2013), Great Britain (Vale et al. 2018), and Russia (Steindl et al. 2021), underline the necessity to continue research in the field of medical chemical countermeasures, with a special focus on acetylcholinesterase (AChE) reactivators. Exposure to OPNAs leads to a covalent binding of the organophosphorus compound (OP) to AChE resulting in an inactive form of the pivotal enzyme (Holmstedt, 1959). This leads to an accumulation of acetylcholine (ACh) in the synaptic cleft and at neuromuscular junctions (King and Aaron, 2015; Costanzi et al. 2018), resulting in a cholinergic toxidrome by overstimulation of muscarinic and nicotinic ACh receptors (Amend et al. 2020; Ciottone and Gregory, 2018). The corresponding respiratory symptoms are salivation, bronchorrhea, bronchoconstriction, paralysis of intercostal muscles and the diaphragm, as well as disturbance in the respiratory drive. Ultimately, death may occur due to asphyxiation (Grob, 1956; Lee, 2003). Standard treatment consists of the administration of a muscarinic antagonist (atropine and/or scopolamine), to counteract the ACh effect, combined with an oxime (obidoxime, pralidoxime, or HI-6). The latter are used to reactivate the OPNA-inhibited AChE to counteract the nicotine receptor overstimulation (Newmark, 2004). Benzodiazepines (diazepam, midazolam) are administered as anticonvulsants for neuroprotection (Masson, 2011). The effectiveness of oximes after exposure to OPNAs is under debate (Worek and Thiermann, 2013; Eddleston, 2022; Thiermann and Worek, 2022) and the standard treatment does not address all

Abbreviations: AA, Airway area; ACh, Acetylcholine; AChE, Acetylcholinesterase; ADOC, 4-amino-2-((diethylamino)methyl)phenol; ATCh, Acetylthiocholine; BuChE, Butyrylcholinesterase; DMEM, Dulbecco's Modified Eagle's Medium; DPBS, Dulbecco's Phosphate Buffered Saline; DTNB, 5,5′-dithiobis(2-nitrobenzoic acid); Eto, Ethopropazine; GB, Sarin; GF, Cyclosarin; HEPES, 4-(2-Hydroxyethyl)-piperazin-1-ethansulfonsäure; hPCLS, human Precision-cut lung slices; IAA, Initial airway area; NOX, non-oxime; OBI, Obidoxime; OP, Organophosphorus compound; OPNA, Organophosphorus nerve agent; PCLS, Precision-cut lung slices; P/S, Penicillin/Streptomycin; PTE, Phosphotriesterase C23AL; SEM, Standard error of the mean; 3D, three dimensional.

* Corresponding author.
E-mail address: timowille@bundeswehr.org (T. Wille).
[1] Current address: Bundeswehr Medical Academy, Division Medical CBRN Defense, Munich, Germany

https://doi.org/10.1016/j.toxlet.2023.12.014
Received 22 September 2023; Received in revised form 12 December 2023; Accepted 22 December 2023
Available online 29 December 2023

life-threatening respiratory symptoms (Worek et al. 2020). For this reason, the search for more effective antidotes, with a special focus on improved AChE reactivators, is still ongoing. Even though the activity of AChE isolated from red blood cells can be measured in a standardized manner (Ellman et al. 1961; Worek et al. 2012), data on AChE activity in lung tissue are scarce (Peng et al. 2014; Wang et al. 2016; Wigenstam et al. 2022; Baba et al. 2014). The Ellman assay measures the formation of 5-thio-2-nitrobenzoate and is based on an enzymatic reaction leading to a color change, which is analyzed using a photometer (Fig. 1). New reactivators are typically prescreened using in vitro models, and after first promising results they are tested in vivo (Worek and Thiermann, 2013). Between these two steps, the use of precision-cut lung slices (PCLS) instead of living animals would be desirable to promote the idea of 3 R (Replacement, Reduction, Refinement) (Russell and Burch, 1960). Contrary to in vitro and in vivo models the use of PCLS enables high throughput toxicity- and therapeutics-screenings with samples from only one individual. This is possible since a great number of technical replicates can be produced from one lung. Additionally, the use of PCLS is important for a better understanding of AChE-related functions in a model more complex than isolated AChE since PCLS are three dimensional (3D) lung tissue. More profound knowledge regarding the AChE activity impact would shed light on the interactions of the molecular and functional levels of respiratory symptoms. As a potential test system PCLS can be used for this purpose. Previous studies proved the benefits of PCLS as a model for studying lung damage through exposure to OPs (Herbert et al. 2020; Tigges et al. 2022). The advantages of using PCLS as ex vivo tissue instead of cell culture are the 3D, morphological organization of all resident cell types (Liu et al. 2019) and the possibility to examine airway responsiveness (Martin et al. 1996). The observation of airway alterations is important since respiratory symptoms, such as bronchoconstriction and bronchorrhea, are linked to OPNA poisoning and are clinically relevant endpoints. Here, we established a model for OPNA-poisoning and subsequent reactivator treatment to quantify bronchoconstriction as airway area (AA) changes and to measure correspondent AChE activity in PCLS. We therefore selected the reactivators obidoxime (OBI), HI-6 and the experimental non-oxime (NOX) reactivator NOX-6 for our study. We opted for OBI and HI-6 due to their well-established status as widely studied oximes. Additionally, the inclusion of NOX-6 served the dual purpose of assessing the use of PCLS as a test system for novel reactivators and exploring the impact of a NOX structure in our investigation.

2. Materials and methods

2.1. Materials

For the PCLS preparation low melting agarose was obtained from Sigma-Aldrich (Deisenhofen, Germany). A Tyrode buffer (pH 7.4; composition see supplementary information) was freshly prepared and used for slicing of the PCLS. Dulbecco's modified Eagle's medium/nutrient mixture F-12 (1:1) with 15 mmol/L HEPES and sodium bicarbonate, without L-glutamine and phenol red (DMEM/F-12, Sigma-Aldrich) supplemented with 1% penicillin/streptomycin (P/S, 10,000 units penicillin and 10 mg streptomycin/mL; Sigma-Aldrich) was used for the further storage, washing and the measurements of PCLS. For the photometric measurements Dulbecco's Phosphate Buffered Saline (1X) (DPBS) with calcium and magnesium (Gibco by Thermo Fisher Scientific, Waltham, USA) was used additionally. 5,5′-dithiobis(2-nitrobenzoic acid) (DTNB), as a chromogen for the Ellman reaction; acetylthiocholine iodide (ATCh), as a substrate for the Ellman reaction; Triton-X, to lyse cells; and ethopropazine (Eto), as a selective and potent butyrylcholinesterase (BuChE) inhibitor, were purchased from Sigma-Aldrich. The Eto stock solution (6 mmol/L) was prepared with 0.01 mmol/L HCL (final Eto concentration 0.02 mmol/L). The phosphotriesterase PTE C23AL (PTE; 48 mg/mL; final concentration 0.48 mg/mL) was kindly supplied by the Weizmann Institute of Science and hydrolyzed excess OPNAs. The organophosphorus nerve agents (Fig. 2 *a*) sarin (isopropylmethylphosphonofluoridate, GB), cyclosarin (cyclohexylmethylphosphonofluoridate, GF) and VX (O-ethyl-S-[2-(diisopropylamino)-ethyl]-methylphosphonothioate) (≥ 98% by GC–MS, ^{1}H NMR and ^{31}P NMR) were made available by the German Ministry of Defence (Bonn, Germany). OPNA stock solutions (0.1% v/v) were prepared with acetonitrile (Merck KgaA). They were stored at room temperature and were diluted with distilled water before the experiment

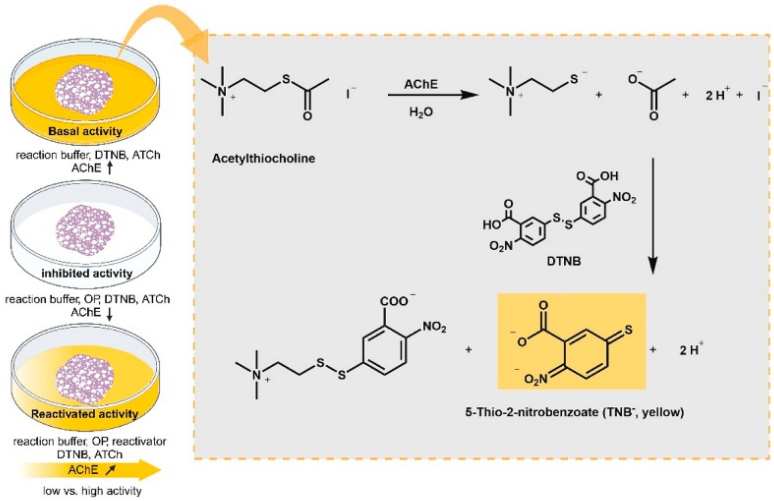

Fig. 1. Experimental setup of the acetylcholinesterase (AChE) measurements in intact PCLS. AChE activity was determined with a modified Ellman assay. Four PCLS were stacked on each other in the cavity of a 24-well-plate. Different reagents were applied at various time points (see Table 1 for further information) to measure all the conditions. The stronger the formation of the yellow product, the higher is the AChE activity. The scheme on the right shows the Ellman reaction. (Figure made in BioRender.com).

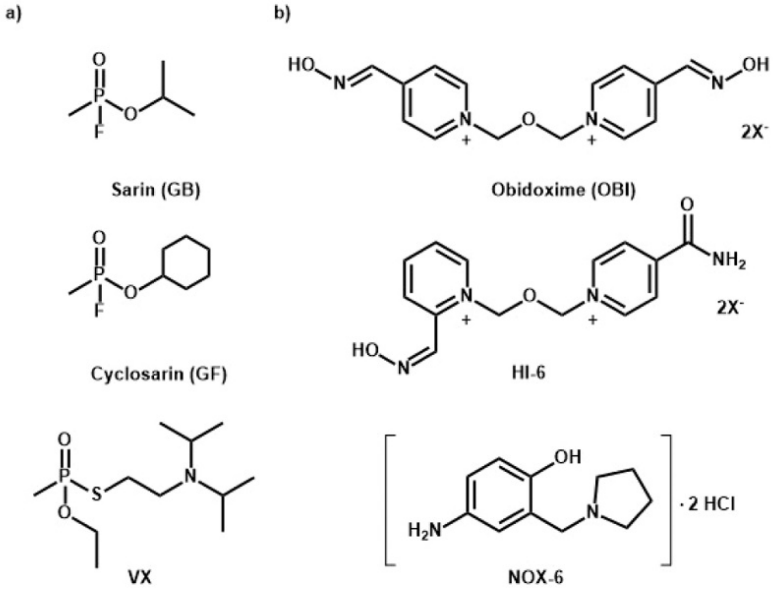

Fig. 2. Structure of organophosphorus nerve agents and reactivators. The figure shows the chemical structures of the organophosphorus nerve agents (OPNAs) used in this study (a) and the medical countermeasures used (b).

(concentration of the OPNA working solution 256 µmol/L, final OPNA concentration 1 µmol/L, final ACN concentration < 0.03%). As reactivators (Fig. 2 *b*) OBI (1,1'-(oxybis-methylene)bis[4-(hydroxyamino) methyl] pyridinium dichloride) (Merck KGaA), HI-6 (1-[([4-amino-carbonyl-pyridinio]-methoxy)-methyl]– 2-[hydroxyiminomethyl]-pyridinium dichloride monohydrate (Dr. Clement, Defence Research Establishment Suffield, Ralston, Alberta, Canada) and the experimental non-oxime reactivator NOX-6 (Phenol, 4-amino-2-(1-pyrrolidinyl-methyl)-, dihydrochloride) (> 95% by ^{1}H NMR, synthesized in house) were used (de Koning et al. 2018). Stock solutions of the reactivators were prepared in distilled water and stored at – 80 °C (oximes 2 mmol/L, non-oxime 10 mmol/L) until the day of the experiment (final oxime concentration 30 µmol/L, final non-oxime concentration 100 µmol/L). Acetylcholine (ACh) was acquired from Sigma-Aldrich; a stock solution (0.1 mol/L) was prepared with DMEM/F-12 and stored at – 80 °C. On the day of the experiment the ACh working solution (50 µmol/L, final ACh concentration 0.5 µmol/L) was freshly prepared and stored on ice.

2.2. Animals

Male Wistar rats (250-350 g) were bought from Charles River (Sulzfeld, Germany) and kept in a standard animal housing facility for at least seven days prior to the preparation of the PCLS, to allow proper acclimatization. The rats had access to food and water *ad libidum* and were kept under standard conditions (12 h light/dark circle, 20–24 °C, 45–65% humidity range) (Herbert et al. 2017). All experiments conducted agreed with the German Animal Welfare Act of 18th May 2006 (BGBl. I S. 1206, 1313) and the European Parliament and Council Directive of 22nd September 2010 (2010/63/EU). In total, lungs were removed from 39 rats.

2.3. Preparation of PCLS

PCLS were prepared as described before (Herbert et al. 2019; Tigges et al. 2021) with minor modifications. In summary, the rats were anesthetized with a mixture of 75 mg/kg ketamine (Ketavet 100 mg/mL, Zoetis Deutschland GmbH, Berlin, Germany) and 10 mg/kg xylazine (Xylasel 20 mg/mL, Selectavet Dr. Otto Fischer GmbH, Weyarn-Holzolling, Germany) and euthanized by cervical dislocation of the neck and additional exsanguination. Subsequently the trachea was cannulated, and the lung was filled with a 37 °C warm agarose solution (1.5% in DMEM/F-12 + P/S). Tissue cylinders (8 mm diameter) were obtained with a biopsy punch after the agarose had hardened on ice for 30 min. A Krumdieck tissue slicer (Alabama Research and Development, Munford, AL, USA) was used to cut the cylinders into 250 - 300 µm thick PCLS. As slicing medium ice-cold Tyrode buffer was used. All PCLS were pooled together and washed with fresh, prewarmed DMEM/F-12 + P/S three times after 30 min and two times after 60 min storage in an incubator (HeraCell 240i, Thermo Fisher Scientific, Waltham, MA) at 37 °C and 5% CO_2 on a shaker with 60 rpm. This procedure removes most of the excess agarose and cellular debris.

2.4. Determination of the AChE activity in intact PCLS

AChE activity was determined 24 h after slicing, this ensured stable viability since PCLS remain intact for up to 14 days under standard cell culture conditions with frequent medium changes (Neuhaus et al. 2017; Tigges et al. 2021). A photometric method based on the modified Ellman assay (Worek et al. 2012) (Fig. 1) was applied to measure the AChE activity. Due to a low AChE activity in PCLS, four intact PCLS were pooled per condition. The 24-well-plate cavities contained a prewarmed mixture of DMEM/F-12 + P/S with DPBS + 0.1% Triton-X. PCLS were stacked and pinned together in the center of a cavity by shortened sterile cannulas (Sterican, 21 G x 1 1/2, B. Braun SE Melsungen, Germany). Mounting of PCLS was necessary to prevent floating and to enable the circular photometric measurement during a defined period of time. To ensure determination of AChE activity only, BuChE was inhibited by Eto (final concentration 0.02 mmol/L) prior to the addition of other reagents. They were then exposed to various OPNAs (VX, GB, GF; final

concentration 1 μmol/L) and reactivators (OBI, HI-6; final concentration 30 μmol/L; NOX-6, final concentration 100 μmol/L). PTE (final concentration 0.048 mg/mL) was added after AChE inhibition to remove excess OPNA (Cherny et al. 2013; Worek et al. 2014) and to avoid a re-inhibition of AChE. For all experiments the (i) basal activity, the (ii) basal activity + reactivator, the (iii) residual activity after OPNA exposure and the (iv) restored activities after OPNA exposure + reactivator treatment were measured at 37 °C / 436 nm (Spark, Tecan Group Ltd., Männedorf, Switzerland) (Table 1). Blanks without any use of tissue but with all the reagents required were measured additionally and subtracted from measured values, making sure the reagent mixture would not influence the results. Depending on the reactivator properties, different workflows had to be chosen:

The effect of the established reactivators HI-6 and OBI was measured continuously. Depending on which values had to be obtained different reagents were combined. The use of Eto, DTNB and ATCh was mandatory in all assays. The required final composition and the incubation periods can be found in Table 1 *a)*. The change of absorption was measured for 30 min.

The effect of NOX-6 was measured discontinuously using VX-inhibited PCLS. This was necessary due to its high intrinsic inhibitory activity (de Koning et al. 2018; Horn et al. 2018): Therefore, five washing steps were included (5 ×1000 μl prewarmed DMEM/F12 + P/S). The required final composition of the reagents and the incubation periods can be found in Table 1 *b)*. After a 30 min incubation time, washing and preincubation with DTNB the change of extinction was measured for three minutes after adding ATCh. In doing so, an experimental setup which was as close as possible to the continuous measurements was obtained.

2.5. Video microscopy of airways in intact PCLS

A PCLS was mounted with a stainless-steel wire in prewarmed DMEM/F-12 + P/S in a cavity of a 24-well plate and analyzed with an inverted, camera-connected microscope (Axio Observer 5, Axiocam 503 mono, Carl Zeiss Microscopy GmbH, Jena, Germany). Each PCLS was then examined for various factors to ensure adequate airway quality and viability. The following factors were necessary for this purpose: an intact muscular layer, the occurrence of ciliary beating and the ability to contract following an ACh stimulus. The PCLS were then placed back

Table 1
a) Basic information about the experimental design and required concentrations of the continuous measurement setup. b) Basic information about the experimental design and required concentrations of the discontinuous measurement setup.

a)

	Basal activity		Basal activity + Reactivator		Residual activity		Restored activity	
Reagents	concentration	incubation time [min]	concentration	incubation time [min]	concentration	incubation time [min]	concentration	incubation time [min]
Eto [mmol/L]	0.02	10	0.02	10	0.02	10	0.02	10
DTNB [mmol/L]	0.40		0.40		0.40		0.40	
OPNA [μmol/L]	-	-	-	-	1.00	30	1.00	
PTE [mg/ml]	-	-	-	-	-		0.48	5
Oxime [μmol/L]	-	-	30.00	30	-		30.00	30
ATCh [mmol/L]	0.56	30	0.56		0.56		0.56	

b)

	Basal activity		Basal activity + Reactivator		Residual activity		Restored activity	
Reagents	concentration	incubation time [min]	concentration	incubation time [min]	concentration	incubation time [min]	concentration	incubation time [min]
Eto [mmol/L]	0.02	30	0.02	10	0.02	10	0.02	10
VX [μmol/L]	-	-	-	-	1.00	30	1.00	
PTE [mg/ml]	-	-	-	-	-	-	0.48	5
NOX-6 [μmol/L]	-	-	100.00	30	-	-	100.00	30
5 x washing steps with prewarmed DMEM/F-12 + P/S								
DTNB [mmol/L]	0.40	10	0.40	10	0.40	10	0.40	10
ATCh [mmol/L]	0.56	3	0.56	3	0.56	3	0.56	3

For all experiments the (i) basal activity, the (ii) basal activity + reactivator, the (iii) residual activity after organophosphorus nerve agent (OPNA) exposure and the (iv) restored activities after OPNA exposure + reactivator treatment were measured at 37 °C / 436 nm. Four PCLS were used for each measurement and the total volume of the reagent mixtures was 1280 μl for each experiment. a) The effect of the established reactivators HI-6 and obidoxime (OBI) was measured continuously after exposure to VX, sarin (GB) or cyclosarin (GF). Ethopropazine (Eto), 5,5′-dithiobis(2-nitrobenzoic acid) (DTNB) and acetylthiocholine (ATCh) were used in all measurements. Depending on the requirements, different reagents (OPNAs and oximes) were added additionally. The required final composition and the incubation periods can be found in the table. If a reagent was not added to the measurement setup this is marked by a dash. b) The effect of non-oxime 6 (NOX-6) was measured discontinuously using VX-inhibited PCLS. Five washing steps were performed between the first incubation period with Eto, VX, phosphotriesterase C23AL (PTE), NOX-6 and the second incubation period previously to the addition of DTNB. Eto, DTNB and ATCh were used in all measurements. Depending on the requirements, different reagents (VX or NOX-6) were added additionally. The required final composition and the incubation periods can be found in the table. If a reagent was not added to the measurement setup this is marked by a dash.

into the incubator (37 °C, 5% CO_2) to equilibrate for one hour before starting the actual experiment. The Zen Pro Software (Version 3.4.91, Carl Zeiss Microscopy GmbH) was used to calculate the initial airway area (IAA), which was set as 100%. For this purpose, the software determined the enclosed space, after we outlined the airway walls. Since the enclosed space doesn't show any cellular structures the outlining of the airway could be done very precise. Then the PCLS were exposed to GB or GF (final concentration 1 µmol/L), ACh (final concentration 0.5 µmol/L), the PTE (final conc. 0.048 mg/mL) and OBI (final concentration 30 µmol/L) in intervals of five minutes. Changes in the AA were observed for 30 min after treatment with OBI. In total, 14 images were taken throughout the whole experiment to document the AA changes from onset to end of experiment (Fig. 3 *a*). The IAA was compared to the AA of the contracted airways as well as to the re-opened ones.

Measurements in a discontinuous setup with five additional washing steps were performed for NOX-6, too (Fig. 3 *b*). Since flushing induced pressure changes, the results were invalidated, because washing led to a provoked reopening of the airways even without the use of a reactivator. Therefore, the effect on the airways of NOX-6 after OPNA exposure could not be observed.

2.6. Data analysis

All data are presented as means ± standard error of the mean (SEM). Statistical analyses were performed using GraphPad Prism Version 5.04 (GraphPad Software, San Diego, CA). Statistics were determined by one-way analysis of variance (ANOVA) followed by a Tukey's multiple comparison test or an unpaired two-tailed standard t-test. Detailed animal numbers (*n*) used for each experiment can be found in the figure legends. $p < 0.05$ was considered being statistically significant.

3. Results

3.1. AChE activity

AChE activity was determined by a modified Ellman assay (Worek et al. 2012). Inhibition and reactivation rates were calculated in relation to the basal activity. Exposure of PCLS to three different OPNAs caused an almost complete inhibition of the AChE. The residual AChE activity in PCLS after exposure to VX was 11.9 ± 2.1%, 11.0 ± 1.2% after GB and 11.7 ± 1.4% after GF (mean ± SEM, Fig. 4 *a*). Reactivation data for the established reactivators showed significant higher AChE activities with HI-6 and OBI compared to OPNA exposure alone for VX (VX + HI-6 50.7 ± 1.2%, VX + OBI 70.7 ± 2.5%) and GB (GB + HI-6 64.4 ± 0.7%, GB + OBI 83.0 ± 6.5%). For GF, however, (GF + HI-6 15.4 ± 2.7%, GF + OBI 12.01 ± 2.4%) no significant reactivation could be observed for OBI and HI-6 (Fig. 4 *a*).

Reactivation data for the experimental non-oxime reactivator NOX-6 for VX-inhibited PCLS showed a significantly higher AChE activity (53.3 ± 3.7%) compared to the AChE activity after VX 17.3 ± 4.0% suggesting substantial reactivation in lung tissue (Fig. 4 *b*). NOX-6 and VX were selected based on prior findings of human in vitro experiments from de Koning et al., where this combination demonstrated the most promising results for AChE reactivation compared to GB/GF/PXE (de Koning et al. 2018).

3.2. Airway responsiveness

Changes of AA were assessed and calculated after the different treatment options (Fig. 5 *a*). A stimulation with ACh and GB (13.4 ± 4.0%) or GF (13.2 ± 4.0%) without OBI treatment led to an irreversible decrease of the AA (Fig. 5 *a*). No visual changes could be observed for GF + OBI treated airways (Fig. 6, *green line*). After the addition of OBI to the GB-exposed airways, dilation was observed immediately (Fig. 6, *blue line*). The therapeutic efficacy of OBI treatment was superior in GB-exposed PCLS compared to GF-exposed PCLS. By the

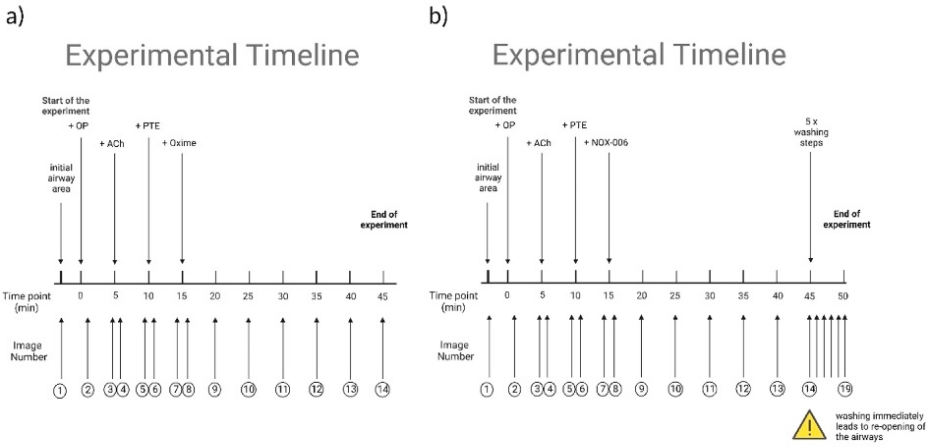

Fig. 3. Experimental timeline of the measurement of the airway responsiveness without washing (a) and with additional washing steps (b). One PCLS per well is weighted with a steel wire in a 24-well plate and placed under an inverted, camera-connected microscope. The airways were identified and tested for their ability to contract after an acetylcholine (ACh) stimulus. Afterwards the PCLS were then stored in the incubator at 37 °C for another hour to return to their original state. The initial airway area (IAA) was photographed before the experiment. Then the PCLS were poisoned with sarin (GB) (a) / cyclosarin (GF) (a) / VX (b) (all 1 µM). After 5 min of incubation ACh (0,5 µM) was added and after another 5 min PTE A203L (PTE) (0,48 mg/mL) was added to scavenge the free nerve agents. 5 min later obidoxime (OBI) (30 µM) (a) / non-oxime (NOX-6) (100 µM) (b) was added. Changes in the airway area (AA) were documented by 14 snapshots (a). Five additional washing steps were conducted afterwards when NOX-6 was used (b). Snapshots were made for 5 more minutes. Thus, changes in the AA were documented by 19 snapshots (b). Due to the sensitivity of the airways to pressure changes approach b) was not feasible. The airways opened immediately during the washing process. Since washing steps would have been required to measure the effect of NOX-6 on the airways, it was not possible to make a statement about its possible airway reopening properties. The washing steps would have been required due to NOX-6 high intrinsic inhibitory potency. (Figure made in BioRender.com).

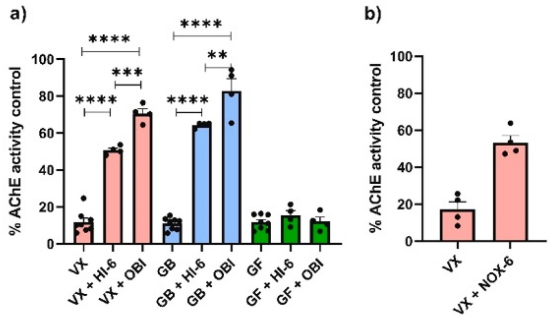

Fig. 4. Acetylcholinesterase (AChE) activity in intact PCLS after exposure to organophosphorus nerve agents (OPNAs) and after administration of established and experimental reactivators. PCLS were exposed to VX, sarin (GB), cyclosarin (GF) (all 1 µmol/L) for rapid AChE inhibition. Phosphotriesterase C23AL (PTE) was then added to facilitate cleavage of the respective excess AChE inhibitor. Subsequently, HI-6 or obidoxime (OBI) (both 30 µmol/L) were added to mimic oxime treatment and the AChE activity changes were measured continuously (for experimental setup see Table 1 a). Statistical comparisons were performed by using the one-way analysis of variance (ANOVA) followed by a Tukey's multiple comparison test (a). Data are presented as mean ± SEM n = 12 – 24 PCLS from 4 – 8 animals. Asterisks indicate significant differences to the control (****$p < 0.0001$, ***$p < 0.0003$, **$p < 0.0047$). AChE activity of PCLS which were exposed to VX (1 µmol/L), cleaved by PTE, and then exposed to the potential medical countermeasure non-oxime (NOX-6) (100 µmol/L), an experimental non-oxime reactivator, were observed for 3 min after a 30 min incubation time followed by five washing steps (experimental setup see Table 1 b). Statistical comparisons were performed by using two-tailed standard t-test (b). Data are presented as mean ± SEM n = 16 - 20 PCLS from 4 animals. Asterisks indicate significant differences to the control (***$p < 0.0006$).

end of the experiment the AA increased up to 73.6 ± 6.5% after GB + OBI treatment, whereas no increase of the AA was observed in the GF + OBI group (11.3 ± 2.8%) (Fig. 5 *a*). Exemplarily snapshots of the AA changes can be seen in Fig. 5 *b*.

3.3. Comparison of AChE reactivation vs. airway reopening

A comparison of the AChE activity with the airway response showed comparable results (Fig. 4 vs 5). There was no significant difference regarding both parameters in the slopes after a 30 min treatment with OBI subsequently to OPNA exposure (Fig. 7). The feasibility to reactivate VX- and GB-inhibited AChE was higher than for GF-inhibited AChE (Fig. 4).

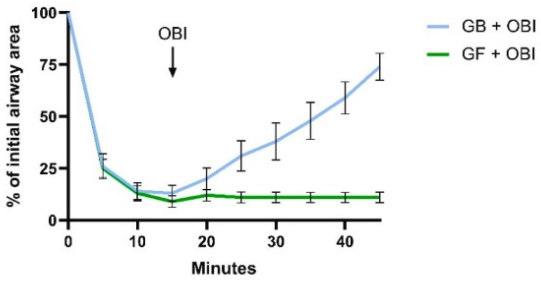

Fig. 6. Airway responsiveness after treatment with obidoxime. PCLS were exposed to sarin (GB) or cyclosarin (GF) (both 1 µmol/L), 5 min later acetylcholine (ACh) (0.5 µmol/L) was applied, another 5 min later phosphotriesterase C23AL (PTE) (0.048 mg/mL) was added to scavenge free organophosphorus nerve agents (OPNAs). After five more minutes obidoxime (OBI) (30 µmol/L) was administered. Airway area alterations were observed for 45 min in total, whereas the therapeutic time frame after addition of OBI amounted to 30 min. Data are presented as mean + SEM n = 3–4 airways from 4–5 different animals.

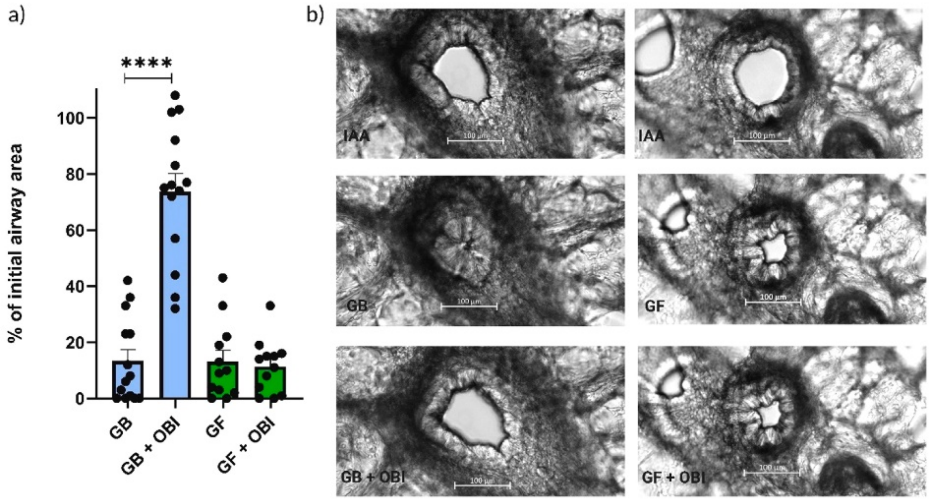

Fig. 5. Effect of therapeutically relevant oxime concentrations on airway areas. The initial airway area (IAA) was photographed before any exposure and was set as 100%. Then PCLS were exposed to either sarin (GB) or cyclosarin (GF) (both 1 µmol/L), acetylcholine (ACh) (0.5 µmol/L), PTE C23AL (PTE) (0.048 mg/mL) and to obidoxime (OBI) (30 µmol/L) (See Fig. 6 for further information). Airway area (AA) changes were then measured with a video microscopic setup for 45 min - in total 14 images were taken (Fig. 3). Data were compared via the unpaired two-tailed standard t-test (a). Data are given as mean ± SEM n = 3 - 4 airways from at least 4 - 5 different animals. (****$p < 0.0001$). Representative images of airways, for initial airway area (IAA), after exposure to GB or GF and with subsequent OBI administration are shown in (b). The white scale displays 100 µm.

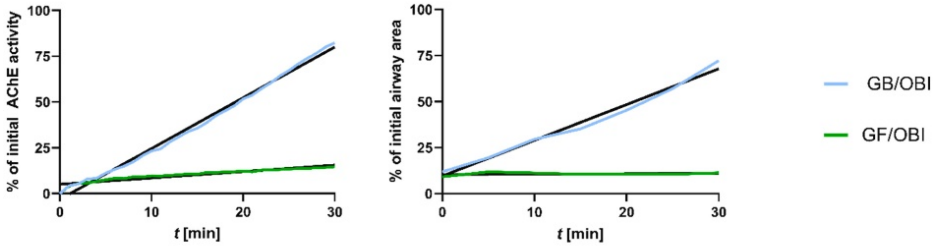

Fig. 7. Comparison of the slopes of the acetylcholinesterase (AChE) reactivation vs. the airway reopening during a 30 min time frame. Treatment with obidoxime (OBI) (30 μmol/L) after exposure to sarin (GB) or cyclosarin (GF) (both 1 μmol/L). Data were compared via the unpaired two-tailed standard t-test. Slopes were determined with simple linear regression. Slope of % of AChE activity: GB/OBI = 2.8, GF/OBI = 0.3. Slope % of initial airway area: GB/OBI = 1.9, GF/OBI = 0.

4. Discussion

To expand the options for assessing potential AChE reactivators after OPNA poisoning, more reliable and faster test systems are needed. For this reason, PCLS as an ex vivo model were used in this study. Here, insights into AChE activity changes and the airway responsivity after exposure to OPNAs and subsequent reactivator administration are provided. To determine the AChE activity in intact PCLS, a modified Ellman assay was applied. To the best of our knowledge, an experimental setup analyzing AChE activity in intact PCLS has not been published before. Reactivator properties are mostly evaluated by using AChE isolated from erythrocytes (Worek et al. 1999; Worek et al. 2016). Alternatively, some in vivo studies used rat lung tissue homogenate (Peng et al. 2014; Wang et al. 2016; Wigenstam et al. 2022) and found that the AChE activity was strongly diminished after OPNA exposure. Yet, these studies do not allow conclusions on the functional level. The use of PCLS overcomes this drawback as next to the AChE activity (molecular level), AA changes (functional level) can be analyzed as well.

In line with the above cited publications, we measured a significant decrease in AChE activity in viable PCLS after exposure to VX, GB, or GF (Fig. 4). Depending on the OPNA reactivator properties, changes in the AChE activity levels were observed after administration of therapeutic reactivator concentrations mimicking treatment in the clinic. OBI reactivated VX- and GB-inhibited AChE in PCLS best, while reactivation with HI-6 seemed to be comparable to the reactivation potency of OBI, even though it was slightly less effective. Wigenstam et al. measured a lower AChE reactivation rate of PCLS homogenate after exposure to VX and treatment with HI-6 (Wigenstam et al. 2022). One possible reason for those results could be the presence of residual VX in the environment which could have re-inhibited the AChE. The reactivation results of the present study were in line with those previously published, except for the negligible influence of HI-6 on GF-inhibited AChE in intact PCLS (Worek et al. 2002). The fact that GF-inhibited AChE can only be poorly reactivated by the currently available reactivators is well known, but a more increased reactivation rate would have been expected since in vitro data evidenced a higher reactivation capability for HI-6 in rat and human erythrocyte AChE (Worek et al. 2002). GF exerts a strong inhibitory activity (Worek et al. 2004) which might be one reason for the results in the current study. Possible species-specific differences should be noted, too, just as the way the AChE is present (Worek et al. 2002). Potential differences might be because the AChE activity investigated here was assessed in a whole organ model with intact lung structure instead of being isolated from the membranes of erythrocytes. The fact that HI-6 is slightly more beneficial than OBI was expected and there seemed to be a non-significant tendency here for higher reactivation with HI-6 compared to OBI as well (Fig. 4). The experimental non-oxime reactivator NOX-6 was tested after exposure to VX, too. It was chosen since it is a promising new reactivator with a structure based on ADOC (4-amino-2((diethylamino)methyl)phenol) and due to its different structural properties (no oxime substituent, a hydroxyl group, and an amino group in para position of it and a pyrrolidine group) compared to the well-known oximes. Yet, it needs to be pointed out that its high intrinsic AChE inhibition (de Koning et al. 2018) hampers a continuous test setup like the one used for OBI and HI-6. For this reason, the experimental setup had to be adjusted and five washing steps were included to wash out the reactivator (Table 1 *b)*. The AChE reactivation observations were in line with previously published results pertaining to human-AChE isolated from erythrocytes as well (de Koning et al. 2018; Horn et al. 2018).

Initially, the effects of reactivators on airway contraction were analyzed in a similar fashion to the AChE enzyme activity measurements, including five wash steps (Fig. 3 *b*). However, flushing-associated pressure changes resulted in an increase in the AA (> 100%) in the absence of AChE reactivators. Thus, flushes were discontinued, and continuous video microscopic measurements (Fig. 3 *a*) were used to investigate the ability of airways to dilate after GF and GB exposure and OBI treatment (Fig. 6). This way, dilation effects of the reactivators could be shown. The results after exposure to GF and GB with respective OBI treatment showed a correlation between AChE activity analyzed by a modified Ellman assay and airway area as a surrogate readout for bronchoconstriction (Fig. 7). Therefore, reactivators might not only support the reactivation of AChE by first forming a Michaelis-type-oxime-phosphyl-AChE-conjugate and then removing the phosphyl moiety by the formation of a phosphyloxime but also indirectly via counteracting the bronchoconstriction, thus addressing both, nicotinic and muscarinic signaling. This highlights additional benefits of reactivators after OPNA or OP pesticide exposure. Hitherto muscarinic antagonists like atropine and scopolamine are mostly used to counteract bronchoconstriction and other muscarinic signs (Eddleston et al. 2008; Robenshtok et al. 2002). Unfortunately, antimuscarinics may lead to unwanted side effects like tachycardia, intestinal atony, and pyrexia (Steindl et al. 2021; Moffatt et al. 2010; Aurbek et al. 2006; Thiermann et al. 2011). Thus, it would be desirable to use atropine doses that are as low as reasonably possible (Bloch-Shilderman et al. 2019; Wigenstam et al. 2021). An advantage of reactivators over muscarinic antagonists, which only competitively antagonize ACh, is the possibility to enable the degradation of ACh implying that the reactivators act further upstream. This might lead to shorter artificial ventilation times and fewer ventilator-associated complications. Herbert et al. have demonstrated the beneficial use of a combination of the beta-2-agonists formoterol or salbutamol with atropine (Herbert et al. 2019). Wigenstam et al. have underlined those findings and furthermore recommended the use of the potassium channel-opening vasodilator cromakalim and magnesium sulfate with atropine to reduce the atropine dose (Wigenstam et al. 2022). The results of those studies may help to prevent unintended adverse effects from atropine therapy, by reducing its dose. Mitra et al. could not show a significant decrease in the amount of atropine needed by using magnesium sulfate in combination with *N*-acetylcysteine (Mitra et al. 2023). With our work, a new platform to test those different approaches is given and experimental data regarding the beneficial effects

of different reactivators, even without the use of atropine, is provided. More research with human PCLS (hPCLS) is necessary to ascertain any potential non-conformance for this model regarding species-specific differences. With respect to species-specific variations regarding anatomical, physiological and pharmacological differences between humans and rodents extrapolation of those findings would require careful consideration (Bonniaud et al. 2018). Information about isolated AChE (Clement and Erhardt, 1994) or enzymes of the CYP family (Yilmaz et al. 2019), and airway area alterations (Seehase et al. 2011), already point to possible species differences. Therefore, it would be valuable to determine if the correlation between AChE activity changes and AA changes in hPCLS are as high as determined in this study, too. Additionally, the use of hPCLS would be beneficial according to the 3 R principles.

5. Conclusion

Analysis of AChE activity in intact PCLS is a new method that will help to identify promising reactivators early and to understand mechanistic interactions. The correlation of AChE activity and the airway response indicates that - next to antimuscarinic drugs - reactivators may play a role in the treatment of life-threatening airway constriction after OPNA exposure.

Funding

This work was supported from the German Research Foundation (GRK 2338, Targets in Toxicology); project P02 (to T.W. and F.W.); F.G. received a PhD stipend in the GRK 2338.

CRediT authorship contribution statement

Gölitz Fee: Formal analysis, Investigation, Visualization, Writing – original draft, Methodology. **Herbert Julia:** Investigation, Writing – review & editing. **Worek Franz:** Conceptualization, Funding acquisition, Project administration, Validation, Writing – review & editing. **Wille Timo:** Conceptualization, Funding acquisition, Project administration, Supervision, Writing – review & editing.

Declaration of Competing Interest

The authors declare that they have no known competing financial interests or personal relationships that could have appeared to influence the work reported in this paper.

Data availability

Data will be made available on request.

Appendix A. Supporting information

Supplementary data associated with this article can be found in the online version at doi:10.1016/j.toxlet.2023.12.014.

References

Amend, Niko, Niessen, Karin V., Seeger, Thomas, Wille, Timo, Worek, Franz, Thiermann, Horst, 2020. Diagnostics and treatment of nerve agent poisoning-current status and future developments (S). Ann. N. Y. Acad. Sci. 1479 (1), 13–28. https://doi.org/10.1111/nyas.14336.

Aurbek, N., Thiermann, H., Szinicz, L., Eyer, P., Worek, F., 2006. Analysis of inhibition, reactivation and aging kinetics of highly toxic organophosphorus compounds with human and pig acetylcholinesterase (S). Toxicology 224 (1-2), 91–99. https://doi.org/10.1016/j.tox.2006.04.030.

Baba, Naseer Ahmad, Raina, Rajinder, Verma, Pawan Kumar, Sultana, Mudasir, 2014. Alterations in plasma and tissue acetylcholinesterase activity following repeated oral exposure of chlorpyrifos alone and in conjunction with fluoride in wistar rats (S.). Proc. Natl. Acad. Sci., India, Sect. B Biol. Sci. 84 (4), 969–972. https://doi.org/10.1007/s40011-013-0286-3.

Bloch-Shilderman, E., Yacov, G., Cohen, I., Egoz, I., Gutman, H., Gez, R., et al., 2019. Repetitive antidotal treatment is crucial in eliminating eye pathology, respiratory toxicity and death following whole-body VX vapor exposure in freely moving rats (S.). Arch. Toxicol. 93 (5), 1365–1384. https://doi.org/10.1007/s00204-019-02401-0.

Bonniaud, Philippe, Fabre, Aurélie, Frossard, Nelly, Guignabert, Christophe, Inman, Mark, Kuebler, Wolfgang M., et al., 2018. Optimising experimental research in respiratory diseases: an ERS statement. Eur. Respir. J. 51 (5) https://doi.org/10.1183/13993003.02133-2017.

Cherny, Izhack, Greisen, Per, Ashani, Yacov, Khare, Sagar D., Oberdorfer, Gustav, Leader, Haim, et al., 2013. Engineering V-type nerve agents detoxifying enzymes using computationally focused libraries (S.). : *ACS Chem. Biol.* 8 (11), 2394–2403. https://doi.org/10.1021/cb4004892.

Ciottone, M.D., Gregory, R., 2018. Toxidrome recognition in chemical-weapons attacks (S.). N. Engl. J. Med. 378 (17), 1611–1620. https://doi.org/10.1056/NEJMra1705224.

Clement, John G., Erhardt, Nancy, 1994. In vitro oxime-induced reactivation of various molecular forms of soman-inhibited acetylcholinesterase in striated muscle from rat, monkey and human. Arch. Toxicol. 68, 648–655 (S.).

Costanzi, Stefano, Machado, John-Hanson, Mitchell, Moriah, 2018. Nerve agents: what they are, how they work, how to counter them (S.). ACS Chem. Neurosci. 9 (5), 873–885. https://doi.org/10.1021/acschemneuro.8b00148.

Dolgin, Elie, 2013. Syrian gas attack reinforces need for better anti-sarin drugs (S.). Nat. Med. 19 (10), 1194–1195. https://doi.org/10.1038/nm1013-1194.

Eddleston, Michael, 2022. CON: oximes should not be used routinely in organophosphorus insecticide poisoning (S.). Br. J. Clin. Pharmacol. 88 (12), 5070–5073. https://doi.org/10.1111/bcp.15217.

Eddleston, Michael, Buckley, Nick A., Eyer, Peter, Dawson, Andrew H., 2008. Management of acute organophosphorus pesticide poisoning (S.). Lancet 371 (9612), 597–607. https://doi.org/10.1016/S0140-6736(07)61202-1.

Ellman, G.L., Courtney, K.D., Andres, V., Feather-Stone, R.M., 1961. A new and rapid colorimetric determination of acetylcholinesterase activity (S.). Biochem. Pharmacol. 7, 88–95. https://doi.org/10.1016/0006-2952(61)90145-9.

Grob, David, 1956. The manifestations and treatment of poisoning due to nerve gas and other organic phosphate anticholinesterase compounds. A. M. A. Arch. Intern. Med. 98, 221–239 (S.).

Herbert, Julia, Thiermann, Horst, Worek, Franz, Wille, Timo, 2017. Precision cut lung slices as test system for candidate therapeutics in organophosphate poisoning (S.). Toxicology 389, 94–100. https://doi.org/10.1016/j.tox.2017.07.011.

Herbert, Julia, Thiermann, Horst, Worek, Franz, Wille, Timo, 2019. COPD and asthma therapeutics for supportive treatment in organophosphate poisoning (S.). Clin. Toxicol. 57 (7), 644–651. https://doi.org/10.1080/15563650.2018.1540785.

Herbert, Julia, Laskin, Debra L., Gow, Andrew J., Laskin, Jeffrey D., 2020. Chemical warfare agent research in precision-cut tissue slices-a useful alternative approach (S.). Ann. N. Y. Acad. Sci. 1480 (1), 44–53. https://doi.org/10.1111/nyas.14459.

Holmstedt, Bo, 1959. Pharmacology of organophosphorus cholinesterase inhibitors. Pharmacol. Rev. 11, 567–688.

Horn, Gabriele, de Koning, Martijn Constantijn, Thiermann, Horst, van Grol, Marco, Worek, Franz, 2018. Interactions between acetylcholinesterase, toxic organophosphorus compounds and a short series of structurally related non-oxime reactivators: analysis of reactivation and inhibition kinetics in vitro (S.). Toxicol. Lett. 299, 218–225. https://doi.org/10.1016/j.toxlet.2018.10.004.

King, Andrew M., Aaron, Cynthia K., 2015. Organophosphate and carbamate poisoning (S.). Emerg. Med. Clin. North Am. 33 (1), 133–151. https://doi.org/10.1016/j.emc.2014.09.010.

de Koning, Martijn Constantijn, Horn, Gabriele, Worek, Franz, van Grol, Marco, 2018. Discovery of a potent non-oxime reactivator of nerve agent inhibited human acetylcholinesterase (S.). Eur. J. Med. Chem. 157, 151–160. https://doi.org/10.1016/j.ejmech.2018.08.016.

Lee, Ernest C., 2003. Clinical manifestations of sarin nerve gas exposure (S.). JAMA 290 (5), 659–662. https://doi.org/10.1001/jama.290.5.659.

Liu, Guanghui, Betts, Catherine, Cunoosamy, Danen M., Åberg, Per M., Hornberg, Jorrit J., Sivars, Kinga Balogh, Cohen, Taylor S., 2019. Use of precision cut lung slices as a translational model for the study of lung biology (S.). Respir. Res. 20 (1), 162. https://doi.org/10.1186/s12931-019-1131-x.

Martin, C., Uhlig, S., Ullrich, V., 1996. Videomicroscopy of methacholine-induced contraction of individual airways in precision-cut lung slices (S.). Eur. Respir. J. 9 (12), 2479–2487. https://doi.org/10.1183/09031936.96.09122479.

Masson, Patrick, 2011. Evolution of and perspectives on therapeutic approaches to nerve agent poisoning (S.). Toxicol. Lett. 206 (1), 5–13. https://doi.org/10.1016/j.toxlet.2011.04.006.

Mitra, Jayanta Kumar, Hansda, Upendra, Bandyopadhyay, Debapriya, Sarkar, Satyaki, Sahoo, Joshna, 2023. The role of a combination of N-acetylcysteine and magnesium sulfate as adjuvants to standard therapy in acute organophosphate poisoning: a randomized controlled trial. Heliyon 9 (4), e15376. https://doi.org/10.1016/j.heliyon.2023.e15376.

Moffatt, Alison, Mohammed, Fahim, Eddleston, Michael, Azher, Shifa, Eyer, Peter, Buckley, Nick A., 2010. Hypothermia and fever after organophosphorus poisoning in humans–a prospective case series (S.). J. Med. Toxicol.: Off. J. Am. Coll. Med. Toxicol. 6 (4), 379–385. https://doi.org/10.1007/s13181-010-0012-y.

Neuhaus, Vanessa, Schaudien, Dirk, Golovina, Tatiana, Temann, Ulla-Angela, Thompson, Carolann, Lippmann, Torsten, et al., 2017. Assessment of long-term cultivated human precision-cut lung slices as an ex vivo system for evaluation of chronic cytotoxicity and functionality (S.). J. Occup. Med. Toxicol. 12, 13. https://doi.org/10.1186/s12995-017-0158-5.

Newmark, Jonathan, 2004. Therapy for nerve agent poisoning (S.). Arch. Neurol. 61 (5), 649–652. https://doi.org/10.1001/archneur.61.5.649.
Peng, Xinqi, Perkins, Michael W., Simons, Jannitt, Witriol, Alicia M., Rodriguez, Ashley M., Benjamin, Brittany M., et al., 2014. Acute pulmonary toxicity following inhalation exposure to aerosolized VX in anesthetized rats (S.). Inhal. Toxicol. 26 (7), 371–379. https://doi.org/10.3109/08958378.2014.899410.
Robenshtok, E., Luria, S., Tashma, Z., Hourvitz, A., 2002. Adverse reaction to atropine and the treatment of organophosphate intoxication. Isr. Med Assoc. J. 4, 535–539 (S.).
Russell, W.M.S., Burch, R.L., 1960. The principles of humane experimental technique (S.). Med. J. Aust. 1 (13), 500. https://doi.org/10.5694/j.1326-5377.1960.tb73127.x.
Seehase, S., Schlepütz, M., Switalla, S., Mätz-Rensing, K., Kaup, F.J., Zöller, M., et al., 2011. Bronchoconstriction in nonhuman primates: a species comparison (S.). J. Appl. Physiol. 111 (3), 791–798. https://doi.org/10.1152/japplphysiol.00162.2011.
Steindl, David, Boehmerle, Wolfgang, Körner, Roland, Praeger, Damaris, Haug, Marcel, Nee, Jens, et al., 2021. Novichok nerve agent poisoning (S.). Lancet 397 (10270), 249–252. https://doi.org/10.1016/S0140-6736(20)32644-1.
Thiermann, Horst, Worek, Franz, 2022. Pro: Oximes should be used routinely in organophosphate poisoning (S.). Br. J. Clin. Pharmacol. 88 (12), 5064–5069. https://doi.org/10.1111/bcp.15215.
Thiermann, Horst, Steinritz, Dirk, Worek, Franz, Radtke, Maria, Eyer, Peter, Eyer, Florian, et al., 2011. Atropine maintenance dosage in patients with severe organophosphate pesticide poisoning (S.). Toxicol. Lett. 206 (1), 77–83. https://doi.org/10.1016/j.toxlet.2011.07.006.
Tigges, Jonas, Eggerbauer, Florian, Worek, Franz, Thiermann, Horst, Rauen, Ursula, Wille, Timo, 2021. Optimization of long-term cold storage of rat precision-cut lung slices with a tissue preservation solution. Am. J. Physiol. Lung Cell. Mol. Physiol. 321 (6), L1023–L1035. https://doi.org/10.1152/ajplung.00076.2021.
Tigges, Jonas, Worek, Franz, Thiermann, Horst, Wille, Timo, 2022. Organophosphorus pesticides exhibit compound specific effects in rat precision-cut lung slices (PCLS): mechanisms involved in airway response, cytotoxicity, inflammatory activation and antioxidative defense (S.). Arch. Toxicol. 96 (1), 321–334. https://doi.org/10.1007/s00204-021-03186-x.
Vale, J.Allister, Marrs, Timothy C., Maynard, Robert L., 2018. Novichok: a murderous nerve agent attack in the UK (S.). Clin. Toxicol. 56 (11), 1093–1097. https://doi.org/10.1080/15563650.2018.1469759.
Wang, J., Yu, X.F., Zhao, J.J., Shi, S.M., Fu, L., Sui, D.Y., 2016. Ginsenoside Rg3 attenuated omethoate-induced lung injury in rats (S.). Hum. Exp. Toxicol. 35 (6), 677–684. https://doi.org/10.1177/0960327115597984.
Wigenstam, E., Forsberg, E., Bucht, A., Thors, L., 2021. Efficacy of atropine and scopolamine on airway contractions following exposure to the nerve agent VX (S.). Toxicol. Appl. Pharmacol. 419, 115512. https://doi.org/10.1016/j.taap.2021.115512.
Wigenstam, Elisabeth, Artursson, Elisabet, Bucht, Anders, Thors, Lina, 2022. Supplemental treatment to atropine improves the efficacy to reverse nerve agent induced bronchoconstriction (S. Chem. -Biol. Interact. 364, 110061 https://doi.org/10.1016/j.cbi.2022.110061.
Worek, F., Mast, U., Kiderlen, D., Diepold, C., Eyer, P., 1999. Improved determination of acetylcholinesterase activity in human whole blood (S.). Clin. Chim. Acta; Int. J. Clin. Chem. 288 (1-2), 73–90. https://doi.org/10.1016/s0009-8981(99)00144-8.
Worek, F., Reiter, G., Eyer, P., Szinicz, L., 2002. Reactivation kinetics of acetylcholinesterase from different species inhibited by highly toxic organophosphates (S.). Arch. Toxicol. 76 (9), 523–529. https://doi.org/10.1007/s00204-002-0375-1.
Worek, Franz, Thiermann, Horst, 2013. The value of novel oximes for treatment of poisoning by organophosphorus compounds (S.). Pharmacol. Ther. 139 (2), 249–259. https://doi.org/10.1016/j.pharmthera.2013.04.009.
Worek, Franz, Thiermann, Horst, Szinicz, Ladislaus, Eyer, Peter, 2004. Kinetic analysis of interactions between human acetylcholinesterase, structurally different organophosphorus compounds and oximes (S.). Biochem. Pharmacol. 68 (11), 2237–2248. https://doi.org/10.1016/j.bcp.2004.07.038.
Worek, Franz, Eyer, Peter, Thiermann, Horst, 2012. Determination of acetylcholinesterase activity by the Ellman assay: a versatile tool for in vitro research on medical countermeasures against organophosphate poisoning (S.). Drug Test. Anal. 4 (3-4), 282–291. https://doi.org/10.1002/dta.337.
Worek, Franz, Seeger, Thomas, Reiter, Georg, Goldsmith, Moshe, Ashani, Yacov, Leader, Haim, et al., 2014. Post-exposure treatment of VX poisoned guinea pigs with the engineered phosphotriesterase mutant C23: a proof-of-concept study (S.). Toxicol. Lett. 231 (1), 45–54. https://doi.org/10.1016/j.toxlet.2014.09.003.
Worek, Franz, Koller, Marianne, Thiermann, Horst, Wille, Timo, 2016. Reactivation of nerve agent-inhibited human acetylcholinesterase by obidoxime, HI-6 and obidoxime+HI-6: Kinetic in vitro study with simulated nerve agent toxicokinetics and oxime pharmacokinetics (S.). Toxicology 350-352, 25–30. https://doi.org/10.1016/j.tox.2016.05.001.
Worek, Franz, Thiermann, Horst, Wille, Timo, 2020. Organophosphorus compounds and oximes: a critical review (S.). Arch. Toxicol. 94 (7), 2275–2292. https://doi.org/10.1007/s00204-020-02797-0.
Yilmaz, Yildiz, Williams, Gareth, Walles, Markus, Manevski, Nenad, Krähenbühl, Stephan, Camenisch, Gian, 2019. Comparison of rat and human pulmonary metabolism using precision-cut lung slices (PCLS) (S.). Drug Metab. Lett. 13 (1), 53–63. https://doi.org/10.2174/1872312812666181022114622.

Supplementary Information Publication I:

Tyrode buffer composition:

1.8 mmol/L $CaCl_2 \cdot 2 H_2O$ (Carl Roth, Karlsruhe, Germany), 5.5 mmol/L glucose monohydrate (Merck KGaA), 2.7 mmol/L KCl (Carl Roth), 1.1 mmol/L $MgCl_2 \cdot 6 H_2O$ (Sigma-Aldrich), 137.0 mmol/L NaCl (Carl Roth), 22.0 mmol/L $NaHCO_3$ (Carl Roth) and 0.4 mmol/L $NaH_2PO_4 \cdot 2 H_2O$ (Merck KGaA) in double-distilled water. pH was adjusted to 7.4 by carbogen gassing

4. Publication II

Melo-Narvaez *et al. Respiratory Research* (2025) 26:57
https://doi.org/10.1186/s12931-025-03132-w

Respiratory Research

RESEARCH Open Access

Cold storage of human precision-cut lung slices in TiProtec preserves cellular composition and transcriptional responses and enables on-demand mechanistic studies

M. Camila Melo-Narvaez[1,2†], Fee Gölitz[3,4†], Eshita Jain[1], Janine Gote-Schniering[5,6], Mircea Gabriel Stoleriu[1,7], Wilhelm Bertrams[2], Bernd Schmeck[2,8,9,10,11,15], Ali Önder Yildirim[1,12], Ursula Rauen[13], Timo Wille[3,14*] and Mareike Lehmann[1,2,15*]

Abstract

Background Human precision-cut lung slices (hPCLS) are a unique platform for functional, mechanistic, and drug discovery studies in the field of respiratory research. However, tissue availability, generation, and cultivation time represent important challenges for their usage. Therefore, the present study evaluated the efficacy of a specifically designed tissue preservation solution, TiProtec, complete or in absence (-) of iron chelators, for long-term cold storage of hPCLS.

Methods hPCLS were generated from peritumor control tissues and stored in DMEM/F-12, TiProtec, or TiProtec (-) for up to 28 days. Viability, metabolic activity, and tissue structure were determined. Moreover, bulk-RNA sequencing was used to study transcriptional changes, regulated signaling pathways, and cellular composition after cold storage. Induction of cold storage-associated senescence was determined by transcriptomics and immunofluorescence (IF). Finally, cold-stored hPCLS were exposed to a fibrotic cocktail and early fibrotic changes were assessed by RT-qPCR and IF.

Results Here, we found that TiProtec preserves the viability, metabolic activity, transcriptional profile, as well as cellular composition of hPCLS for up to 14 days. Cold storage did not significantly induce cellular senescence in hPCLS. Moreover, TiProtec downregulated pathways associated with cell death, inflammation, and hypoxia while activating pathways protective against oxidative stress. Cold-stored hPCLS remained responsive to fibrotic stimuli and upregulated extracellular matrix-related genes such as fibronectin and collagen 1 as well as alpha-smooth muscle actin, a marker for myofibroblasts.

†M. Camila Melo-Narvaez and Fee Gölitz contributed equally to this work.

*Correspondence:
Timo Wille
timowille@bundeswehr.org
Mareike Lehmann
mareike.lehmann@uni-marburg.de

Full list of author information is available at the end of the article

Conclusions Optimized long-term cold storage of hPCLS preserves their viability, metabolic activity, transcriptional profile, and cellular composition for up to 14 days, specifically in TiProtec. Finally, our study demonstrated that cold-stored hPCLS can be used for on-demand mechanistic studies relevant for respiratory research.

Keywords Human precision-cut lung slices (hPCLS), 3R, Long-term cold storage, Tissue preservation, Fibrosis, Human lung models, TiProtec

Graphical Abstract

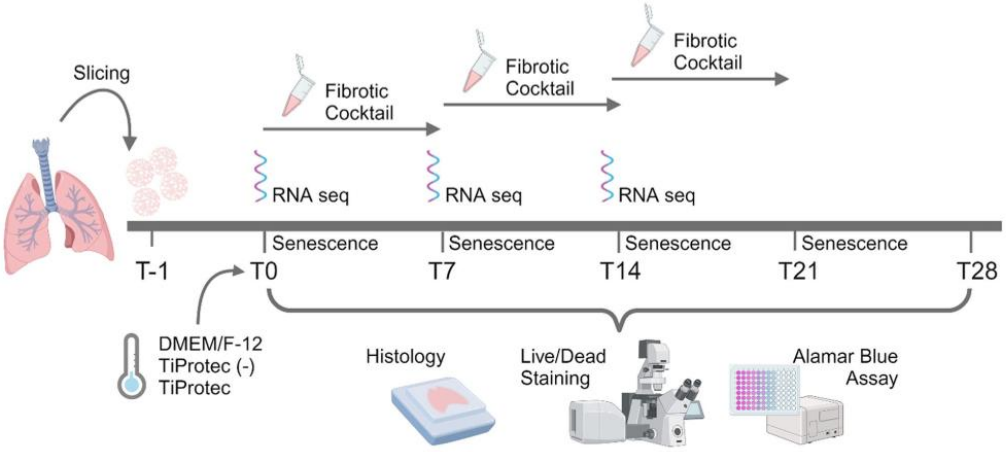

Background

Chronic lung diseases represent a significant health burden and are among the leading causes of morbidity and mortality worldwide [1]. Several models have been used in the past to study respiratory diseases and human derived ex vivo models such as Precision-Cut Lung Slices (PCLS) are versatile models for studying the underlying mechanisms [2–4], evaluating impact of novel therapeutics [5–7], and examining (toxic) environmental impacts on lungs [8–10]. Their importance in basic research and drug development lies in their ability to maintain the intact lung architecture, since resident cell types including epithelial, mesenchymal, and resident innate and adaptive immune cells as well as the extracellular matrix (ECM) are maintained in their native three-dimensional (3D) structure (11–13). Therefore, PCLS can be applied to study various endpoints, including viability, metabolic activity as well as ECM changes in response to a fibrotic stimulation [4, 14–16]. Notably, advanced microscopy technologies can be applied to study longitudinal and functional responses of PCLS [17–22] and recently, single-cell-RNA sequencing datasets obtained from PCLS have provided new insights into the mechanisms of the progression of fibrosis and pointed to possible new therapeutic targets [23, 24]. Furthermore, PCLS can be derived from various species like mice, rats, guinea pigs, sheep, and most importantly humans (hPCLS) [25]. hPCLS can be either generated from diseased or healthy lung tissue. In these cases, disease mechanisms and therapeutic options can be studied. Depending on the size of the lung, several hundred PCLS can be obtained from one lung. Therefore, the use of PCLS also supports the Replacement, Refinement, and Reduction (3R) of animals in relevant studies [26, 27]. Efforts to prolong the viability of PCLS and to optimize their usage have led to improved culture protocols [28–30]. Despite these improvements, there are still challenges with tissue waste and optimal utilization of PCLS because of time constraints and tissue availability [31]. Given the scarcity of human lung tissue samples and the even greater value of samples from diseased patients, an optimized storage protocol for processing large quantities of human PCLS is of high importance for lung research. For these reasons, several groups have developed alternative storage methods, including cryo- [32–34] and cold storage preservation [31]. For both methods, medium changes are not necessary, simplifying handling and shipping of PCLS. This facilitates transport of PCLS between collaborating laboratories, paving the way for setting up PCLS biobanks. Cryopreservation (at -60 to -80 °C), although promising [35], presents risks such as cell damage from ice crystal formation, loss of cell water, and possible degradation of the cell architecture during the freeze-thaw process [4, 36–38]. These risks might be minimized with

cryoprotectants like dimethyl sulfoxide (DMSO), which themselves exert disadvantages like cell membrane toxicity and/or oxidative damage [38, 39]. Cold storage preservation at 4 °C is a more "gentle" method, which we have put forward as a viable option using rat PCLS [31]. With a suitable PCLS storage approach, on-demand experiments using tissue from multiple donors could be conducted simultaneously, tissue sharing with other research groups lacking tissue access would be possible and it would also allow the storage of excess PCLS for future experiments and/or for the repetition of experiments in the case of technical problems in downstream assays. Lowering the storage temperature significantly reduces the metabolic activity of the cells, thereby decreasing the energy needed to maintain cellular functions [31], resulting in higher viability over a longer period of time. Additionally, storing PCLS at 4 °C simplifies transport and storage, as it eliminates the need for liquid nitrogen tanks needed for cryopreservation and significantly facilitates shipping since it eliminates the need for dry ice. Originally, cold storage solutions for lung tissue samples were developed from organ transplant storage solutions. Although beneficial, previous studies have described cold-induced injury characterized by mitochondrial dysfunction and oxidative stress [40–44], well-known inducers of cellular senescence. Senescent cells are characterized by a stable cell cycle arrest, an altered metabolic activity, and the secretion of several pro-inflammatory growth factors and cytokines [45]. Moreover, other studies have reported a cold-induced, iron-dependent mechanism of cellular injury, against which the addition of iron chelators showed protective effects [41, 46, 47]. Previously, we tested two cold storage solutions with rat PCLS in 2021 [31], whereas Horn et al. deployed the same solutions for the cold storage preservation of human HepaRG liver spheroids [48]. Therefore, building upon our previous results [31], this study aims to establish the efficacy of the most promising Solution 1 (without iron chelators or with iron chelators, the latter being commercially available as TiProtec®) for preserving hPCLS. Here, we demonstrate that TiProtec allows the cold storage of hPCLS for up to 14 days maintaining their viability, metabolic activity, major cellular composition, and tissue integrity as well as their capacity to elicit a fibrotic response. Moreover, we describe for the first-time transcriptional changes associated to cold storage preservation of hPCLS, thereby offering a reference atlas for future studies. Finally, this study contributes to an optimized use of hPCLS, enabling banking, sharing, and on-demand processing and usage of hPCLS for translational lung research.

Table 1 Composition of DMEM/F-12 and cold storage preservation TiProtec

	DMEM/F-12	TiProtec
Cl^-	126	103.1
Na^+	133	16
K^+	0.4	93
$H_2PO_4^-$ (41)		1
SO_4^{2-}	0.4	
Mg^{2+}	1	8
Ca^{2+}	2.22	0.05
Glycine	0.25	10
Alanine	0.05	5
α-Ketoglutarate		2
Aspartate	0.05	5
N-Acetylhistidine	0.15	30
Tryptophan	0.05	2
Sucrose		20
Glucose	17.5	10
Hepes Buffer	15	
Deferoxamine*		0.1
LK 614*		0.02
Other compounds	(cf. to Supplementary Table 1)	
pH	7.0-7.6	7.0

Concentrations are given in mmol/L; for a simplified comparison of both solutions the main compounds are displayed here. More detailed information about DMEM/F-12, including other compounds, can be found in the Supplementary Table 1. *Not present in TiProtec (-)

Methods

Aim, design, and setting of the study

To evaluate the effects of long-term cold storage on hPCLS, the special preservation solution TiProtec® and a variant of it, without iron chelators; TiProtec (-), were compared with a standard DMEM/F-12 solution (Table 1). After agarose filling and slicing, 4 mm punches were generated. Slices were kept in culture medium overnight, as previously described and recommended [2, 30]. Accordingly, the day after preparation of hPCLS was defined as baseline (T0) for all experiments. On this day, hPCLS were then transferred to 500 µL of the respective solutions and the samples were stored at 4 °C without medium change until the collection time point (T7, T14, T21, T28). To account for slice-to-slice variability in cellular composition, 4 mm punches derived from the same hPCLS were randomly distributed among the tested cold-storage solutions or baseline stimulations. Prior to functional and stimulation experiments, hPCLS were warmed up for 3 h in standard cell culture conditions (37 °C with 5% CO_2 and 95% O_2) in the same cold storage solution in which they were stored respectively, unless otherwise described.

Ethic statement

The study was approved by the local ethics committee of the Ludwig-Maximilians University of Munich, Germany (Ethic vote 19–630). Written informed consent was obtained for all study participants.

Precision-cut lung slices

Peritumor control tissue from non-chronic lung diseases (N-CLD) patients (Table 2) were obtained from the CPC-M bioArchive at the Comprehensive Pneumology Center (CPC Munich, Germany). Patients were 53.8% male and had a mean age of 70 ± 7.98 years old. PCLS were generated using either a vibratome HyraxV50 (Zeiss, Germany) or 7000smz-2 Vibratome (Campden Instruments, England) [22, 49]. Human lung tissue was filled with 3% of low gelling temperature agarose in hPCLS culture medium: DMEM/F-12 (Thermo Scientific, USA) with phenol red supplemented with 0.1% Fetal Bovine Serum (FBS), 1% penicillin/streptomycin (P/S) and 1% amphotericin B. Filled tissue was kept at 4 °C at least for 1 h before slicing it into 500 µm slices. Using a biopsy puncher, 4 mm slices were generated and cultured in 24-well plates. After cold storage and for any stimulation assay, hPCLS were cultured for up to 7 days (unless otherwise described) in hPCLS culture medium as described before [22, 49] and the medium was changed every 48/72 h.

Materials and chemicals

Low melting point agarose was purchased from Sigma-Aldrich. The Alamar Blue assay and the Live/Dead Staining were performed in DMEM/F-12 (1:1) with 15 mmol/L HEPES and sodium bicarbonate without L-glutamine and phenol red (Sigma-Aldrich, St. Louis, MO/USA; Product ID: D6434-500ML; Table 1). This medium was supplemented with 1% P/S (10,000 units penicillin and 10 mg streptomycin/mL; Sigma-Aldrich). The cold storage solution (TiProtec®; Table 1) was either obtained from Dr. Franz Köhler Chemie (Bensheim, Germany) or prepared in the Institute of Physiological Chemistry, Germany, Essen. The iron chelator-free derivative of this solution (TiProtec (-)) was prepared in the Institute of Physiological Chemistry, Essen. The supplement LK 614 (N-hydroxy-3,4-dimethoxy-N-methylbenzamide) was generously provided by Dr. Franz Koehler Chemie, while deferoxamine mesylate was purchased from Novartis Pharma (Basel, Switzerland). Both chelators were freshly added to obtain the final TiProtec. Both, TiProtec and TiProtec (-) were supplemented with 1% P/S. For fibrosis induction, control and fibrotic cocktails (Table 3) were freshly prepared just before the treatment in DMEM/F-12 supplemented with 1% P/S (Sigma-Aldrich), 1% amphotericin B (Sigma, 250 µg/ml), and 0.1% FBS (PAN Biotech) as previously described [2]. Transforming growth factor-β1 (TGF-β1) was obtained from R&D systems (Product ID: 240-B-002/CF), reconstituted in 0.1% Bovine Serum Albumin (BSA, Sigma) dissolved in 4 mM HCl in Phosphate Buffered Saline (PBS) at a concentration of 1 µg/mL, and aliquots were stored at -20 °C. Tumor necrosis factor-α (TNF-α) was obtained from R&D systems (Product ID: 210-TA-CF), reconstituted in PBS at a concentration of 0.1 mg/ml, and aliquots were stored at -20 °C. Platelet-derived growth factor-AB (PDGF-AB) was obtained from Gibco (Product ID: PHG0134), reconstituted in 10 mM Acetic Acid (Honeywell Research Chemicals) at a concentration of 0.1 mg/ml, and aliquots were stored at -20 °C. Lysophosphatidic acid (LPA) was obtained from Cayman Chemical (Product ID: 62215), reconstituted in PBS at a concentration of 10 mM, and aliquots were stored at -20 °C. BSA was obtained from Sigma (Product ID: A7906-100G).

Table 2 Patient demographics and clinical data

Sex	Age	Smoking status	Tissue Origin
Male	70	ex-smoker	Peritumor
Male	65	ex-smoker	Peritumor
Female	77	never-smoker	Peritumor
Female	65	ex-smoker	Peritumor
Male	83	never-smoker	Peritumor
Female	77	smoker	Peritumor
Male	68	ex-smoker	Peritumor
Male	80	ex-smoker	Peritumor
Male	66	never-smoker	Peritumor
Female	68	ex-smoker	Peritumor
Female	57	ex-smoker	Peritumor
Female	77	ex-smoker	Peritumor
Male	57	smoker	Peritumor
Female	71	ex-smoker	Peritumor
Female	68	ex-smoker	Peritumor

Table 3 Composition of control cocktail (CC) and fibrotic cocktail (FC). Transforming growth factor- β1 (TGF- β1), tumor necrosis factor- α (TNF- α), platelet-derived growth factor-AB (PDGF-AB), Lysophosphatidic acid (LPA), bovine serum albumin (BSA)

Reagent	CC	FC
TGF-β1	0.1% BSA in PBS	5 ng/ml
TNF-α	0.1% BSA in PBS	10 ng/ml
PDGF-AB	10 mM Acetic acid	10 ng/ml
LPA	PBS	5 µM

Viability

To visualize and quantify possible cold storage induced cell death, the Live/Dead™ Viability/Cytotoxicity Staining kit for mammalian cells containing calcein acetoxymethylester (calcein AM) and ethidium homodimer-1 (EtHD-1) from Invitrogen (Thermo Fisher Scientific, Karlsruhe, Germany) was used in combination with confocal microscopy. The cold storage duration was set between 14 and 28 days, based on preliminary experiments that indicated substantial changes in metabolic activity within this interval (Fig. 1C) and to enable a direct comparison to the results of Tigges et al. [31]. Living cells fluoresced green due to the enzymatic cleavage of calcein AM by intracellular esterases, while dead cells fluoresced red as

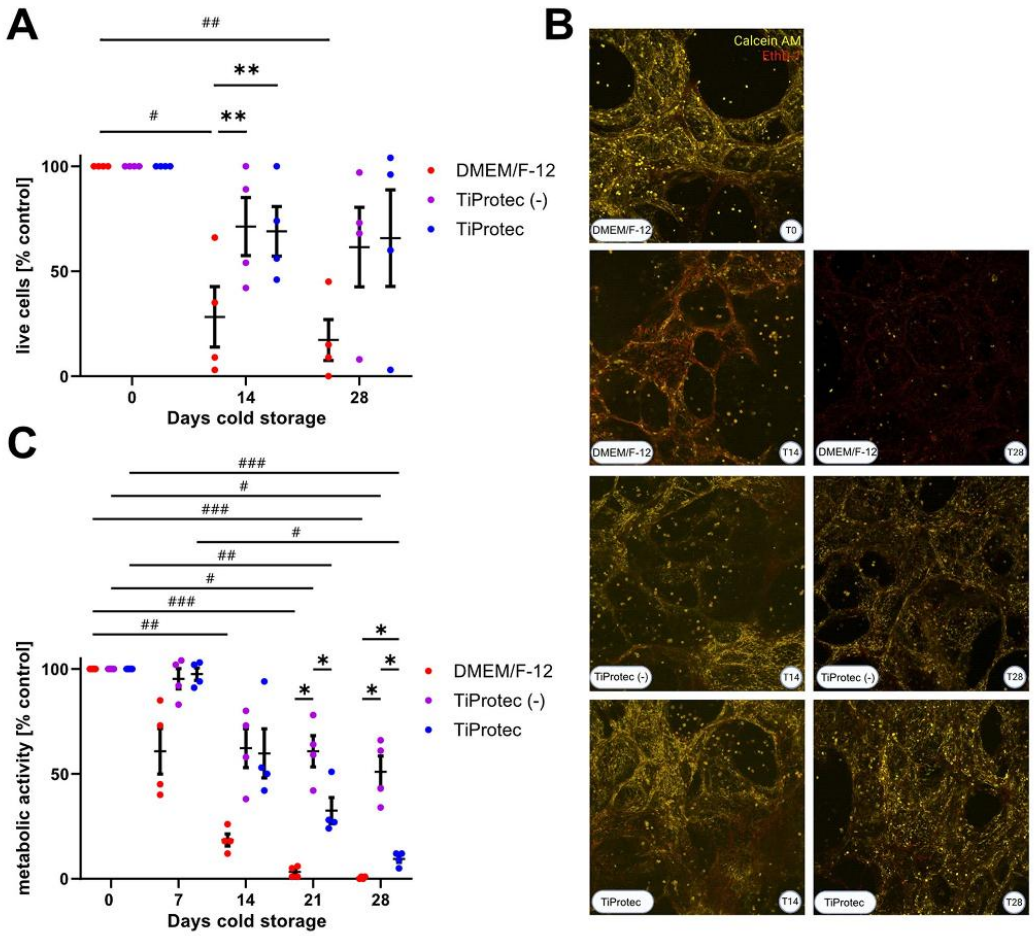

Fig. 1 Viability and metabolic activity after long-term cold storage. After preparation, hPCLS were cold stored in DMEM/F-12, TiProtec, or TiProtec (-), at 4 °C for up to 28 days. **A**) Viability changes were assessed by Calcein AM and EthD-1 staining. Viability is expressed as a percentage of the baseline viability of freshly sliced hPCLS at day 0 (100%). A positive control was also measured, after treating hPCLS with 1% Triton-X. Data set was analyzed using a RM two-way ANOVA followed by a Tukey´s multiple comparison test: * simple effects of the medium and # simple effects of storage time. Data are presented as means ± SEM ($n = 4$ patients, single dots represent average activity from 3 technical replicates per patient). Asterisks indicate significant differences (** $p < 0.01$, # $p < 0.05$, ## $p < 0.01$). **B**) Representative images of Live/Dead™ staining of hPCLS at baseline (T0) and after long-term cold storage. **C**) Quantification of Alamar Blue assay. The baseline metabolic activity was measured on day 0 and set as 100%. A negative control with only medium was also included. Metabolic activity changes are presented as a percentage of the baseline activity of freshly cut hPCLS (T0). Data set was analyzed using a Mixed-effects model followed by a Tukey´s multiple comparison test: * simple effects of the medium and # simple effects of storage time. Data are presented as means ± SEM ($n = 4$–6 patients, single dots represent averaged activity from 3 technical replicates per patient). Asterisks indicate significant differences (* $p < 0.05$, # $p < 0.05$, ## $p < 0.01$, ### $p < 0.001$)

EthD-1, as a cell impermeable dye, binds to the cell nuclei following the loss of plasma membrane integrity [50]. Measurements were generally performed in triplicates of hPCLS for each solution after a rewarming period of 3 h at T14 and T28 after cold storage in the respective solutions. Baseline measurements (T0) and positive controls, for which 1% Triton-X was applied to one hPCLS per patient, were included. The Live/Dead™ Staining kit was used according to the manufacturer's instructions, which involved applying 4 µmol/L calcein AM and 4 µmol/L EthD-1 for staining in DMEM/F-12 for 45 min at room temperature on a vibratory plate in the dark. Then, hPCLS were washed three times with Dulbecco's Phosphate Buffered Saline without Calcium and Magnesium

(DPBS; Thermo Fisher Scientific). Before microscopy, hPCLS were weighted with steel wires to prevent floating during examination with a confocal microscope (Leica DMi-8; Leica Microsystems, Wetzlar, Germany) using a 10x objective. The excitation/emission maxima were 503/565 nm for calcein AM and 592/752 nm for EthD-1. Z-stacks and 3D images were generated, consistently applying the same settings. ImageJ was then used to quantify the live and dead cells. Afterwards, percentages of live/dead cells were calculated at the different collection time points using hPCLS treated with Triton-X as maximum cell death and T0 as 100% viability for each donor.

Metabolic activity

The metabolic activity of hPCLS was determined using an Alamar Blue assay (Invitrogen, Carlsbad, CA/USA). This assay measures the fluorescence intensity of resorufin, which is produced by the reduction of resazurin in live cells as described previously by Tigges et al. [31]. In brief, one hPCLS per solution was placed into a 24-well plate containing 445 µL/well of prewarmed DMEM/F-12. Then, 5 µL of Alamar Blue reagent were added to each well. Afterwards the hPCLS were incubated for 2 h at 37 °C on a vibratory plate. Subsequently, 125 µL of the supernatant were transferred in technical duplicates into a 96-well plate. Control wells, which only contained DMEM/F-12 and Alamar Blue, were treated in the same way as described above and measured in technical duplicates. Fluorescence intensity was measured with a multimode microplate reader (Spark, Tecan Group Ltd., Männedorf, Switzerland), with excitation and emission wavelengths set as 560 nm and 590 nm, respectively. Background fluorescence, represented by the control values, was subtracted from the readings. The measurements were taken at T7, T14, T21, and T28 in hPCLS triplicates for each solution after a rewarming period of 3 h. These timepoints were chosen, since a direct comparison of the results to the ones of Tigges et al. [31] was planned to study whether there were species induced differences. The fluorescence intensity of the various long-term cold-stored hPCLS was then compared with the baseline fluorescence activity measured at T0.

Formalin-fixed paraffin-embedding of PCLS

hPCLS were washed once with 1X PBS, fixed in 4% PFA solution for 1 h at 37 °C, and kept at 4 °C in 1X PBS until used. Fixed hPCLS were transferred to embedding cassettes and processed by a Microm STP 420D Tissue Processor (Thermo Scientific, USA) with the following steps: 50% EtOH (1 cycle, 60 min), 70% EtOH (1 cycle, 60 min), 96% EtOH (2 cycles, 60 min each), 100% EtOH (2 cycles, 60 min each), Paraffin (1 cycle, 30 min), and Paraffin (3 cycles, 45 min each). Then, tissue was embedded in paraffin Type 3 (Thermo Scientific, USA) using the Modular Tissue Embedding Center EC 350 (Thermo Scientific, USA), and blocks were kept at 4 °C until use. Formalin-fixed, paraffin-embedded (FFPE) sections were cut using a Hyrax M55 microtome (Zeiss, Germany) mounted on slides, dried overnight at 40 °C, and kept at 4 °C until use.

Table 4 Antibodies used for immunofluorescence staining

Target Protein	Host	Company	Ref. No
P21	rabbit	Abcam	ab109520
PDPN	sheep	R&D system	AF3670
aSMA	mouse	Millipore Sigma	A5228
FN1	rabbit	Santa cruz	sc-9068

Hematoxylin and eosin staining

Hematoxylin and Eosin (H&E) staining was performed to assess morphological changes in hPCLS after cold storage in DMEM/F-12, TiProtec, or TiProtec (-). Samples were collected at T7, T14, T21, and T28 and FFPE sections were generated. FFPE sections were dried at 60 °C for 30 min to 1 h. Then, they were deparaffinized with the following steps: Xylene (2 cycles, 5 min each), 100% EtOH (2 cycles, 3 min each), 90% EtOH (1 cycle, 3 min), 80% EtOH (1 cycle, 3 min), 70% EtOH (1 cycle, 3 min), and Milli-Q water (1 cycle, 5 min). Then, FFPE sections were stained with hematoxylin for 10 min, rinsed, and then stained with eosin for 45 s followed by final washing step with Milli-Q water. Samples were dehydrated prior to the mounting and then they were imaged with an AxioImager (Zeiss) at 20X magnification.

Immunofluorescence

FFPE sections were deparaffinized and exposed to heat-induced antigen retrieval (10 mM citrate buffer, pH = 6.0, 1 cycle at 125 °C for 30 s, 1 cycle at 90 °C for 10 s). Slides were washed twice with 1X PBS and blocked for 1 h at RT in a humid chamber with 10% Normal Donkey Serum in DAKO Antibody Diluent (Agilent Technologies, USA). Samples were incubated with primary antibodies (Table 4) diluted in DAKO Antibody Diluent (Agilent Technologies, USA) and incubated at 4 °C overnight in a humid chamber. The next day, samples were washed twice in 1X PBS for 5 min and incubated with secondary antibodies (Table 4, diluted 1:250) and DAPI (1:500) prepared in 1% BSA in 1X PBS and incubated for 2 h at RT in a humid chamber. hPCLS were blocked with the Vector® TrueVIEW® Autofluorescence Quenching Kit (Vector laboratories, USA) for 2–3 min at RT in a humid chamber. Finally, hPCLS were mounted using DAKO Fluorescence mounting medium (Agilent Technologies, USA) and imaged using an AxioImager (Zeiss) acquiring at least 3 regions of interest per sample at 20X. Fiji (version 1.53t) was used for automatic quantification of mean

fluorescence intensity or cell percentage, which were normalized to cell count based on DAPI signal.

Determination of baseline senescence

To determine whether the three solutions induce cold storage-related cellular senescence in human PCLS, samples were collected at T0, T7, T14, and T21. These time points were chosen to compare baseline senescence with changes in metabolic activity. For this, 4 mm punches were prepared and stored in DMEM/F-12, TiProtec (-), or TiProtec for the listed time points. At collection points, samples were washed once with 1X PBS and prepared into FFPE sections as previously described. Immunofluorescence was used to determine the expression of the Cyclin Dependent Kinase Inhibitor 1 A (CDKN1A/P21) as a marker for cellular senescence and Podoplanin (PDPN) as a lung structural marker of the alveolar region (Table 4).

Induction of fibrosis

As previously described [2], hPCLS were treated with a control (CC) or fibrotic cocktail (FC) (Table 3) at baseline (T0) or after cold storage in TiProtec solutions (T7, T14). These time points were selected as our findings suggested tissue viability and function were most effectively maintained for up to 14 days of cold storage. For this, both cocktails were prepared in DMEM/F-12 with phenol red supplemented with 0.1% FBS, 1% P/S and 1% amphotericin B. After cold storage and a 3 h rewarming period, hPCLS were washed once with pre-warmed DPBS and then the CC/FC cocktails were added. hPCLS were kept in standard cell culture conditions (37 °C, 5% CO_2) and treatment was replenished after two days. Samples were collected at day 5 after treatment. On the collection day, six 4 mm punches per condition were flash frozen in liquid nitrogen and the corresponding supernatants were collected and kept at -80 °C until use. Moreover, two 4 mm punches were collected for immunostaining, as previously described.

RNA isolation

For RNA isolation we adapted the protocol previously published [51]. In summary, six 4 mm hPCLS were washed once with cold 1X DPBS and snap frozen in liquid nitrogen either at baseline, after cold storage, or after stimulation. Then, 400 µl of TRIzol™ and one 5 mm stainless steel bead (Qiagen, USA) were added to each sample and tissue was homogenized using a TissueLyser II (Qiagen, USA) 3 times at 27 Hz for 1 min. RNA was then precipitated using 100% EtOH, loaded into RNeasy MinElutespin columns, and spun down at full speed (16,000 x g/RFC) for 30 s at RT. Samples were washed once with RW1 buffer and treated with DNAseI diluted in RDD buffer, according to the manufacturer´s instructions (Qiagen, USA). Samples were then sequentially washed with RW1 buffer (12,000 x *g*/RFC for 30 s, RT), RPE Buffer (12,000 x *g*/RFC for 30 s, RT), and 80% EtOH (12,000 x *g*/RFC for 2 min, RT). Columns were air dried at full speed (16,000 x *g*/RFC) for 5 min at room temperature (RT) and RNA was eluted in 20 µl RNase-free water. RNA concentration was determined using a Nanodrop with an average yield of 34.06 ± 10.54% ng/µl (T0), 28.96 ± 10.60% ng/µl (T7 DMEM/F-12), 34.43 ± 24.94% ng/µl (T7 TiProtec (-)), 31.33 ± 6.375 ng/µl (T7 TiProtec), 35.39 ± 12.70% ng/µl (T14 TiProtec (-)), and 44.78 ± 28.68 ng/µl (T14 TiProtec), with not statistical significant differences among conditions as tested by Kruskal-Wallis test, followed by a Dunn´s multiple comparisons test. RNA was stored at -80 °C until further use.

Table 5 Mastermix for cDNA synthesis

Reagent	Article ID	Final concentration
Random Hexamers	N8080127	10 µM
dNTP Mix	R0192	2 mM
5X First– Strand Buffer	18057018	1X
0,1 M DTT	18057018	40 mM
Reverse Transcriptase	28025013	10 U/µl
RNAse Inhibitor	N8080119	4 U/µl

Table 6 Primers for RT-qPCR

Primer	Sequence (5'-3')
*FN1*_fw	CCGACCAGAAGTTTGGGTTCT
*FN1*_rv	CAATGCGGTACATGACCCCT
*ACTA2*_fw	CGAGATCTCACTGACTACCTCATGA
*ACTA2*_rv	AGAGCTACATAACACAGTTTCTCCTTGA
*COL1A1*_fw	CAAGAGGAAGGCCAAGTCGAG
*COL1A1*_rv	TTGTCGCAGACGCAGATCC
*HPRT*_fw	AAGGACCCCACGAAGTGTTG
*HPRT*_rv	GGCTTTGTATTTTGCTTTTCCA

RT-qPCR

500–1000 ng RNA, as determined by Nanodrop quantification, were denatured in 20 µl of RNAse-free water (15 min at 70 °C). Then, the cDNA reaction mix (Table 5) was added to each sample and incubated for one cycle at 20 °C for 10 min, one cycle at 43 °C for 75 min, and one cycle at 99 °C for 5 min. Finally, cDNA was diluted with RNAse-free water and kept at -20 °C until use. The RT-qPCR reaction mix was prepared using Luna® Universal qPCR Master Mix and the desired primer pair (final concentration 5 µM) (Table 6). Samples were loaded in a 96-well plate and incubated in a QuantStudio3 (Thermo Fisher Scientific) following these steps: Pre-incubation: (1 cycle) 50 °C for 2 min. Denaturation: (1 cycle) 95 °C for 10 min. Amplification: (40 cycles) at 95 °C for 3 s and 60 °C for 30 s. Melting curve: (1 cycle) 95 °C for 15 s, 60 °C for 1 min and 95 °C for 15 s. A two-derivative analysis was used to determine Ct values and the 2–ΔΔCt

method [52] was used to calculate the relative fold gene expression.

RNA-bulk-sequencing

Bulk RNA was isolated as described previously from three (DMEM/F-12) and four (TiProtec solutions) different biological replicates at T0 and after 7 and 14 days in cold storage. Time points were selected accordingly to viability and metabolic activity of cold-stored PCLS. Samples were sent to Novogene for quality control, library preparation, and sequencing. RNA quantity and quality was determined using a Bioanalyzer, with no significant differences found among conditions. Messenger RNA was purified from total RNA using poly-T oligo-attached magnetic beads. After fragmentation, the first strand cDNA was synthesized using random hexamer primers. Then, the second strand cDNA was synthesized using dUTP, instead of dTTP. The directional library was ready after end repair, A-tailing, adapter ligation, size selection, USER enzyme digestion, amplification, and purification. The library was checked with Qubit and real-time PCR for quantification and bioanalyzer for size distribution detection. Quantified libraries were pooled and sequenced on Illumina NovaSeq X Plus Series (PE150) platforms, according to effective library concentration and data amount. The gene annotation used for quantification was Ensembl version 108. Quality controls were performed in R (4.2.3) and RStudio (2023.03.0). Raw counts were corrected for batch bias due to biological variance using ComBatseq function in the sva package (3.46.0). Then, differential expression analysis was done using the DESeq2 package (pAdjustMethod = "BH", alpha = 0.05) and shrinkage of the Log-fold change (LFC) [53]. Differentially expressed genes (adjusted p-value < 0.05, LFC > 0) were extracted and used for initial exploration and cell type signature enrichment analysis. Differentially expressed genes (adjusted p-value < 0.05, LFC > 1) were extracted and used for gene set enrichment analyses using the fsgea (1.24.0), DOSE (3.24.2), and Cluster Profiler (4.6.2) packages. Cell type signature enrichment analysis was performed as described in [54, 55], using the top 100 marker genes for each cell type of the publicly available single-cell RNA-seq hPCLS dataset [23]. The enrichment scores (-log10 p-values signed by effect size) reflect either enrichment or depletion of the respective cell types, with positive values indicating enrichment and negative values indicating cell type depletion.

Statistics

All datasets were tested for normality using a Shapiro-Wilk test. Data derived from viability, metabolic activity, and baseline senescence was analyzed using a two-way ANOVA model or Mixed-effect model followed by Tukey`s multiple comparisons test. Data from RT-qPCR after fibrotic stimulation was analyzed using an unpaired t-test (baseline) or a Kruskal-Wallis test followed by a Dunn´s multiple comparisons test (day 7 and day 14). Data from immunofluorescence quantification after fibrotic stimulation was normalized to control cocktail samples and analyzed with one sample t-test. Differences with p-values < 0.05 were considered significant. Data are reported as the mean and standard deviation or standard error of the mean. Single points represent independent biological replicates. All data and graphs were analyzed and generated in GraphPad Prism v.10.0.2.

Results

TiProtec and TiProtec (-) preserve hPCLS viability for more than 14 days

Live/Dead™ staining was performed to assess the cell viability of hPCLS at baseline and after cold storage in DMEM/F-12, TiProtec, and TiProtec without the iron chelators LK 614 and deferoxamine (TiProtec (-)). The baseline cell viability (T0) was measured one day after slicing prior to long-term cold storage. Residual viability after cold storage, expressed as a percentage of the initial viability (100%) was determined after 7, 14, and 28 days of cold storage. In general, hPCLS stored in TiProtec and TiProtec (-) exhibited higher viability than hPCLS stored in DMEM/F-12 (Fig. 1A, B). Preservation of cell viability was time- ($p = 0.0281$) and medium- ($p = 0.0050$), but not patient-dependent. When stored in DMEM/F-12 the viability significantly dropped to 28 ± 25% ($p = 0.0312$) by day 14, and further decreased to 17 ± 17% ($p = 0.0070$) by day 28 (Fig. 1A). In contrast, cold storage in both TiProtec variants did not result in significant viability declines throughout the entire cold storage period (T14: TiProtec (-) = 71 ± 24%, TiProtec = 69 ± 21%; T28: TiProtec (-) = 62 ± 33%, TiProtec = 65 ± 40%). The presence of iron chelators did not significantly affect cold-stored hPCLS viability. TiProtec (-) showed a slight benefit on day 14, while TiProtec had a benefit on day 28. Overall, hPCLS stored in TiProtec with and without iron chelators remained more viable than those in DMEM/F-12 after 14 days (Fig. 1A, B). A similar pattern was seen at 28 days, but the effect was less pronounced. In conclusion, cold storage in TiProtec and TiProtec (-) maintains cellular viability for up to 28 days, with no significant impact from the addition of iron chelators. Accordingly, H&E staining also indicated that tissue integrity is preserved up to 28 days with both cold storage solutions (Suppl. Figure 1).

TiProtec and TiProtec (-) maintain the metabolic activity for up to 14 days

Metabolic activity was measured at baseline (T0 = 100%) and after cold storage (T7, T14, T21, T28). The metabolic

activity was dependent on the duration of storage ($p < 0.0001$) and type of storage solution ($p = 0.0004$). hPCLS stored in TiProtec and TiProtec (-) had a higher metabolic activity than those stored in DMEM/F-12 (Fig. 1C). Indeed, the metabolic activity of hPCLS had a decline already after 7 days of cold storage in DMEM F-12 that continuously decreased over the storing time (Fig. 1C), becoming significant after 14 days with 19 ± 5% ($p = 0.01$), and further decreasing to 3 ± 2% ($p < 0.001$) after 21 days, and to 1 ± 1% ($p < 0.01$) after 28 days. These results indicate that DMEM/F-12 is unsuitable for long-term (> 7 days) cold storage of hPCLS. In contrast, TiProtec and TiProtec (-) performed better, as metabolic activity was not significantly reduced until day 21. Up to 14 days of cold storage, the presence of iron chelators did not have a significant effect on the metabolic activity, as this was comparable for both solutions: TiProtec (-) 62 ± 16%; TiProtec 60 ± 20% (Fig. 1C). The addition of iron chelators (TiProtec) appears not to be beneficial to improve the metabolic activity after cold storage of hPCLS longer than 14 days, as the metabolic activity was significantly lower in its presence: TiProtec (-) 61 ± 13% ($p = 0.0395$), TiProtec 33 ± 11% ($p = 0.0051$) after 21 days and TiProtec (-) 51 ± 13% ($p = 0.0221$), TiProtec 10 ± 3% ($p < 0.001$) after 28 days. TiProtec (-) demonstrated superior performance in maintaining the metabolic activity of hPCLS between days 21 and 28 compared to TiProtec. In conclusion, both versions of TiProtec effectively preserved metabolic activity during cold storage, with minimal loss observed up to 7 days and no significant decline up to 14 days, whereas it was significantly altered from day 21 onwards.

hPCLS stored in TiProtec and TiProtec (-) preserve transcriptional and cellular identity of fresh hPCLS

We have shown for the first time that hPCLS can be stored at least for 14 days at 4 °C without significant changes in viability or metabolic activity. Therefore, we next used bulk-RNA sequencing to characterize the molecular and cellular changes occurring in hPCLS after cold storage in DMEM/F-12 or TiProtec with and without iron chelators for 7 and 14 days when compared to freshly cut hPCLS (T0). First, we performed a principal component analysis (PCA) to visualize and identify the most important factors driving the differences among the evaluated conditions [56]. Here, we found that at day 7, the principal component 1 (PC1) explained 23.4% of the variance indicating differences between freshly cut hPCLS (black symbols) and cold-stored hPCLS (Fig. 2A). Moreover, PC2 explained additional 16.8% of the variance indicating differences among the three cold-storage solutions used (Fig. 2A). Similar sample separation was observed after 14 days, with PC1 explaining 40.8% of the total variance indicating differences depending on cold storage solution (Suppl. Figure 2A). After differential expression analysis, we found that hPCLS stored in DMEM/F-12 for 7 days had the most dramatic transcriptional changes with 447 (3.1% of total genes) differentially expressed genes (DEG) vs. 390 (2.7% of total genes) DEG for TiProtec (-) and 281 (2.0% of total genes) DEG for TiProtec when compared to freshly sliced hPCLS (Fig. 2B). After 14 days, hPCLS cold-stored in TiProtec also displayed the lowest amount of DEG with 297 (2.1% of total genes) vs. 453 (3.1% of total genes) for TiProtec (-) (Suppl. Figure 2B). We next performed a cell type signature enrichment analysis using the top 100 genes for each cellular compartment derived from a single-cell reference atlas previously described for hPCLS [23]. For this, the cell signatures from all cells in hPCLS are used to predict how much each cell type contributes to the global gene expression changes observed in our dataset [54, 55]. Here we observed that cold storage in DMEM/F-12 led to significant transcriptional changes in several cellular compartments of hPCLS, including a relative loss of epithelial cells (Fig. 2C). Storage in TiProtec (-) or TiProtec affected fewer cellular compartments including a predicted relative loss of pro-fibrotic immune cells and myofibroblasts after 7 days (Fig. 2C) and enrichment of mesenchymal cells after 14 days (Suppl. Figure 2C). To further characterize molecular changes in cold-stored hPCLS, we performed an unsupervised hierarchical clustering analysis based on the DEG for TiProtec (-) and TiProtec in comparison to T0 baseline control [56]. Here, we observed that samples stored in TiProtec have a transcriptional profile that is closer to freshly cut hPCLS than those stored in TiProtec (-) (Fig. 2D) with a similar trend after 14 days of cold storage (Suppl. Figure 2B). This together suggests that cold storage in TiProtec or TiProtec (-) maintains not only the viability and metabolic activity of hPCLS but also the transcriptional signature of fresh hPCLS for 14 days. Finally, a gene set enrichment analysis (GSEA) for different molecular pathways showed that cold storage in TiProtec (-) upregulated processes related to stress response, cell death, and development, while TiProtec downregulated most of these pathways (Fig. 2E). Comparison of different pathways after 7- and 14-days cold storage in both TiProtec solutions revealed a sustained downregulation of pathways associated to stress response, inflammation, and cell death in TiProtec (Fig. 2F, Suppl. Figure 3B). The main differences over time in hPCLS stored in TiProtec were an increase of cell cycle and the decrease in mesenchymal activation pathways at day 14 (Fig. 2F), while hPCLS stored in TiProtec (-) showed activation of these pathways already at day 7 (Suppl. Figure 4). In conclusion, TiProtec allows the cold storage of hPCLS for up to 14 days preserving gene expression signatures of cold-stored hPCLS and downregulating pathways associated with stress response, cell

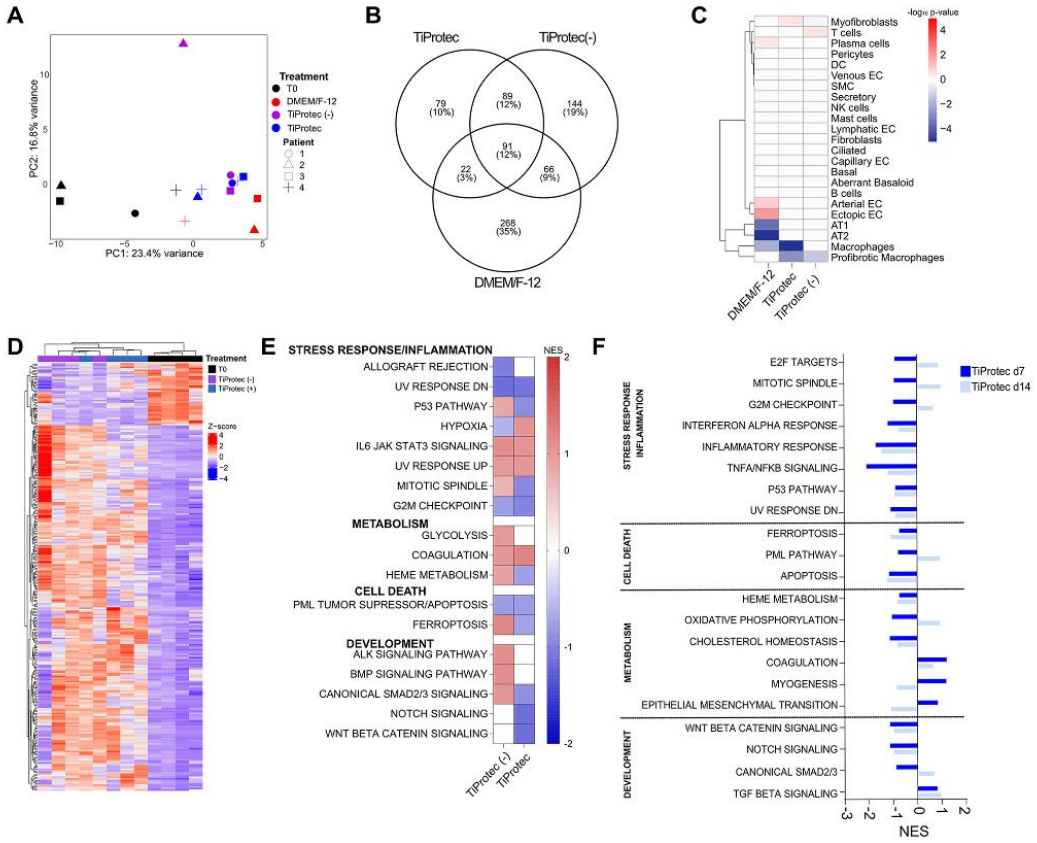

Fig. 2 Transcriptional changes in hPCLS after cold storage. **A**) Principal component analysis for freshly cut hPCLS (T0) and after 7 days of cold storage in DMEM/F-12, TiProtec (-), and TiProtec. Shapes show three (DMEM/F-12) or four (T0, TiProtec (-), TiProtec)) different biological replicates and colors indicate the cold storage solution. **B**) Venn diagram of differentially expressed genes (DEG) after 7 days of cold storage when compared to T0 baseline control (LFC > 0). **C**) Cell type signature enrichment analysis of main cellular compartments in hPCLS based on DEG displayed in B. **D**) Heatmap of DEG after 7 days of cold storage in TiProtec (-) or TiProtec when compared to T0 baseline control (LFC > 1). **E**) Deregulated pathways in hPCLS after 7 days of cold storage in TiProtec or TiProtec (-) based on DEG from D. **F**) Deregulated pathways in hPCLS after 7 and 14 days of cold storage in TiProtec based on DEG in comparison to T0 control (LFC > 1).

death, and inflammation providing a long-term protective effect in hPCLS from cold storage-induced inflammation and oxidative stress.

TiProtec and TiProtec (-) prevent inflammation, hypoxia, and maintain cellular composition in hPCLS

Then, we investigated the transcriptional changes associated with a better cold storage preservation of TiProtec and TiProtec (-) in comparison to DMEM/F-12. For this, we extracted the DEG of hPCLS after 7 days of cold storage in both solutions using DMEM/F-12 as reference. Here, we found that TiProtec shows a different profile than TiProtec (-) (Fig. 3A). Gene set enrichment analysis showed that both solutions downregulate interferon-associated inflammatory response in hPCLS (Fig. 3B). However, TiProtec seems much more effective in downregulating other metabolic functions as well as oxidative-stress response and hypoxia in comparison to TiProtec (-) (Fig. 3B), as shown by a stronger regulation of up- and downstream regulators of these pathways including Quiescin sulfhydryl oxidase 1 (*QSOX1*) and Fatty Acid Synthase (*FASN*) after cold-storage in TiProtec (Fig. 3C). Finally, cold storage in TiProtec preserved the identity of cellular populations such as alveolar type II cells and pericytes, both being one of the most susceptible and commonly altered cell types in cultured hPCLS (Fig. 3D) [23]. This together supports the idea that TiProtec allows long-term cold storage of hPCLS by preventing

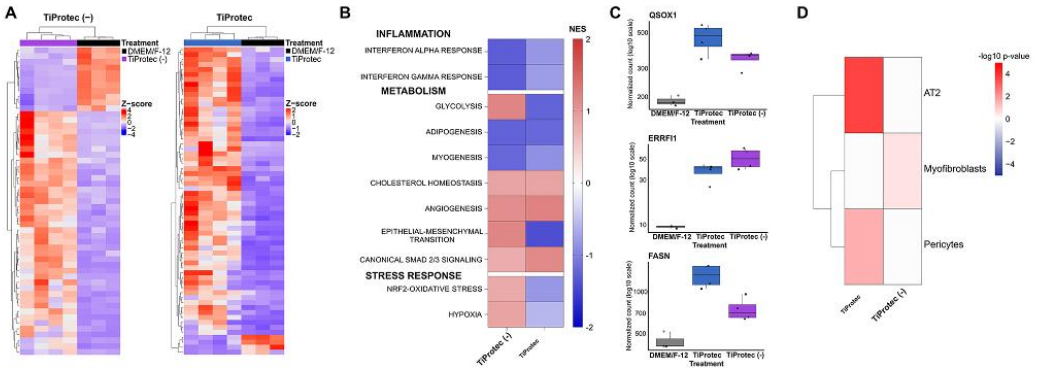

Fig. 3 Transcriptional changes induced by TiProtec and TiProtec (-) in comparison to DMEM/F-12 after 7 days of cold storage. **A**) Heatmap of differentially expressed genes (DEG) after 7 days of cold storage when compared to DMEM/F-12 in hPLCS obtained from three (DMEM/F-12) or four (TiProtec (-), TiProtec) different donors. **B**) Gene set enrichment analysis of deregulated pathways in hPCLS after cold storage based on DEG from A. **C**) Normalized counts of up- and -downstream regulators of oxidative stress-associated pathways after 7 days of cold storage in DMEM/F-12, TiProtec (-), or TiProtec. Single points with different shapes represent three (DMEM/F-12) or four (TiProtec solutions) different biological replicates. **D**) Cell type signature enrichmentanalysis in hPCLS after cold storage with TiProtec or TiProtec (-) when compared to DMEM/F-12 for 7 days

inflammation and oxidative stress responses and preserving vulnerable cell types (up to 14 days).

Cold storage does not induce cellular senescence in hPCLS

Given our previous results, suggesting a protective effect of cold storage for stress-induced inflammatory response, in both TiProtec solutions, we aimed to determine whether TiProtec or TiProtec (-) protected hPCLS from cold storage induced-senescence. For this, we first explored the gene expression of senescence-associated markers, cyclin dependent kinase inhibitor 1 A (*CDKN1A/P21*), tumor suppressor 53 (*TP53*), and growth differentiation factor 15 (*GDF-15*), in our dataset after 7 days of cold storage in both TiProtec variants in comparison to DMEM/F-12. Here we did not find significant differences in the expression of the evaluated genes (Fig. 4A). Moreover, a gene set enrichment analysis revealed an increase of pathways linked to senescence induction but no change in widely accepted senescence gene lists including SenMayo [57] (Fig. 4B). These results were also confirmed in situ, where we evaluated the nuclear protein levels of CDKN1A/P21 after 7, 14, and 21 days of cold storage in DMEM/F-12, TiProtec, or TiProtec (-) and compared it to standard culture at 37 °C, CO_2 for 7 days. Here, we observed similarly low levels of CDKN1A/P21 expression after cold storage in comparison to standard cell culture of hPCLS (Fig. 4C, D), suggesting that cold storage does not induce cellular senescence in hPCLS, and this effect does not depend on the presence of chelators.

Cold-stored hPCLS can be used in a clinically relevant fibrosis model

Human PCLS have been widely used to model and study chronic lung diseases such as idiopathic pulmonary fibrosis (IPF) [2, 49, 58]. Among them, the use of a fibrotic cocktail induces structural and cellular changes in hPCLS recapitulating early stages of lung fibrosis characterized by upregulation of alpha smooth muscle actin (*ACTA2*, aSMA) a marker for activated myofibroblasts, as well as extracellular matrix proteins like Fibronectin (*FN1*) and Collagen 1A1 (*COL1A1*) after 5 days of treatment [2]. Therefore, we were interested in evaluating whether cold-stored hPCLS retain their capacity to response to pro-fibrotic stimuli. To this end, we exposed hPCLS to control (CC) or fibrotic (FC) cocktail directly after slicing (T0 baseline) or after being cold stored in TiProtec (-) or TiProtec for 7 and 14 days. hPCLS stored in TiProtec (-) and TiProtec retained their fibrotic response even after 14 days of cold storage as shown by higher gene expression of *ACTA2*, *FN1*, and *COL1A1* after FC treatment in comparison to CC as observed at baseline (Fig. 5A). On protein level, as assessed by immunostaining, we observed a similar trend of upregulation of aSMA and FN1 in hPCLS stored in both solutions after FC treatment (Fig. 5B and Suppl. Figure 5A). The increase in FN1 upon FC showed a significant correlation between samples treated at day 0 and samples treated after cold storage, suggesting a similar fibrotic response before and after cold storage (Suppl. Figure 5B). In conclusion, TiProtec (-) and TiProtec can effectively maintain the fibrotic response capacity of hPCLS after 14 days of cold storage.

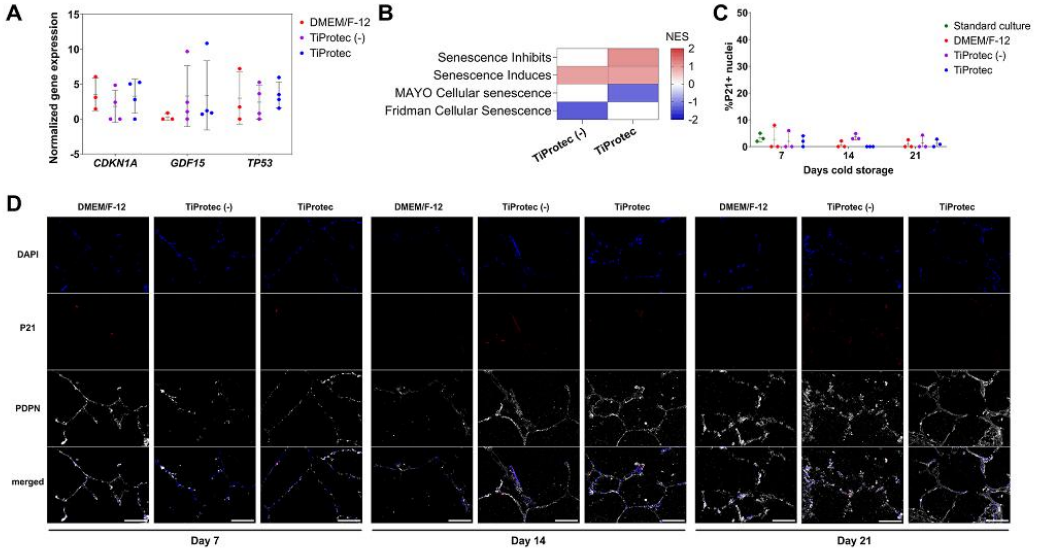

Fig. 4 Senescence response in cold-stored hPCLS. **A**) Normalized counts for senescence-associated genes: *CDKN1A/P21*, *GDF-15*, and *TP53*. Single points represent independent donors (N = three (DMEM/F-12)) or four (T0, TiProtec (-), TiProtec)). **B**) Heatmap of enrichment scores after GSEA for senescence-related pathways of DEG from day 7 cold storage in TiProtec (-) or TiProtec in comparison to DMEM/F-12. **C**) Quantification of P21/CDKN1A + nuclei in hPCLS after standard cell culture for 7 days or cold storage in DMEM/F-12, TiProtec (-), or TiProtec for 7, 14, and 21 days. Single points represent independent donors (*N* = 3). **D**) Representative images of immunostaining for P21/CDKN1A and Podoplanin (PDPN, structural marker for alveolar region) in hPCLS after cold storage in DMEM/F-12, TiProtec (-), or TiProtec for 7, 14, and 21 days. Scale bar = 100 µm.

Discussion

Chronic lung diseases remain a leading cause of morbidity and mortality worldwide [1]. hPCLS are a versatile model for studying disease-associated mechanisms [2, 3], pre-clinical drug testing [5–7], and toxicology assessments [8–10]. hPCLS maintain the intact 3D lung architecture and contain all the resident cell types like airway epithelial cells, type I and type II alveolar cells, fibroblasts, immune cells (e.g. alveolar macrophages), and smooth muscle cells [11–13]. However, one of the main limitations that researchers face while working with hPCLS is the limited tissue availability. This limitation, compounded by the low throughput slice generation and lack of adequate storage options, forces researchers to use freshly generated hPCLS immediately and discard any remaining tissue, since it not possible to keep them for later experiments. Additionally, researchers not working at major transplant or thoracic surgery centers do not have access to fresh lung tissue. Therefore, having the possibility to store, ship, and use hPCLS on-demand is of great importance for the community.

Here, we studied the potential for long-term cold storage of hPCLS in DMEM/F-12, TiProtec, and TiProtec without iron chelators. After 7 days, viability and metabolic activity were reduced and a significant reduction in immune cells such as macrophages as well as a significant decrease in specific epithelial populations such as alveolar type I and type II cells [31] just after 7 days of cold storage were observed with DMEM/F-12, suggesting that long-term storage in this solution is not feasible. TiProtec is a derivative of the organ preservation solution Custodiol-N [59–62], that is optimized for blood vessels, cells, and tissue storage [47, 63]. It was originally optimized for the cold storage of cells and vascular grafts [44, 47, 63, 64]. Since then, it has been used for cold storage of human HepaRG liver spheroids, human hepatocytes, liver-on-chip organ models, endothelialized gas-exchange membranes, and muscle tissue [48, 64–67]. Its tissue preserving properties are attributed to the presence of the amino acids alanine and glycine, which prevent hypoxic cell injury [68–70]; a risk that is particularly high for hPCLS due to their thickness (500 µm) [71]. The inhibition of the formation of nonspecific, hypoxia-induced plasma membrane pores by glycine (and to a lesser extent by alanine)– and subsequent inhibition of sodium and calcium influx into the hypoxic cells– has been shown to be the molecular mechanism of this protection [68, 70, 72, 73]. In addition, TiProtec includes α-ketoglutarate, shown to act as an antioxidant [74] and as an intermediate in the tricarboxylic acid cycle supporting ATP production and stabilizing cellular membranes in conjunction with tryptophan [75]. High aspartate

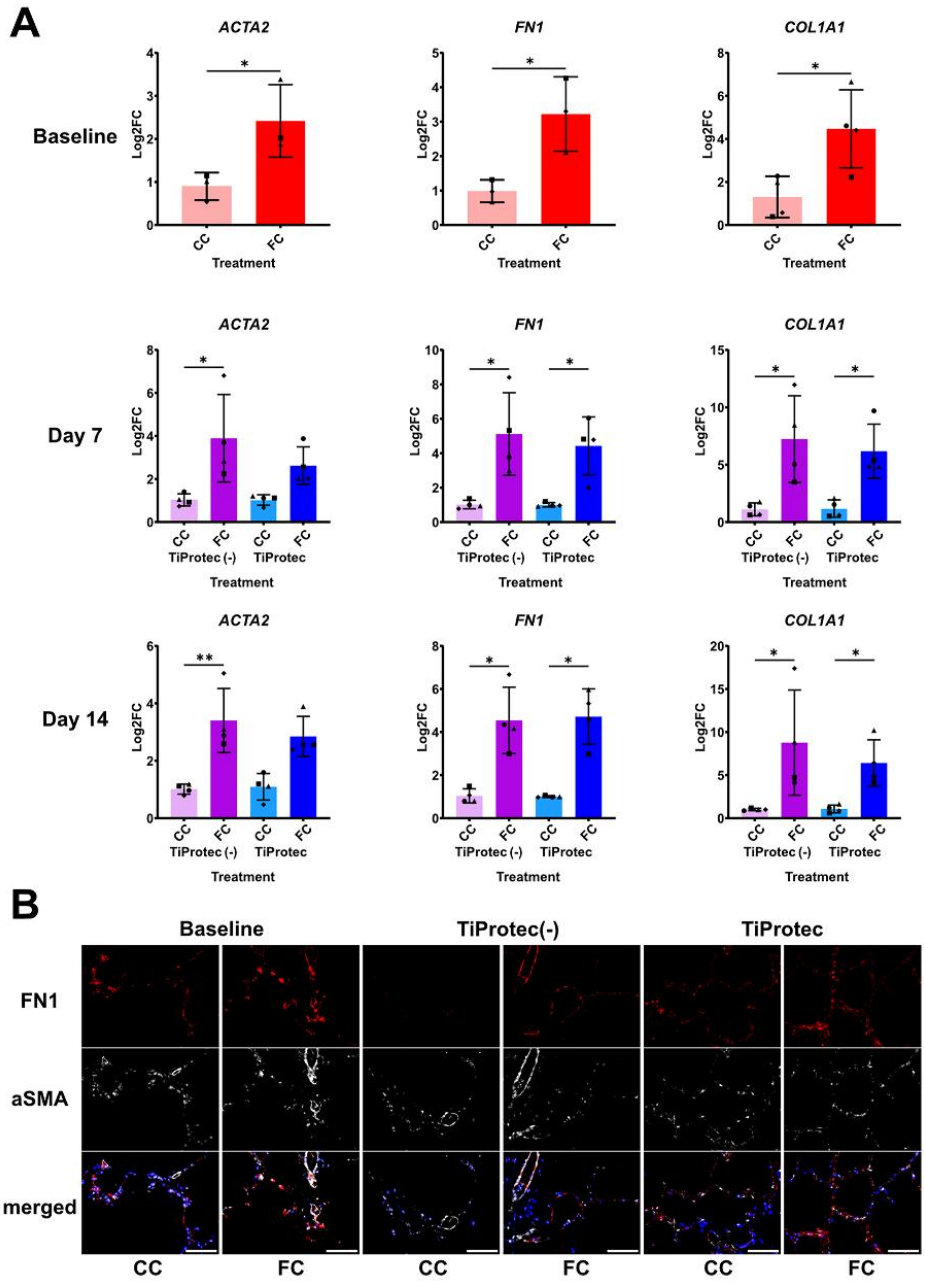

Fig. 5 Evaluation of early-fibrotic changes in cold-stored hPCLS after fibrotic stimulation. **A**) RT-qPCR of the extracellular matrix-related genes *COL1A1* and *FN1* and the myofibroblasts marker, *ACTA2*, in hPCLS treated with control (CC) or fibrotic cocktail (FC) at baseline or after 7 and 14 days of cold storage with TiProtec or TiProtec (-). Single points with different shapes represent independent biological replicates ($N=4$). * $p<0.05$, ** $p<0.01$ after unpaired-t-test (baseline) or Kruskal-Wallis test followed by Dunn´s multiple comparison test (day 7, day 14). **B**) Representative images of immunostaining for fibrosis-related proteins (aSMA and FN1) in hPCLS treated with CC or FC at baseline or after 7 days of cold storage with TiProtec or TiProtec (-). Scale bar = 100 µm.

concentrations ensure the energy supply through the tricarboxylic acid cycle, *N*-acetylhistidine maintains pH balance at a slightly acidic, protective pH, and sucrose prevents osmotic cell swelling [47, 76, 77]. Low calcium levels offer protection against various types of cellular injuries [78, 79]. The iron chelators LK 614, a small lipophilic hydroxamic acid derivative, and deferoxamine, a large, hydrophilic hexadentate chelator of Fe^{3+}, were incorporated into TiProtec to inhibit iron-dependent reactive oxygen species (ROS) formation, the major pathway of hypothermic injury in many cell types [41, 43, 64, 80]. Hypothermia has been shown to trigger the release of tightly bound iron ions into the „free" form, i.e. to lead to an increase in the cellular chelatable, redox-active iron pool [43, 80, 81]. These iron ions then give rise to the formation of highly reactive oxygen species and subsequent mitochondrial permeability transition [41, 43, 80, 81]. This iron-dependent, ROS-mediated cold-induced injury occurred in many cell types such as human and rat hepatocytes, diverse macro- and microvascular endothelial cells, rat renal tubules, proximal tubular cells and, of note, the lung tumor cell line A549 [40, 41, 43, 46, 47, 81, 82]. It proved to be inhibitable by the iron chelators deferoxamine, 2,2´-dipyridyl, and 1,10-phenanthroline as well as by the combination of deferoxamine and LK 614 [40, 41, 43, 82]. Our findings demonstrate that TiProtec outperforms DMEM/F-12 in preserving hPCLS during long-term cold storage across all analyzed endpoints. Long-term cold storage for up to 14 days was possible without significant reductions in viability or metabolic activity (Fig. 1A, C*)*, while storage for up to 28 days in TiProtec showed minimal changes regarding viability and histological changes. Interestingly, most of our results are consistent with findings from Tigges et al. [31], which points to no species-specific differences in viability and metabolic activity between human and rat PCLS.

Given the finding that iron-dependent injury is the major cold-induced injury in many cell types including the lung tumor cell line A549, it is surprising that the addition of the iron chelators LK 614 and deferoxamine did not only not improve cellular metabolic function after cold storage of hPCLS– a finding that would point to a relative low sensitivity of hPCLS, similar to rat PCLS [31, 43, 46], to iron-dependent hypothermic injury (likely due to a certain degree of hypoxia in the thick slices, limiting the formation of reactive oxygen species); the iron chelators even enhanced loss of metabolic activity following prolonged cold storage periods (Fig. 1C). Possibly, this unfavorable effect of the chelators in our current model is related to unwanted cellular iron depletion. Iron depletion by deferoxamine has been described to lead to apoptosis during incubation at 37 °C [83–85]. It appears worthwhile to assess whether rewarming in a chelator-free solution or cell culture medium instead of TiProtec would yield superior metabolic recovery. This is of particular interest as transcriptomics analysis and the evaluation of senescence induction suggest that the addition of iron chelators is beneficial for the cold storage of hPCLS. However, the major effect of TiProtec and Tiprotec (-) on viability and metabolic activity in our model is thus likely due to the protective effects of the amino acids glycine and alanine against hypoxic injury/energy deficiency injury.

This is the first study addressing the transcriptional changes associated with cold storage of hPCLS and providing a reference gene expression dataset that can be used for future studies. A cell type signature enrichment analysis revealed the preservation of most cellular compartments upon cold storage on the transcriptional level. In addition, transcriptional signatures revealed downregulation of pathways related to inflammation as well as, cell death, and oxidative stress, which are detrimental for cellular function after cold storage because they can lead to cellular senescence and lower regeneration capacity in the explanted tissues [31, 86, 87]. This confirms that TiProtec confers its tissue protective functions via regulation of these stress response pathways in lung tissue. Consistently, TiProtec and TiProtec (-) also shielded hPCLS from senescence induced by cold storage. These observations suggest that lung slices may exhibit greater resistance to cold storage-induced senescence, a phenomenon previously described in organs stored in such conditions [86, 87]. Future studies will need to focus on cell-type specific regulation of stress pathways and their upstream regulators upon cold storage. The downregulation of pathways related to inflammation is likely to be– in part– the result of lower injury in TiProtec and TiProtec (-) (Fig. 1A, C) and thus less activation of innate immune cells by released danger-associated molecular patterns (DAMPs). In addition, the amino acid glycine is a potent anti-inflammatory agent [73, 88, 89]. Glycine is known to activate glycine receptors which are glycine-gated chloride channels. These are expressed by macrophages [88], including alveolar macrophages, and other immune cells. Activation of the glycine-gated chloride channels leads to chloride influx and hyperpolarization that decreases the open probability of calcium channels and thus macrophage/immune cell activation. Thus, both, the cytoprotective effect of glycine (action on non-specific, hypoxia-induced membrane pores) and the inhibitory effect of glycine on macrophage activation likely contribute to the downregulation of pathways related to inflammation observed here. The maintenance of low inflammation and senescence levels during cold storage in TiProtec and TiProtec (-) are a great advantage since this is of high importance for the usage of these hPCLS in disease-relevant translational research. Moreover, as the anti-inflammatory effect requires the presence of the

ligand glycine, the anti-inflammatory effect is observed during and immediately after cold storage but is unlikely to compromise the subsequent use of the cold-stored hPCLS in (inflammatory) disease models after the hPCLS have been returned to their usual culture medium.

The downregulation of the hypoxia response in the iron chelator-containing solution (Fig. 3B) is unexpected as deferoxamine is well known to activate hypoxia-inducible factor-1a (HIF-1a) [90, 91]. However, one must consider that samples for this analysis were taken directly after cold storage without any rewarming. Processes like the translocation of HIF-1a to the nucleus might need rewarming (e.g. for reconstitution of disintegrated microtubules), similarly, the transcriptional response to HIF-1a might require more physiological temperatures. Additional assessment of these responses after rewarming would therefore be an important next step.

Finally, to assess the functional response of the cold-stored hPCLS, we exposed them to a fibrotic cocktail, previously used to study the pathobiology of IPF [2, 23, 49]. hPCLS cold-stored in TiProtec preserved their responsiveness to fibrotic stimuli when compared to freshly cut hPCLS. This highlights the applicability of this storage technique for translational lung research applications as well as increasing collaborative potential since this method allows the transfer of hPCLS with very simple transportation requirements [32]. Additionally, the evaluation of other disease-relevant stimuli [92] would determine the broad applicability of this cold storage method. Beyond its implications for basic research, cold storage of hPCLS in TiProtec holds significant potential for advancing therapeutic applications. By enabling the preservation of hPCLS for at least up to 14 days, this approach can support drug discovery and screening in chronic lung disease models, providing a more physiologically relevant platform compared to traditional 2D cell cultures. Moreover, TiProtec facilitates the simultaneous use of hPCLS from different patients through a possible stockpiling strategy, which could allow for high-throughput therapeutic testing. This capability is particularly advantageous for investigating inter-patient variability and tailoring treatments to specific disease phenotypes or patient populations. By offering a scalable solution for preserving and utilizing patient-derived lung tissue, TiProtec could accelerate the development of personalized therapies and enhance the translational potential of preclinical lung disease models. However, this study is limited by the fact that lung tissue derived from different disease identities and sources was not used, as our experiments were restricted to tissues from patients undergoing cancer resection surgery [93]. Furthermore, changes in cellular composition were assessed only at the transcriptomic level and not in a cell-type specific manner; future studies should incorporate cell-type specific analysis on the protein level. Additionally, further research is needed to characterize the differential susceptibility to cold storage or cryopreservation of slices with different compositions and a side-to-side comparison to other long-term storage options including cryopreservation would be desirable. Although cryopreservation has the inherent danger of damaging cells, it might allow for longer storage time and Patel et al. report that the cryopreserved hPCLS retain viability and immune responsiveness for up to 28 days [32]. Despite these limitations, our findings provide a foundation for further exploration of this storage method and its applicability to studying disease-specific mechanisms.

Conclusions

In conclusion, our study presents a novel method for long-term cold storage of hPCLS that preserves their viability, metabolic activity, transcriptional profile, and cellular composition for up to 14 days. From the 3 solutions tested, TiProtec performed the best and therefore, we would recommend the usage of this solution for future studies. Finally, our study demonstrated that cold-stored hPCLS can be used for on-demand mechanistic studies relevant for respiratory research.

Supplementary Information

The online version contains supplementary material available at https://doi.org/10.1186/s12931-025-03132-w.

Supplementary Material 1

Supplementary Material 2

Supplementary Material 3

Supplementary Material 4

Supplementary Material 5

Supplementary Material 6

Acknowledgements

We gratefully acknowledge the provision of human biomaterial and clinical data from the CPC-M bioArchive and its partners at the Asklepios Biobank Gauting, the LMU Hospital and the Ludwig-Maximillians-Universität München. We thank the patients and their families for their support.

Author contributions

Conceptualization, T.W, M.L.Formal analysis, F.G., M.C.M.N, W.B.Funding acquisition, T.W, M.L., A.O.Y, B.S.Investigation, T.W, M.L., F.G., M.C.M.N, M.G.S.Methodology, F.G., M.C.M.N, E.J., J.G. S., U.R.Supervision, T.W, M.L.Visualization, F.G., M.C.M.N, E.J.; J.G.S.Writing—original draft, T.W, M.L., F.G., M.C.M.NWriting—review & editing T.W, M.L., F.G., M.C.M.N, U.R., J.G.S.All authors have read and agreed to the published version of the manuscript.

Funding

Open Access funding enabled and organized by Projekt DEAL.
This work was supported from the German Research Foundation (GRK 2338, Targets in Toxicology); project P02 (to Timo Wille and Franz Worek). Fee Gölitz received a PhD stipend in the GRK 2338. ML, AÖY, and BS acknowledge support from the German Center for Lung Research (DZL). ML acknowledges support from the Deutsche Forschungsgemeinschaft (DFG, German Research Foundation)– 512453064, Federal Institute for Risk assessment (Bundesinstitut

für Risikobewertung, BfR) 60-0102-01.P588, and the von Behring Röntgen Foundation (71_0011).

Data availability
No datasets were generated or analysed during the current study.

Declarations

Institutional review board statement
The study was conducted in accordance with the Declaration of Helsinki and approved by the local ethics committee of the Ludwig-Maximilians University of Munich, Germany (Ethic vote 19–630).

Informed consent statement
Informed consent was obtained from all subjects involved in the study.

Consent to publish
Not Applicable.

Competing interests
U.R. is one of the inventors of TiProtec. She is stated as one of the inventors in the patent on this preservation solution, but the patent is held by Dr. Franz Köhler Chemie. The other authors declare no conflicts of interest.

Author details
[1]Comprehensive Pneumology Center with the CPC-M bioArchive and Institute of Lung Health and Immunity, Helmholtz Center Munich, German Center for Lung Research (DZL), Munich, Germany
[2]Institute for Lung Research, Philipps-University Marburg, German Center for Lung Research (DZL), Marburg, Germany
[3]Bundeswehr Institute of Pharmacology and Toxicology, Munich, Germany
[4]Walther-Straub-Institute of Pharmacology and Toxicology, Ludwig-Maximilians-University, Munich, Germany
[5]Department of Rheumatology and Immunology, Department of Pulmonary Medicine, Allergology and Clinical Immunology, Inselspital, Bern University Hospital, University of Bern, Bern, Switzerland
[6]Lung Precision Medicine (LPM), Department for BioMedical Research (DBMR), University of Bern, Bern, Switzerland
[7]Division for Thoracic Surgery Munich, Ludwig-Maximilians-University of Munich (LMU) and Asklepios Lung Clinic Munich-Gauting, Gauting, Germany
[8]Core Facility Flow Cytometry - Bacterial Vesicles, Philipps-University Marburg, Marburg, Germany
[9]Department of Medicine, Pulmonary and Critical Care Medicine, University Medical Center Marburg, Philipps-University Marburg, German Center for Lung Research (DZL), Marburg, Germany
[10]Center for Synthetic Microbiology (Synmikro), Philipps-University Marburg, Marburg, Germany
[11]Member of the German Center of Infectious Disease Research, Marburg, Germany
[12]Institute of Experimental Pneumology (IEP), Ludwig-Maximilians University of Munich (LMU), Munich, Germany
[13]Institute of Physiological Chemistry, University Hospital Essen, Essen, Germany
[14]Department of CBRN Medical Defense, Bundeswehr Medical Academy, Munich, Germany
[15]Institute for Lung Health (ILH), German Center for Lung Research (DZL), Giessen, Germany

Received: 25 October 2024 / Accepted: 31 January 2025
Published online: 17 February 2025

References

1. GBD Chronic Respiratory Disease Collaborators. Prevalence and attributable health burden of chronic respiratory diseases, 1990–2017: a systematic analysis for the Global Burden of Disease Study 2017. Lancet Respir Med. 2020 A.D. 8:585–596. https://doi.org/10.1016/S2213-2600(20)30105-3. Cited in: PMID: 32526187.
2. Alsafadi HN, Staab-Weijnitz CA, Lehmann M, Lindner M, Peschel B, Königshoff M, Wagner DE. An ex vivo model to induce early fibrosis-like changes in human precision-cut lung slices. Am J Physiol Lung Cell Mol Physiol. 2017 A.D. 312:L896-L902. https://doi.org/10.1152/ajplung.00084.2017. Cited in: PMID: 28314802.
3. Wohlsen A, Martin C, Vollmer E, Branscheid D, Magnussen H, Becker WM, Lepp U, Uhlig S. The early allergic response in small airways of human precision-cut lung slices. Eur Respir J. 2003 A.D. 21:1024–1032. https://doi.org/10.1183/09031936.03.00027502. Cited in: PMID: 12797499.
4. Lehmann M, Krishnan R, Sucre J, Kulkarni HS, Pineda RH, Anderson C, Banovich NE, Behrsing HP, Dean CH, Haak A et al. Precision Cut Lung Slices: Emerging Tools for Preclinical and Translational Lung Research. An Official American Thoracic Society Workshop Report. Am J Respir Cell Mol Biol. Epub ahead of print. https://doi.org/10.1165/rcmb.2024-0479ST. Cited in: PMID: 39499861.
5. Gölitz F, Herbert J, Worek F, Wille T. AChE reactivation in precision-cut lung slices following organophosphorus compound poisoning. Toxicol Lett. 2024 A.D. 392:75–83. https://doi.org/10.1016/j.toxlet.2023.12.014. Cited in: PMID: 38160862.
6. Huang X, Li L, Ammar R, Zhang Y, Wang Y, Ravi K, Thompson J, Jarai G. Molecular characterization of a precision-cut rat lung slice model for the evaluation of antifibrotic drugs. Am J Physiol Lung Cell Mol Physiol. 2019 A.D. 316:L348-L357. https://doi.org/10.1152/ajplung.00339.2018. Cited in: PMID: 30489156.
7. Danov O, Jiménez Delgado SM, Obernolte H, Seehase S, Dehmel S, Braubach P, Fieguth H-G, Matschiner G, Fitzgerald M, Jonigk D et al. Human lung tissue provides highly relevant data about efficacy of new anti-asthmatic drugs. PLoS One. 2018 A.D. 13:e0207767. https://doi.org/10.1371/journal.pone.0207767. Cited in: PMID: 30500834.
8. Herbert J, Kelty JS, Laskin JD, Laskin DL, Gow AJ. Menthol flavoring in e-cigarette condensate causes pulmonary dysfunction and cytotoxicity in precision cut lung slices. Am J Physiol Lung Cell Mol Physiol. 2023 A.D. 324:L345-L357. https://doi.org/10.1152/ajplung.00222.2022. Cited in: PMID: 36692165.
9. Lauenstein L, Switalla S, Prenzler F, Seehase S, Pfennig O, Förster C, Fieguth H, Braun A, Sewald K. Assessment of immunotoxicity induced by chemicals in human precision-cut lung slices (PCLS). Toxicol In Vitro. 2014 A.D. 28:588–599. https://doi.org/10.1016/j.tiv.2013.12.016. Cited in: PMID: 24412833.
10. Switalla S, Knebel J, Ritter D, Krug N, Braun A, Sewald K. Effects of acute in vitro exposure of murine precision-cut lung slices to gaseous nitrogen dioxide and ozone in an air-liquid interface (ALI) culture. Toxicol Lett. 2010 A.D. 196:117–124. https://doi.org/10.1016/j.toxlet.2010.04.004. Cited in: PMID: 20394810.
11. Liu G, Betts C, Cunoosamy DM, Åberg PM, Hornberg JJ, Sivars KB, Cohen TS. Use of precision cut lung slices as a translational model for the study of lung biology. Respir Res. 2019 A.D. 20:162. https://doi.org/10.1186/s12931-019-1131-x. Cited in: PMID: 31324219.
12. Lyons-Cohen MR, Thomas SY, Cook DN, Nakano H. Precision-cut Mouse Lung Slices to Visualize Live Pulmonary Dendritic Cells. J Vis Exp. Epub ahead of print. https://doi.org/10.3791/55465. Cited in: PMID: 28448013.
13. Liberati TA, Randle MR, Toth LA. In vitro lung slices: a powerful approach for assessment of lung pathophysiology. Expert Rev Mol Diagn. 2010 A.D. 10:501–508. https://doi.org/10.1586/erm.10.21. Cited in: PMID: 20465504.
14. Koziol-White C, Gebski E, Cao G, Panettieri RA. Precision cut lung slices: an integrated ex vivo model for studying lung physiology, pharmacology, disease pathogenesis and drug discovery. Respir Res. 2024 A.D. 25:231. https://doi.org/10.1186/s12931-024-02855-6. Cited in: PMID: 38824592.
15. Tigges J, Worek F, Thiermann H, Wille T. Organophosphorus pesticides exhibit compound specific effects in rat precision-cut lung slices (PCLS): mechanisms involved in airway response, cytotoxicity, inflammatory activation and antioxidative defense. Arch Toxicol. 2022 A.D. 96:321–334. https://doi.org/10.1007/s00204-021-03186-x. Cited in: PMID: 34778934.
16. Henjakovic M, Sewald K, Switalla S, Kaiser D, Müller M, Veres TZ, Martin C, Uhlig S, Krug N, Braun A. Ex vivo testing of immune responses in precision-cut lung slices. Toxicol Appl Pharmacol. 2008 A.D. 231:68–76. https://doi.org/10.1016/j.taap.2008.04.003. Cited in: PMID: 18504053.
17. Herbert J, Thiermann H, Worek F, Wille T. Precision cut lung slices as test system for candidate therapeutics in organophosphate poisoning. Toxicology. 2017 A.D. 389:94–100. https://doi.org/10.1016/j.tox.2017.07.011. Cited in: PMID: 28743514.
18. Schlepütz M, Uhlig S, Martin C. Electric field stimulation of precision-cut lung slices. J Appl Physiol (1985). 2011 A.D.110:545–54. https://doi.org/10.1152/japplphysiol.00409.2010. Cited in: PMID: 21109600.

19. Martin C, Uhlig S, Ullrich V. Videomicroscopy of methacholine-induced contraction of individual airways in precision-cut lung slices. Eur Respir J. 1996 A.D. 9:2479–2487. https://doi.org/10.1183/09031936.96.09122479. Cited in: PMID: 8980957.
20. Milara J, Roger I, Montero P, Artigues E, Escrivá J, Perez-Vizcaino F, Cortijo J. Targeting IL-11 system as a treatment of pulmonary arterial hypertension. Pharmacol Res. 2023 A.D. 197:106985. https://doi.org/10.1016/j.phrs.2023.106985. Cited in: PMID: 37949331.
21. Ressmeyer AR, Larsson AK, Vollmer E, Dahlèn SE, Uhlig S, Martin C. Characterisation of guinea pig precision-cut lung slices: comparison with human tissues. Eur Respir J. 2006 A.D. 28:603–611. https://doi.org/10.1183/09031936.06.00004206. Cited in: PMID: 16737991.
22. Uhl FE, Vierkotten S, Wagner DE, Burgstaller G, Costa R, Koch I, Lindner M, Meiners S, Eickelberg O, Königshoff M. Preclinical validation and imaging of Wnt-induced repair in human 3D lung tissue cultures. Eur Respir J. 2015 A.D. 46:1150–1166. https://doi.org/10.1183/09031936.00183214. Cited in: PMID: 25929950.
23. Lang NJ, Gote-Schniering J, Porras-Gonzalez D, Yang L, de Sadeleer LJ, Jentzsch RC, Shitov VA, Zhou S, Ansari M, Agami A et al. Ex vivo tissue perturbations coupled to single-cell RNA-seq reveal multilineage cell circuit dynamics in human lung fibrogenesis. Sci Transl Med. 2023 A.D. 15:eadh0908. https://doi.org/10.1126/scitranslmed.adh0908. Cited in: PMID: 38055803.
24. Heinzelmann K, Hu Q, Hu Y, Dobrinskikh E, Ansari M, Melo-Narváez MC, Ulke HM, Leavitt C, Mirita C, Trudeau T et al. Single-cell RNA sequencing identifies G-protein coupled receptor 87 as a basal cell marker expressed in distal honeycomb cysts in idiopathic pulmonary fibrosis. Eur Respir J. 2022 A.D. 59. https://doi.org/10.1183/13993003.02373-2021. Cited in: PMID: 35604813.
25. Schlepütz M, Rieg AD, Seehase S, Spillner J, Perez-Bouza A, Braunschweig T, Schroeder T, Bernau M, Lambermont V, Schlumbohm C et al. Neurally mediated airway constriction in human and other species: a comparative study using precision-cut lung slices (PCLS). PLoS One. 2012 A.D. 7:e47344. https://doi.org/10.1371/journal.pone.0047344. Cited in: PMID: 23056631.
26. Bonniaud P, Fabre A, Frossard N, Guignabert C, Inman M, Kuebler WM, Maes T, Shi W, Stampfli M, Uhlig S et al. Optimising experimental research in respiratory diseases: an ERS statement. Eur Respir J 2018 D; 51. https://doi.org/10.1183/13993003.02133-2017. Cited in: PMID: 29773606.
27. Russell WMS, Burch RL. The principles of Humane experimental technique. Med J Australia 1960 D; 1:500. https://doi.org/10.5694/j.1326-5377.1960.tb73127.x
28. Preuß EB, Schubert S, Werlein C, Stark H, Braubach P, Höfer A, Plucinski EKJ, Shah HR, Geffers R, Sewald K et al. The Challenge of Long-Term Cultivation of Human Precision-Cut Lung Slices. Am J Pathol. 2022 A.D. 192:239–253. https://doi.org/10.1016/j.ajpath.2021.10.020. Cited in: PMID: 34767811.
29. Patel V, Amin K, Allen D, Ukishima L, Wahab A, Grodi C, Behrsing H. Comparison of Long-term Human Precision-cut Lung Slice Culture Methodology and Response to Challenge: An Argument for Standardisation. Altern Lab Anim. 2021 A.D. 49:209–222. https://doi.org/10.1177/02611929211061884. Cited in: PMID: 34836458.
30. Temann A, Golovina T, Neuhaus V, Thompson C, Chichester JA, Braun A, Yusibov V. Evaluation of inflammatory and immune responses in long-term cultured human precision-cut lung slices. Hum Vaccin Immunother. 2017 A.D. 13:351–358. https://doi.org/10.1080/21645515.2017.1264794. Cited in: PMID: 27929748.
31. Tigges J, Eggerbauer F, Worek F, Thiermann H, Rauen U, Wille T. Optimization of long-term cold storage of rat precision-cut lung slices with a tissue preservation solution. Am J Physiol Lung Cell Mol Physiol. 2021 A.D. 321:L1023-L1035. https://doi.org/10.1152/ajplung.00076.2021. Cited in: PMID: 34643087.
32. Patel VS, Amin K, Wahab A, Marimoutou M, Ukishima L, Alvarez J, Battle K, Stucki AO, Clippinger AJ, Behrsing HP. Cryopreserved human precision-cut lung slices provide an immune competent pulmonary test system for on-demand use and long-term cultures. Toxicol Sci. 2023 A.D. 191:253–265. https://doi.org/10.1093/toxsci/kfac136. Cited in: PMID: 36617185.
33. Bai Y, Krishnamoorthy N, Patel KR, Rosas I, Sanderson MJ, Ai X. Cryopreserved Human Precision-Cut Lung Slices as a Bioassay for Live Tissue Banking. A Viability Study of Bronchodilation with Bitter-Taste Receptor Agonists. Am J Respir Cell Mol Biol. 2016 A.D. 54:656–663. https://doi.org/10.1165/rcmb.2015-0290MA. Cited in: PMID: 26550921.
34. Rosner SR, Ram-Mohan S, Paez-Cortez JR, Lavoie TL, Dowell ML, Yuan L, Ai X, Fine A, Aird WC, Solway J et al. Airway contractility in the precision-cut lung slice after cryopreservation. Am J Respir Cell Mol Biol. 2014 A.D. 50:876–881. https://doi.org/10.1165/rcmb.2013-0166MA. Cited in: PMID: 24313705.
35. Marimoutou M, Patel V, Kim JH, Schaible N, Alvarez J, Hughes J, Obermok M, Rodríguez CI, Kallarakal T, Suki B et al. The Fibrotic phenotype of Human Precision-Cut lung slices is maintained after Cryopreservation. Toxics 2024 D; 12:637. https://doi.org/10.3390/toxics12090637
36. Azam I, Benson JD. Multiscale transport and 4D time-lapse imaging in precision-cut liver slices (PCLS). PeerJ. 2024 A.D. 12:e16994. https://doi.org/10.7717/peerj.16994. Cited in: PMID: 38426134.
37. Gao D, Critser JK. Mechanisms of cryoinjury in living cells. ILAR J. 2000 A.D. 41:187–196. https://doi.org/10.1093/ilar.41.4.187. Cited in: PMID: 11123179.
38. Pegg DE. Principles of cryopreservation. Methods Mol Biol. 2015 A.D. 1257:3–19. https://doi.org/10.1007/978-1-4939-2193-5_1. Cited in: PMID: 25428001.
39. Elliott GD, Wang S, Fuller BJ, Cryoprotectants. A review of the actions and applications of cryoprotective solutes that modulate cell recovery from ultra-low temperatures. Cryobiology. 2017 A.D. 76:74–91. https://doi.org/10.1016/j.cryobiol.2017.04.004. Cited in: PMID: 28428046.
40. Rauen U, Polzar B, Stephan H, Mannherz HG, de Groot H. Cold-induced apoptosis in cultured hepatocytes and liver endothelial cells: mediation by reactive oxygen species. FASEB J. 1999 A.D. 13:155–168. https://doi.org/10.1096/fasebj.13.1.155. Cited in: PMID: 9872940.
41. Rauen U, Kerkweg U, Weisheit D, Petrat F, Sustmann R, de Groot H. Cold-induced apoptosis of hepatocytes: mitochondrial permeability transition triggered by nonmitochondrial chelatable iron. Free Radic Biol Med. 2003 A.D. 35:1664–1678. https://doi.org/10.1016/j.freeradbiomed.2003.09.018. Cited in: PMID: 14680689.
42. Kerkweg U, Jacob M, de Groot H, Mannherz H-G, Rauen U. Cold-induced apoptosis of rat liver endothelial cells: contribution of mitochondrial alterations. Transplantation. 2003 A.D. 76:501–508. https://doi.org/10.1097/01.tp.0000069830.78758.1c. Cited in: PMID: 12923435.
43. Rauen U, de Groot H. New insights into the cellular and molecular mechanisms of cold storage injury. J Investig Med. 2004 A.D. 52:299–309. https://doi.org/10.1136/jim-52-05-29. Cited in: PMID: 15551652.
44. Pless-Petig G, Walter B, Bienholz A, Rauen U. Mitochondrial Impairment as a Key Factor for the Lack of Attachment after Cold Storage of Hepatocyte Suspensions. Cell Transplant. 2017 A.D. 26:1855–1867. https://doi.org/10.1177/0963689717743254. Cited in: PMID: 29390882.
45. Basisty N, Kale A, Jeon OH, Kuehnemann C, Payne T, Rao C, Holtz A, Shah S, Sharma V, Ferrucci L et al. A proteomic atlas of senescence-associated secretomes for aging biomarker development. PLoS Biol. 2020 A.D. 18:e3000599. https://doi.org/10.1371/journal.pbio.3000599. Cited in: PMID: 31945054.
46. Pizanis N, Gillner S, Kamler M, de Groot H, Jakob H, Rauen U. Cold-induced injury to lung epithelial cells can be inhibited by iron chelators - implications for lung preservation. Eur J Cardiothorac Surg. 2011 A.D. 40:948–955. https://doi.org/10.1016/j.ejcts.2011.01.052. Cited in: PMID: 21398140.
47. Wille T, de Groot H, Rauen U. Improvement of the cold storage of blood vessels with a vascular preservation solution. Study in porcine aortic segments. J Vasc Surg. 2008 A.D. 47:422–431. https://doi.org/10.1016/j.jvs.2007.09.048. Cited in: PMID: 18164170.
48. Horn G, Kranawetvogl T, John H, Weigel C, Rauen U, Worek F, Wille T. Human HepaRG liver spheroids: cold storage protocol and study on pyridinium oxime-induced hepatotoxicity in vitro. Chem Biol Interact. 2023 A.D. 369:110285. https://doi.org/10.1016/j.cbi.2022.110285. Cited in: PMID: 36442613.
49. Lehmann M, Buhl L, Alsafadi HN, Klee S, Hermann S, Mutze K, Ota C, Lindner M, Behr J, Hilgendorff A et al. Differential effects of Nintedanib and Pirfenidone on lung alveolar epithelial cell function in ex vivo murine and human lung tissue cultures of pulmonary fibrosis. Respir Res. 2018 A.D. 19:175. https://doi.org/10.1186/s12931-018-0876-y. Cited in: PMID: 30219058.
50. Neuhaus V, Schaudien D, Golovina T, Temann U-A, Thompson C, Lippmann T, Bersch C, Pfennig O, Jonigk D, Braubach P et al. Assessment of long-term cultivated human precision-cut lung slices as an ex vivo system for evaluation of chronic cytotoxicity and functionality. J Occup Med Toxicol. 2017 A.D. 12:13. https://doi.org/10.1186/s12995-017-0158-5. Cited in: PMID: 28559920.
51. Stegmayr J, Alsafadi HN, Langwiński W, Niroomand A, Lindstedt S, Leigh ND, Wagner DE. Isolation of high-yield and -quality RNA from human precision-cut lung slices for RNA-sequencing and computational integration with larger patient cohorts. Am J Physiol Lung Cell Mol Physiol. 2021 A.D. 320:L232-L240. https://doi.org/10.1152/ajplung.00401.2020. Cited in: PMID: 33112185.
52. Livak KJ, Schmittgen TD. Analysis of relative gene expression data using real-time quantitative PCR and the 2(-Delta Delta C(T)) Method. Methods. 2001 A.D. 25:402–408. https://doi.org/10.1006/meth.2001.1262. Cited in: PMID: 11846609.

53. Love MI, Huber W, Anders S. Moderated estimation of fold change and dispersion for RNA-seq data with DESeq2. Genome Biol. 2014 A.D. 15:550. https://doi.org/10.1186/s13059-014-0550-8. Cited in: PMID: 25516281.
54. Lauer D, Magnin CY, Kolly LR, Wang H, Brunner M, Chabria M, Cereghetti GM, Gabryś HS, Tanadini-Lang S, Uldry A-C et al. Radioproteomics stratifies molecular response to antifibrotic treatment in pulmonary fibrosis. JCI Insight. 2024 A.D. 9. https://doi.org/10.1172/jci.insight.181757. Cited in: PMID: 39012714.
55. Mayr CH, Simon LM, Leuschner G, Ansari M, Schniering J, Geyer PE, Angelidis I, Strunz M, Singh P, Kneidinger N et al. Integrative analysis of cell state changes in lung fibrosis with peripheral protein biomarkers. EMBO Mol Med. 2021 A.D. 13:e12871. https://doi.org/10.15252/emmm.202012871. Cited in: PMID: 33650774.
56. Koch CM, Chiu SF, Akbarpour M, Bharat A, Ridge KM, Bartom ET, Winter DR. A Beginner's Guide to Analysis of RNA Sequencing Data. Am J Respir Cell Mol Biol. 2018 A.D. 59:145–157. https://doi.org/10.1165/rcmb.2017-0430TR. Cited in: PMID: 29624415.
57. Saul D, Kosinsky RL, Atkinson EJ, Doolittle ML, Zhang X, LeBrasseur NK, Pignolo RJ, Robbins PD, Niedernhofer LJ, Ikeno Y et al. A new gene set identifies senescent cells and predicts senescence-associated pathways across tissues. Nat Commun. 2022 A.D. 13:4827. https://doi.org/10.1038/s41467-022-32552-1. Cited in: PMID: 35974106.
58. Melo-Narváez MC, Bramey N, See F, Heinzelmann K, Ballester B, Steinchen C, Jain E, Federl K, Hu Q, Dhakad D et al. Stimuli-Specific Senescence of Primary Human Lung Fibroblasts Modulates Alveolar Stem Cell Function. Cells. 2024 A.D. 13. https://doi.org/10.3390/cells13131129. Cited in: PMID: 38994981.
59. Bruns W, Koehler G, de Groot H, Rauen U. Inventors. Protective solution for preventing ischaemia damage. EP20070012466 20030514. May 14, 2003.
60. Pizanis N, Petrov A, Heckmann J, Wiswedel I, Wohlschläger J, de Groot H, Jakob H, Rauen U, Kamler M. A new preservation solution for lung transplantation: evaluation in a porcine transplantation model. J Heart Lung Transplant. 2012 A.D. 31:310–317. https://doi.org/10.1016/j.healun.2011.11.009. Cited in: PMID: 22226803.
61. Minor T, Paul A, Efferz P, Wohlschlaeger J, Rauen U, Gallinat A. Kidney transplantation after oxygenated machine perfusion preservation with Custodiol-N solution. Transpl Int. 2015 A.D. 28:1102–1108. https://doi.org/10.1111/tri.12593. Cited in: PMID: 25882869.
62. Hoyer DP, Benkö T, Gallinat A, Lefering R, Kaths M, Kribben A, Korth J, Rauen U, Treckmann JW, Paul A. HTK-N as a new preservation solution for human kidney preservation: Results of a pilot randomized controlled clinical phase II trial in living donor transplantation. Clin Transplant. 2022 A.D. 36:e14543. https://doi.org/10.1111/ctr.14543. Cited in: PMID: 34813125.
63. Garbe S, Zatschler B, Müller B, Dieterich P, Ebner A, Rauen U, Matschke K, Deussen A. Preservation of human artery function following prolonged cold storage with a new solution. J Vasc Surg. 2011 A.D. 53:1063–1070. https://doi.org/10.1016/j.jvs.2010.10.093. Cited in: PMID: 21227623.
64. Pless G, Sauer IM, Rauen U. Improvement of the cold storage of isolated human hepatocytes. Cell Transplant. 2012 A.D. 21:23–37. https://doi.org/10.3727/096368911X580509. Cited in: PMID: 21669032.
65. Wille T, Gonder S, Thiermann H, Seeger T, Rauen U, Worek F. Evaluation of functional and structural alterations in muscle tissue after short-term cold storage in a new tissue preservation solution. Cells Tissues Organs. 2011 A.D. 194:501–509. https://doi.org/10.1159/000324148. Cited in: PMID: 21494014.
66. Gröger M, Dinger J, Kiehntopf M, Peters FT, Rauen U, Mosig AS. Preservation of Cell Structure, Metabolism, and Biotransformation Activity of Liver-On-Chip Organ Models by Hypothermic Storage. Adv Healthc Mater. 2018 A.D. 7. https://doi.org/10.1002/adhm.201700616. Cited in: PMID: 28960916.
67. Pflaum M, Merhej H, Peredo A, De A, Dipresa D, Wiegmann B, Wolkers W, Haverich A, Korossis S. Hypothermic preservation of endothelialized gas-exchange membranes. Artif Organs. 2020 A.D. 44:e552-e565. https://doi.org/10.1111/aor.13776. Cited in: PMID: 32666514.
68. Frank A, Rauen U, de Groot H. Protection by glycine against hypoxic injury of rat hepatocytes: inhibition of ion fluxes through nonspecific leaks. J Hepatol. 2000 A.D. 32:58–66. https://doi.org/10.1016/S0168-8278(00)80190-7. Cited in: PMID: 10673068.
69. Brecht M, de Groot H. Protection from hypoxic injury in cultured hepatocytes by glycine, alanine, and serine. Amino Acids. 1994 A.D. 6:25–35. https://doi.org/10.1007/bf00808120. Cited in: PMID: 24190740.
70. Dong Z, Patel Y, Saikumar P, Weinberg JM, Venkatachalam MA. Development of porous defects in plasma membranes of adenosine triphosphate-depleted madin-darby canine kidney cells and its inhibition by glycine. Lab Invest 1998 D; 78:657–68. Cited in: PMID: 9645756.
71. Pias SC. Pathways of Oxygen Diffusion in Cells and Tissues: Hydrophobic Channeling via Networked Lipids. Adv Exp Med Biol. 2020 A.D. 1232:183–190. https://doi.org/10.1007/978-3-030-34461-0_23. Cited in: PMID: 31893409.
72. Nishimura Y, Lemasters JJ. Glycine blocks opening of a death channel in cultured hepatic sinusoidal endothelial cells during chemical hypoxia. Cell Death Differ. 2001 A.D. 8:850–858. https://doi.org/10.1038/sj.cdd.4400877. Cited in: PMID: 11526438.
73. Petrat F, Boengler K, Schulz R, de Groot H. Glycine, a simple physiological compound protecting by yet puzzling mechanism(s) against ischaemia-reperfusion injury: current knowledge. Br J Pharmacol. 2012 A.D. 165:2059–2072. https://doi.org/10.1111/j.1476-5381.2011.01711.x. Cited in: PMID: 22044190.
74. Long LH, Halliwell B. Artefacts in cell culture: α-Ketoglutarate can scavenge hydrogen peroxide generated by ascorbate and epigallocatechin gallate in cell culture media. Biochem Biophys Res Commun. 2011 A.D. 406:20–24. https://doi.org/10.1016/j.bbrc.2011.01.091. Cited in: PMID: 21281600.
75. Bretschneider HJ. Myocardial protection., Thorac Cardiovasc S. 1980 A.D. 28:295–302. https://doi.org/10.1055/s-2007-1022099. Cited in: PMID: 6161427.
76. Koop A, Piper HM. Protection of energy status of hypoxic cardiomyocytes by mild acidosis. J Mol Cell Cardiol. 1992 A.D. 24:55–65. https://doi.org/10.1016/0022-2828(92)91159-3. Cited in: PMID: 1564730.
77. Baust JM. Advances in media for Cryopreservation and hypothermic storage. Medicine: Materials Science; 2005.
78. Hochachka PW. Defense strategies against hypoxia and hypothermia. Science. 1986 A.D. 231:234–241. https://doi.org/10.1126/science.2417316. Cited in: PMID: 2417316.
79. Upadhya GA, Topp SA, Hotchkiss RS, Anagli J, Strasberg SM. Effect of cold preservation on intracellular calcium concentration and calpain activity in rat sinusoidal endothelial cells. Hepatology. 2003 A.D. 37:313–323. https://doi.org/10.1053/jhep.2003.50069. Cited in: PMID: 12540781.
80. Rauen U, Petrat F, Li T, de Groot H. Hypothermia injury/cold-induced apoptosis–evidence of an increase in chelatable iron causing oxidative injury in spite of low O2-/H2O2 formation. FASEB J. 2000 A.D. 14:1953–1964. https://doi.org/10.1096/fj.00-0071com. Cited in: PMID: 11023979.
81. Salahudeen AK. Cold ischemic injury of transplanted kidneys: new insights from experimental studies. Am J Physiol Renal Physiol. 2004 A.D. 287:F181-7. https://doi.org/10.1152/ajprenal.00098.2004. Cited in: PMID: 15271685.
82. Bienholz A, Walter B, Pless-Petig G, Guberina H, Kribben A, Witzke O, Rauen U. Characterization of injury in isolated rat proximal tubules during cold incubation and rewarming. PLoS One. 2017 A.D. 12:e0180553. https://doi.org/10.1371/journal.pone.0180553. Cited in: PMID: 28672023.
83. Kim JL, Lee D-H, Na YJ, Kim BR, Jeong YA, Lee SI, Kang S, Joung SY, Lee S-Y, Oh SC et al. Iron chelator-induced apoptosis via the ER stress pathway in gastric cancer cells. Tumour Biol. 2016 A.D. 37:9709–9719. https://doi.org/10.1007/s13277-016-4878-4. Cited in: PMID: 26803514.
84. Simonart T, Degraef C, Andrei G, Mosselmans R, Hermans P, van Vooren JP, Noel JC, Boelaert JR, Snoeck R, Heenen M. Iron chelators inhibit the growth and induce the apoptosis of Kaposi's sarcoma cells and of their putative endothelial precursors. J Invest Dermatol. 2000 A.D. 115:893–900. https://doi.org/10.1046/j.1523-1747.2000.00119.x. Cited in: PMID: 11069629.
85. Fukuchi K, Tomoyasu S, Tsuruoka N, Gomi K. Iron deprivation-induced apoptosis in HL-60 cells. FEBS Lett. 1994 A.D. 350:139–142. https://doi.org/10.1016/0014-5793(94)00755-1. Cited in: PMID: 8062913.
86. Bourdens M, Jeanson Y, Taurand M, Juin N, Carrière A, Clément F, Casteilla L, Bulteau A-L, Planat-Bénard V. Short exposure to cold atmospheric plasma induces senescence in human skin fibroblasts and adipose mesenchymal stromal cells. Sci Rep. 2019 A.D. 9:8671. https://doi.org/10.1038/s41598-019-45191-2. Cited in: PMID: 31209329.
87. Saba H, Munusamy S, Macmillan-Crow LA. Cold preservation mediated renal injury: involvement of mitochondrial oxidative stress. Ren Fail. 2008 A.D. 30:125–133. https://doi.org/10.1080/08860220701813327. Cited in: PMID: 18300110.
88. Wheeler MD, Ikejema K, Enomoto N, Stacklewitz RF, Seabra V, Zhong Z, Yin M, Schemmer P, Rose ML, Rusyn I et al. Glycine: a new anti-inflammatory immunonutrient. Cell Mol Life Sci. 1999 A.D. 56:843–856. https://doi.org/10.1007/s000180050030. Cited in: PMID: 11212343.
89. Zhong Z, Wheeler MD, Li X, Froh M, Schemmer P, Yin M, Bunzendaul H, Bradford B, Lemasters JJ. L-Glycine: a novel antiinflammatory, immunomodulatory, and cytoprotective agent. Curr Opin Clin Nutr Metab Care. 2003 A.D. 6:229–240. https://doi.org/10.1097/00075197-200303000-00013. Cited in: PMID: 12589194.

90. Semenza GL. Targeting hypoxia-inducible factor 1 to stimulate tissue vascularization. J Investig Med. 2016 A.D. 64:361–363. https://doi.org/10.1097/JIM.0000000000000206. Cited in: PMID: 25955799.
91. Stockmann C, Fandrey J. Hypoxia-induced erythropoietin production: a paradigm for oxygen-regulated gene expression. Clin Exp Pharmacol Physiol. 2006 A.D. 33:968–979. https://doi.org/10.1111/j.1440-1681.2006.04474.x. Cited in: PMID: 17002676.
92. Lam M, Lamanna E, Organ L, Donovan C, Bourke JE. Perspectives on precision cut lung slices-powerful tools for investigation of mechanisms and therapeutic targets in lung diseases. Front Pharmacol. 2023 A.D. 14:1162889. https://doi.org/10.3389/fphar.2023.1162889. Cited in: PMID: 37261291.
93. Leard LE, Holm AM, Valapour M, Glanville AR, Attawar S, Aversa M, Campos SV, Christon LM, Cypel M, Dellgren G et al. Consensus document for the selection of lung transplant candidates: An update from the International Society for Heart and Lung Transplantation. J Heart Lung Transplant. 2021 A.D. 40:1349–1379. https://doi.org/10.1016/j.healun.2021.07.005. Cited in: PMID: 34419372.

Publisher's note

Supplementary Information Publication II:

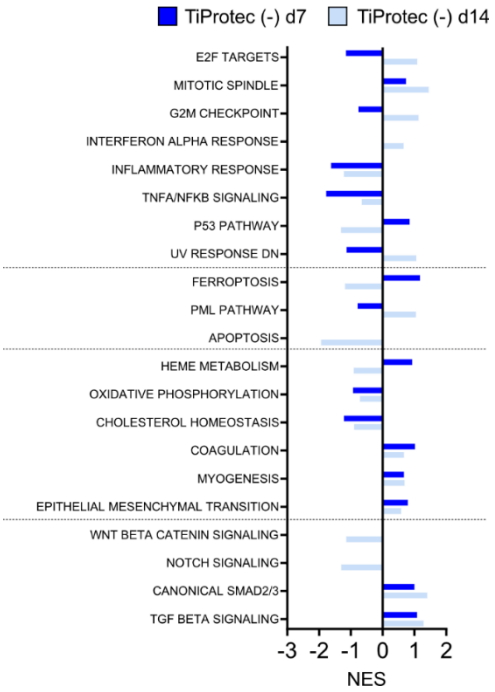

Supplementary Fig. 1

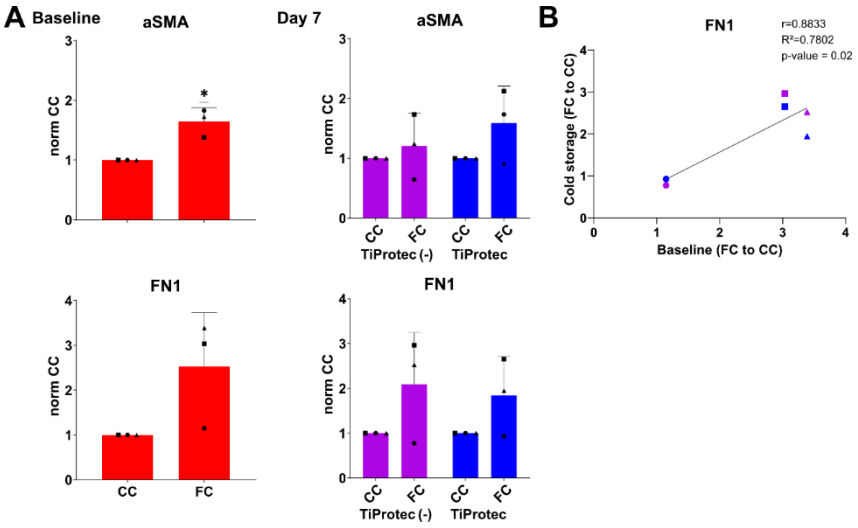

Supplementary Fig. 2

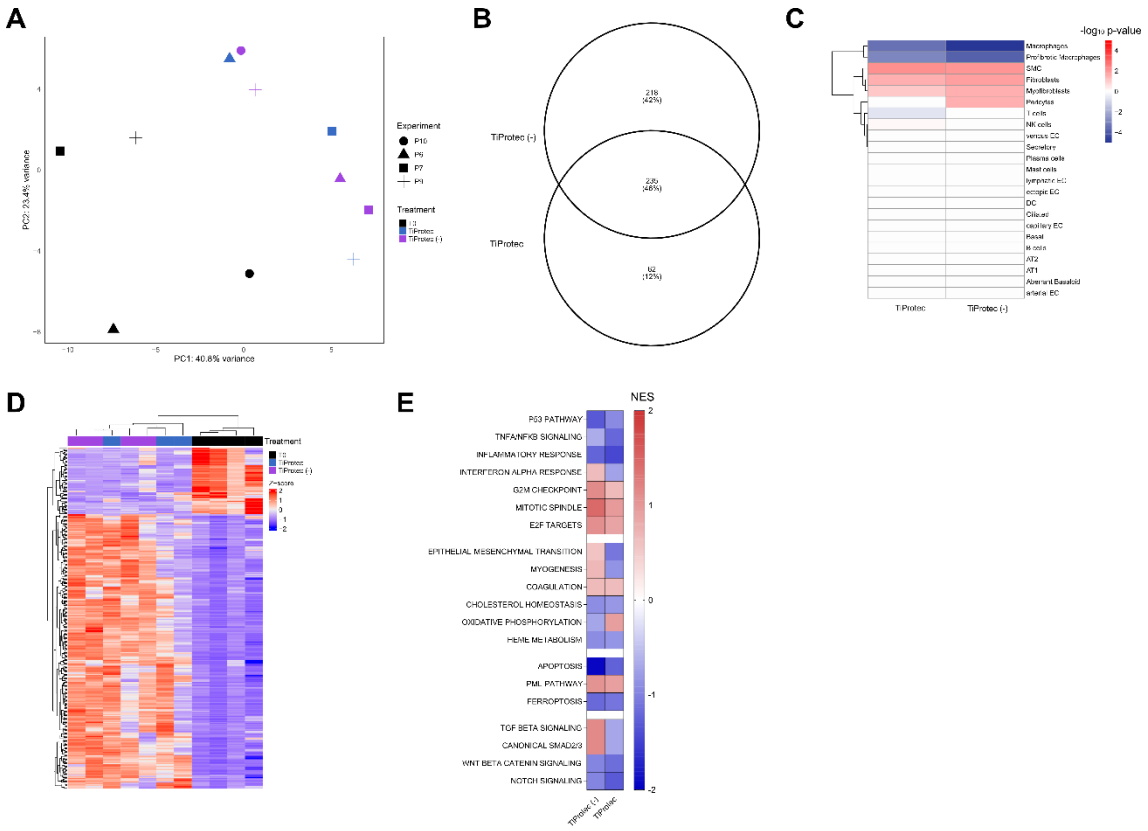

Supplementary Fig. 3

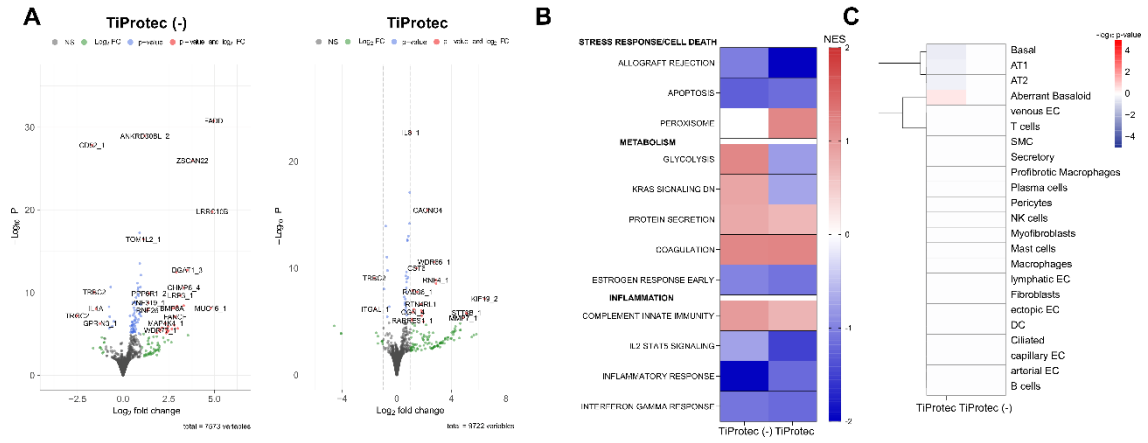

Supplementary Fig. 4

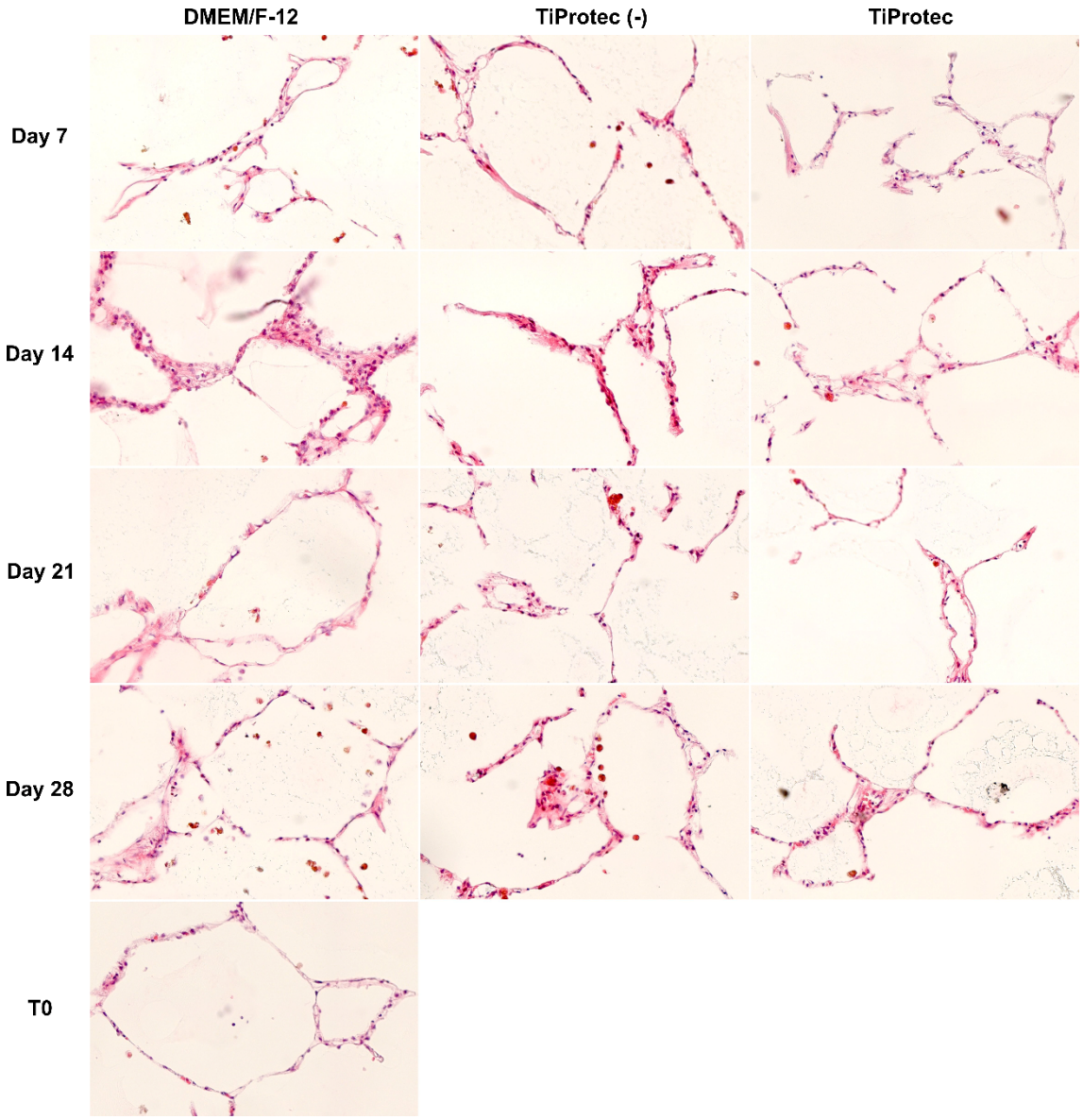

Supplementary Fig. 5

References

Aktories, Klaus; Flockerzi, Veit; Förstermann, Ulrich; Hofmann, Franz; Forth, Wolfgang; Henschler, Dietrich; Rummel, W. (Hg.) (2022): Allgemeine und spezielle Pharmakologie und Toxikologie. Lehrbuch und Nachschlagewerk für Studierende der Medizin, Zahnmedizin, Pharmazie und Veterinärmedizin, für Ärzte, Zahnärzte, Apotheker und Tierärzte sowie für Wissenschaftlerinnen und Wissenschaftler verwandter Disziplinen. Urban-&-Fischer-Verlag. 13. Auflage. München: Elsevier.

Alkondon, Manickavasagom; Aracava, Yasco; Pereira, Edna F. R.; Albuquerque, Edson X. (2009): A single in vivo application of cholinesterase inhibitors has neuron type-specific effects on nicotinic receptor activity in guinea pig hippocampus. In: *The Journal of pharmacology and experimental therapeutics* 328 (1), S. 69–82. DOI: 10.1124/jpet.108.146068.

Alsafadi, Hani N.; Staab-Weijnitz, Claudia A.; Lehmann, Mareike; Lindner, Michael; Peschel, Britta; Königshoff, Melanie; Wagner, Darcy E. (2017): An ex vivo model to induce early fibrosis-like changes in human precision-cut lung slices. In: *American journal of physiology. Lung cellular and molecular physiology* 312 (6), 896-902. DOI: 10.1152/ajplung.00084.2017.

Alsafadi, Hani N.; Uhl, Franziska E.; Pineda, Ricardo H.; Bailey, Kolene E.; Rojas, Mauricio; Wagner, Darcy E.; Königshoff, Melanie (2020): Applications and Approaches for Three-Dimensional Precision-Cut Lung Slices. Disease Modeling and Drug Discovery. In: *American journal of respiratory cell and molecular biology* 62 (6), S. 681–691. DOI: 10.1165/rcmb.2019-0276TR.

Ashani, Yacov; Bhattacharjee, Apurba K.; Leader, Haim; Saxena, Ashima; Doctor, Bhupendra P. (2003): Inhibition of cholinesterases with cationic phosphonyl oximes highlights distinctive properties of the charged pyridine groups of quaternary oxime reactivators. In: *Biochemical pharmacology* 66 (2), S. 191–202. DOI: 10.1016/s0006-2952(03)00204-1.

Aurbek, Nadine; Herkert, Nadja M.; Koller, Marianne; Thiermann, Horst; Worek, Franz (2010): Kinetic analysis of interactions of different sarin and tabun analogues with human acetylcholinesterase and oximes: is there a structure-activity relationship? In: *Chemico-biological interactions* 187 (1-3), S. 215–219. DOI: 10.1016/j.cbi.2010.01.035.

Becker, Christian; Worek, Franz; John, Harald (2010): Chromatographic analysis of toxic phosphylated oximes (POX): a brief overview. In: *Drug testing and analysis* 2 (10), S. 460–468. DOI: 10.1002/dta.167.

Bey, T.; Walter, F. G. (2002): Sarin, Soman, Tabun und VX. In: *Notfall & Rettungsmedizin* 5 (6), S. 462–468. DOI: 10.1007/s10049-002-0462-0.

Box, George E. P. (1976): Science and Statistics. In: *Journal of the American Statistical Association* 71 (356), S. 791–799. DOI: 10.1080/01621459.1976.10480949.

Chauhan, S.; D'Cruz, R.; Faruqi, S.; Singh, K. K.; Varma, S.; Singh, M.; Karthik, V. (2008): Chemical warfare agents. In: *Environmental toxicology and pharmacology* 26 (2), S. 113–122. DOI: 10.1016/j.etap.2008.03.003.

Cherny, Izhack; Greisen, Per; Ashani, Yacov; Khare, Sagar D.; Oberdorfer, Gustav; Leader, Haim et al. (2013): Engineering V-type nerve agents detoxifying enzymes using computationally focused libraries. In: *ACS chemical biology* 8 (11), S. 2394–2403. DOI: 10.1021/cb4004892.

Dodge, J. T.; Mitchell, C.; Hanahan, D. J. (1963): The preparation and chemical characteristics of hemoglobin-free ghosts of human erythrocytes. In: *Archives of Biochemistry and Biophysics* 100 (1), S. 119–130. DOI: 10.1016/0003-9861(63)90042-0.

Dolgin, Elie (2013): Syrian gas attack reinforces need for better anti-sarin drugs. In: *Nature medicine* 19 (10), S. 1194–1195. DOI: 10.1038/nm1013-1194.

Eddleston, Michael; Buckley, Nick A.; Eyer, Peter; Dawson, Andrew H. (2008): Management of acute organophosphorus pesticide poisoning. In: *Toxicology in vitro : an international journal published in association with BIBRA* 371 (9612), S. 597–607. DOI: 10.1016/S0140-6736(07)61202-1.

Eddleston, Michael; Eyer, Peter; Worek, Franz; Mohamed, Fahim; Senarathna, Lalith; Meyer, Ludwig von et al. (2005): Differences between organophosphorus insecticides in human self-poisoning: a prospective cohort study. In: *The Lancet* 366 (9495), S. 1452–1459. DOI: 10.1016/S0140-6736(05)67598-8.

EFSA (2024): European Food Safety Authority. Online verfügbar unter https://www.efsa.europa.eu/en, zuletzt aktualisiert am 21.11.2024, zuletzt geprüft am 21.11.2024.

Elliott, Gloria D.; Wang, Shangping; Fuller, Barry J. (2017): Cryoprotectants: A review of the actions and applications of cryoprotective solutes that modulate cell recovery from ultra-low temperatures. In: *Cryobiology* 76, S. 74–91. DOI: 10.1016/j.cryobiol.2017.04.004.

Ellman, G. L.; Courtney, K. D.; Andres, V.; Feather-Stone, R. M. (1961): A new and rapid colorimetric determination of acetylcholinesterase activity. In: *Biochemical pharmacology* 7, S. 88–95. DOI: 10.1016/0006-2952(61)90145-9.

European Comission (2024): EU Pesticides Database - Active substances. Online verfügbar unter https://ec.europa.eu/food/plant/pesticides/eu-pesticides-database/start/screen/active-substances, zuletzt aktualisiert am 14.11.2024, zuletzt geprüft am 10.12.2024.

Eyer, Peter (2003): The role of oximes in the management of organophosphorus pesticide poisoning. In: *Toxicological reviews* 22 (3), S. 165–190. DOI: 10.2165/00139709-200322030-00004.

Goldsmith, Moshe; Eckstein, Simone; Ashani, Yacov; Greisen, Per; Leader, Haim; Sussman, Joel L. et al. (2016): Catalytic efficiencies of directly evolved phosphotriesterase variants with structurally different organophosphorus compounds in vitro. In: *Archives of toxicology* 90 (11), S. 2711–2724. DOI: 10.1007/s00204-015-1626-2.

Grob, D. (1956): The manifestations and treatment of poisoning due to nerve gas and other organic phosphate anticholinesterase compounds. In: *A.M.A. archives of internal medicine* 98 (2), S. 221–239. DOI: 10.1001/archinte.1956.00250260095010.

Gunnell, David; Eddleston, Michael (2003): Suicide by intentional ingestion of pesticides: a continuing tragedy in developing countries. In: *International journal of epidemiology* 32 (6), S. 902–909. DOI: 10.1093/ije/dyg307.

Herbert, Julia; Kelty, Jacklyn S.; Laskin, Jeffrey D.; Laskin, Debra L.; Gow, Andrew J. (2023): Menthol flavoring in e-cigarette condensate causes pulmonary dysfunction and cytotoxicity in precision cut lung slices. In: *American journal of physiology. Lung cellular and molecular physiology* 324 (3), 345-357. DOI: 10.1152/ajplung.00222.2022.

Herbert, Julia; Thiermann, Horst; Worek, Franz; Wille, Timo (2019): COPD and asthma therapeutics for supportive treatment in organophosphate poisoning. In: *Clinical toxicology (Philadelphia, Pa.)* 57 (7), S. 644–651. DOI: 10.1080/15563650.2018.1540785.

Holmstedt, B. (1959): Pharmacology of organophosphorus cholinesterase inhibitors. In: *Pharmacological reviews* 11, S. 567–688.

John, Harald; van der Schans, Marcel J.; Koller, Marianne; Spruit, Helma E. T.; Worek, Franz; Thiermann, Horst; Noort, Daan (2018): Fatal sarin poisoning in Syria 2013: forensic verification within an international laboratory network. In: *Forensic toxicology* 36 (1), S. 61–71. DOI: 10.1007/s11419-017-0376-7.

Kalász, H.; Nurulain, S. M.; Veress, G.; Antus, S.; Darvas, F.; Adeghate, E. et al. (2015): Mini review on blood-brain barrier penetration of pyridinium aldoximes. In: *Journal of applied toxicology : JAT* 35 (2), S. 116–123. DOI: 10.1002/jat.3048.

Karalliedde, Lakshman; Feldman, Stanley; Henry, John; Marrs, Timothy (2001): Organophosphates and Health: Imperial College Press.

Koning, Martijn Constantijn de; Horn, Gabriele; Worek, Franz; van Grol, Marco (2018): Discovery of a potent non-oxime reactivator of nerve agent inhibited human acetylcholinesterase. In: *European journal of medicinal chemistry* 157, S. 151–160. DOI: 10.1016/j.ejmech.2018.08.016.

Koziol-White, Cynthia; Gebski, Eric; Cao, Gaoyaun; Panettieri, Reynold A. (2024): Precision cut lung slices: an integrated ex vivo model for studying lung physiology, pharmacology, disease pathogenesis and drug discovery. In: *Respir Res* 25 (1), S. 231. DOI: 10.1186/s12931-024-02855-6.

Lehmann, Mareike; Krishnan, Ramaswamy; Sucre, Jennifer; Kulkarni, Hrishikesh S.; Pineda, Ricardo H.; Anderson, Christopher et al. (2024): Precision Cut Lung Slices:

Emerging Tools for Preclinical and Translational Lung Research. An Official American Thoracic Society Workshop Report. In: *American journal of respiratory cell and molecular biology*. DOI: 10.1165/rcmb.2024-0479ST.

Liu, Guanghui; Betts, Catherine; Cunoosamy, Danen M.; Åberg, Per M.; Hornberg, Jorrit J.; Sivars, Kinga Balogh; Cohen, Taylor S. (2019): Use of precision cut lung slices as a translational model for the study of lung biology. In: *Respir Res* 20 (1), S. 162. DOI: 10.1186/s12931-019-1131-x.

Marrs, T. C. (1993): Organophosphate poisoning. In: *Pharmacology & therapeutics* 58 (1), S. 51–66. DOI: 10.1016/0163-7258(93)90066-m.

Marrs, Timothy C. (2007): Toxicology of Organophosphate Nerve Agents. In: Timothy C. Marrs, Robert L. Maynard und Frederick R. Sidell (Hg.): Chemical Warfare Agents: Wiley, S. 191–221.

Martin, C.; Uhlig, S.; Ullrich, V. (1996): Videomicroscopy of methacholine-induced contraction of individual airways in precision-cut lung slices. In: *The European respiratory journal* 9 (12), S. 2479–2487. DOI: 10.1183/09031936.96.09122479.

Moffatt, Alison; Mohammed, Fahim; Eddleston, Michael; Azher, Shifa; Eyer, Peter; Buckley, Nick A. (2010): Hypothermia and Fever after organophosphorus poisoning in humans--a prospective case series. In: *J. Med. Toxicol.* 6 (4), S. 379–385. DOI: 10.1007/s13181-010-0012-y.

Nakagawa, Tomomasa; Tu, Anthony T. (2018): Murders with VX: Aum Shinrikyo in Japan and the assassination of Kim Jong-Nam in Malaysia. In: *Forensic toxicology* 36 (2), S. 542–544. DOI: 10.1007/s11419-018-0426-9.

Neuhaus, Vanessa; Danov, Olga; Konzok, Sebastian; Obernolte, Helena; Dehmel, Susann; Braubach, Peter et al. (2018): Assessment of the Cytotoxic and Immunomodulatory Effects of Substances in Human Precision-cut Lung Slices. In: *Journal of visualized experiments : JoVE* (135). DOI: 10.3791/57042.

Neuhaus, Vanessa; Schaudien, Dirk; Golovina, Tatiana; Temann, Ulla-Angela; Thompson, Carolann; Lippmann, Torsten et al. (2017): Assessment of long-term cultivated human precision-cut lung slices as an ex vivo system for evaluation of chronic cytotoxicity and functionality. In: *Journal of occupational medicine and toxicology (London, England)* 12, S. 13. DOI: 10.1186/s12995-017-0158-5.

Organisation for the Prohibition of Chemical Weapons (07.06.2020): Chemical Weapons Convention (CWC). Online verfügbar unter https://www.opcw.org/sites/default/files/documents/CWC/CWC_en.pdf, zuletzt geprüft am 21.11.2024.

Paddenberg, Renate; Mermer, Petra; Goldenberg, Anna; Kummer, Wolfgang (2014): Videomorphometric analysis of hypoxic pulmonary vasoconstriction of intra-pulmonary arteries using murine precision cut lung slices. In: *Journal of visualized experiments : JoVE* (83). DOI: 10.3791/50970.

Pegg, David E. (2015): Principles of cryopreservation. In: *Methods in molecular biology (Clifton, N.J.)* 1257, S. 3–19. DOI: 10.1007/978-1-4939-2193-5_1.

Russell, W. M. S.; Burch, R. L. (1992): The principles of humane experimental technique / W.M.S. Russell and R.L. Burch. Special ed. South Mimms, Potters Bar, Herts, England: Universities Federation for Animal Welfare.

Schrader, G. (1950): Organische Phosphor-Verbindungen als neuartige lnsektizide (Auszug). In: *Angewandte Chemie* 62 (20), S. 471–473. DOI: 10.1002/ange.19500622002.

Schrader, G.; Lorenz, W.; Mühlmann, R. (1958): Monothio-pyrophosphorsäure-tetraalkylester – ihre Herstellung und ihre Eigenschaften. In: *Angewandte Chemie* 70 (22-23), S. 690–694. DOI: 10.1002/ange.19580702204.

Seehase, S.; Schlepütz, M.; Switalla, S.; Mätz-Rensing, K.; Kaup, F. J.; Zöller, M. et al. (2011): Bronchoconstriction in nonhuman primates: a species comparison. In: *Journal of applied physiology (Bethesda, Md. : 1985)* 111 (3), S. 791–798. DOI: 10.1152/japplphysiol.00162.2011.

Sinko, Goran; Calić, Maja; Bosak, Anita; Kovarik, Zrinka (2007): Limitation of the Ellman method: cholinesterase activity measurement in the presence of oximes. In: *Analytical biochemistry* 370 (2), S. 223–227. DOI: 10.1016/j.ab.2007.07.023.

Steindl, David; Boehmerle, Wolfgang; Körner, Roland; Praeger, Damaris; Haug, Marcel; Nee, Jens et al. (2021): Novichok nerve agent poisoning. In: *The Lancet* 397 (10270), S. 249–252. DOI: 10.1016/S0140-6736(20)32644-1.

Tigges, Jonas; Eggerbauer, Florian; Worek, Franz; Thiermann, Horst; Rauen, Ursula; Wille, Timo (2021): Optimization of long-term cold storage of rat precision-cut lung slices with a tissue preservation solution. In: *American journal of physiology. Lung cellular and molecular physiology* 321 (6), 1023-1035. DOI: 10.1152/ajplung.00076.2021.

Tigges, Jonas; Worek, Franz; Thiermann, Horst; Wille, Timo (2022): Organophosphorus pesticides exhibit compound specific effects in rat precision-cut lung slices (PCLS): mechanisms involved in airway response, cytotoxicity, inflammatory activation and antioxidative defense. In: *Archives of toxicology* 96 (1), S. 321–334. DOI: 10.1007/s00204-021-03186-x.

Urbina, Fabio; Lentzos, Filippa; Invernizzi, Cédric; Ekins, Sean (2022): Dual Use of Artificial Intelligence-powered Drug Discovery. In: *Nature machine intelligence* 4 (3), S. 189–191. DOI: 10.1038/s42256-022-00465-9.

Vale, J. Allister; Marrs, Timothy C.; Maynard, Robert L. (2018): Novichok: a murderous nerve agent attack in the UK. In: *Clinical toxicology (Philadelphia, Pa.)* 56 (11), S. 1093–1097. DOI: 10.1080/15563650.2018.1469759.

Wigenstam, E.; Forsberg, E.; Bucht, A.; Thors, L. (2021): Efficacy of atropine and scopolamine on airway contractions following exposure to the nerve agent VX. In: *Toxicology and Applied Pharmacology* 419. DOI: 10.1016/j.taap.2021.115512.

Wigenstam, Elisabeth; Artursson, Elisabet; Bucht, Anders; Thors, Lina (2022): Supplemental treatment to atropine improves the efficacy to reverse nerve agent induced bronchoconstriction. In: *Chemico-biological interactions* 364. DOI: 10.1016/j.cbi.2022.110061.

Wille, T.; Thiermann, H.; Worek, F. (2010): Development of a high-throughput screening for nerve agent detoxifying materials using a fully-automated robot-assisted biological assay. In: *Toxicology in vitro : an international journal published in association with BIBRA* 24 (3), S. 1026–1031. DOI: 10.1016/j.tiv.2009.11.023.

Worek, F.; Aurbek, N.; Thiermann, H. (2007): Reactivation of organophosphate-inhibited human AChE by combinations of obidoxime and HI 6 in vitro. In: *Journal of applied toxicology : JAT* 27 (6), S. 582–588. DOI: 10.1002/jat.1241.

Worek, F.; Diepold, C.; Eyer, P. (1999): Dimethylphosphoryl-inhibited human cholinesterases: inhibition, reactivation, and aging kinetics. In: *Archives of toxicology* 73 (1), S. 7–14. DOI: 10.1007/s002040050580.

Worek, F.; Reiter, G.; Eyer, P.; Szinicz, L. (2002): Reactivation kinetics of acetylcholinesterase from different species inhibited by highly toxic organophosphates. In: *Archives of toxicology* 76 (9), S. 523–529. DOI: 10.1007/s00204-002-0375-1.

Worek, Franz; Eyer, Peter; Thiermann, Horst (2012): Determination of acetylcholinesterase activity by the Ellman assay: a versatile tool for in vitro research on medical countermeasures against organophosphate poisoning. In: *Drug testing and analysis* 4 (3-4), S. 282–291. DOI: 10.1002/dta.337.

Worek, Franz; Jenner, John; Thiermann, Horst (Hg.) (2016a): Chemical Warfare Toxicology. Cambridge: Royal Society of Chemistry (Issues in Toxicology).

Worek, Franz; Thiermann, Horst (2013): The value of novel oximes for treatment of poisoning by organophosphorus compounds. In: *Pharmacology & therapeutics* 139 (2), S. 249–259. DOI: 10.1016/j.pharmthera.2013.04.009.

Worek, Franz; Thiermann, Horst; Szinicz, Ladislaus; Eyer, Peter (2004): Kinetic analysis of interactions between human acetylcholinesterase, structurally different organophosphorus compounds and oximes. In: *Biochemical pharmacology* 68 (11), S. 2237–2248. DOI: 10.1016/j.bcp.2004.07.038.

Worek, Franz; Thiermann, Horst; Wille, Timo (2020): Organophosphorus compounds and oximes: a critical review. In: *Archives of toxicology* 94 (7), S. 2275–2292. DOI: 10.1007/s00204-020-02797-0.

Worek, Franz; Wille, Timo; Koller, Marianne; Thiermann, Horst (2016b): Toxicology of organophosphorus compounds in view of an increasing terrorist threat. In: *Archives of toxicology* 90 (9), S. 2131–2145. DOI: 10.1007/s00204-016-1772-1.

Acknowledgements

I would like to express my appreciation to the following individuals who have played pivotal roles in the successful completion of my Ph.D. thesis:

First and foremost, I would like to thank my primary supervisor, Prof. Dr. med. Timo Wille. His continuous support, the excellent supervision and his generous investment of time have been invaluable. I am grateful for his professional advice and for the motivation he gave to me.

My gratitude also extends to Prof. Dr. med. Franz Worek, who always had an open ear and excellent professional advice. In his capacity as the head of the Bundeswehr Institute of Pharmacology and Toxicology I want to thank him and Prof. Dr. med. Horst Thiermann, his predecessor, for the exceptional working conditions they facilitated, and which were crucial to the success of my dissertation.

I thank Dr. Jonas Tigges, who shared his knowledge with me, introduced me to the world of PCLS and who consistently trusted in me. I am grateful for the foundation he laid for my work.

I thank the members of my thesis advisory committee, Prof. Dr. med. Thomas Gudermann and Prof. Dr. phil. nat. Anette Nicke. Their additional scientific advice and external perspectives enriched my work. Additionally, I want to thank Prof. Dr. Thomas Gudermann in his role as a speaker of GRK 2338 and express my gratitude for the outstanding scientific program provided by the Research Training Group and the DFG.

I am grateful for my colleagues and friends from the GRK 2338 and the Bundeswehr Institute of Pharmacology and Toxicology - with special thanks to Paula Helena Sieber. Furthermore, I want to thank Prof. Dr. Mareike Lehmann and Dr. María Camila Melo-Narváez for the possibility to collaborate with both. The scientific discussions, encouraging advice, and support have created a vibrant academic community that enriched my research experience.

To my parents (Dres. Eva E. Wille and Peter Gölitz), my nanny, her daughter (Ruth Leonhard, Heike Leonhard), and my boyfriend (Paul Schäfer), I owe thanks for their constant support and motivation. The function of neutral, independent and sometimes even sceptic observers could not have been performed better by anyone than my parents. They always endorsed me, when help was needed. Without all their endless encouragement, this journey would have been much more challenging.